INFORMATION TO USERS

This manuscript has been reproduced from the microfilm master. UMI films the text directly from the original or copy submitted. Thus, some thesis and dissertation copies are in typewriter face, while others may be from any type of computer printer.

The quality of this reproduction is dependent upon the quality of the copy submitted. Broken or indistinct print, colored or poor quality illustrations and photographs, print bleedthrough, substandard margins, and improper alignment can adversely affect reproduction.

In the unlikely event that the author did not send UMI a complete manuscript and there are missing pages, these will be noted. Also, if unauthorized copyright material had to be removed, a note will indicate the deletion.

Oversize materials (e.g., maps, drawings, charts) are reproduced by sectioning the original, beginning at the upper left-hand corner and continuing from left to right in equal sections with small overlaps. Each original is also photographed in one exposure and is included in reduced form at the back of the book.

Photographs included in the original manuscript have been reproduced xerographically in this copy. Higher quality 6" x 9" black and white photographic prints are available for any photographs or illustrations appearing in this copy for an additional charge. Contact UMI directly to order.

UMI

A Bell & Howell Information Company
300 North Zeeb Road, Ann Arbor MI 48106-1346 USA
313/761-4700 800/521-0600

THE STRUCTURAL DIFFERENCES OF FIVE FORMS OF ALPHA-LACTALBUMIN AS REVEALED BY FTIR SPECTROSCOPY

by

Hui Zhong

A dissertation submitted to the Graduate Faculty in Physics in partial fulfillment of the requirements for the degree of Doctor of Philosophy, The City University of New York

1999

This manuscript has been read and acepted for the Graduate Faculty in Physics in the satisfaction of the dissertation requirement for the degree of Doctor of Philosophy.

3/9/99
Date

Robert Callender
Chair of Examing Comittee

3/10/99
Date

Executive Officer

Supervisory Committee

The City University of New York

Abstract

THE STRUCTURAL DIFFERENCES OF FIVE FORMS OF ALPHA-LACTABUMIN AS REVEALED BY FTIR SPECTROSCOPY

By

Hui Zhong

Adviser: Professor Robert Callender

We have performed heat induced thermal denaturation study on bovine α-lactalbumin by application of Fourier transformation spectroscopy. Different modified forms of this protein, including the apo form (calcium free α-LA), the cam-3ss form (disrupted 6-120 disulfide bond) and the apo cam-3ss form, were studied in addition to the intact protein so as to find the influence of the ligand calcium and disulfide bond 6-120 on the folding and stability of α-lactalbumin.

The sharp bands of the IR spectrum for the native α-lactalbumin exhibits rigid structural features of the native protein. At low temperature, the bands at 1653 and 1638 cm^{-1} are assigned to the contribution from the helical structures. The weak band at 1629 cm^{-1} is associated with β-structure. The bands above 1660 cm^{-1} are attributable to the turn structures. At high temperature, all denatured forms show a wide dominant bands

centered at 1645 cm^{-1}, a feature found in denatured α-lactalbumin. This band most likely arises from the random structure and solvated helices.

The transition curves of the intact protein indicate gradual melting behavior of the β-structure below 60 °C. The major transition happening in the mid 60 °C involves substantial decrease of the bands at 1638 and 1653 cm^{-1}, and this relates to the denaturation of helical structures.

The cam-3ss form exhibits similar melting to the intact protein. However, the major transition temperature shifts down to the mid fifties compared to the mid sixties of the intact protein as result of the broken disulfide bond. In addition, a small structure change is found at room temperature and is thought to be caused by local relaxation in the region around the broken disulfide bond. Therefore, a major role of the disulfide bond 6-120 is to stabilize protein.

The thermal denaturation studies of the calcium free forms of α-lactalbumin are investigated with AgCl windows instead of CaF_2 windows to avoid the possible calcium contamination. The transition curves of the apo form of α-lactabumin show two transitions instead of one transition found in the calcium bound forms. The transition at low temperature (around 20 °C) involves substantial decrease of the band at 1638 and 1653 cm^{-1}, indicative of the denaturation of the helical structures. On the other hand, the band at 1629 cm^{-1} increases, suggesting the increased formation of β-structure. The second transition happens around 40 °C. The remaining components, largely β-structure, are unfolded through this transition.

The apo cam-3ss form of α-LA shows one major transition in the experimental range. Further analysis of the spectra suggests a low temperature transition below 5 °C. The unstructured helical domain at 5 °C provides the evidence of melting of helical structures through this transition. The high temperature transition happens around 40 °C, similar to that of the apo form.

The non-cooperative transition behavior of the two structural domains in the calcium free forms of α-lactalbumin suggests these two domains melt independently. The presence of the calcium ion gives to rise a cooperative transition. The function of the disulfide bond 6-120 is to stabilize the helical domain rather than the whole protein.

On the basis of traditional model that suggests helical domain is formed first without the formation of β-structural domain (classic molten globules), this thermal denaturation study further infers that β-domain folds first, followed by binding of calcium ion, which then triggers the complete folding of the helical domain during the folding process of α-lactalbumin from molten globule to native protein.

Acknowledgments

I would like to express my sincere gratitude to Professor Robert H Callender for his guidance, patience and inspiration, leading me into an active research field which was exciting to me. His style of research had a great influence on me.

I would like to thank Dr. Rudolf Gilmanshin for his valuable suggestion, discussion and helps from which I have been benefited a lot. His extensive experiences and discernment are good guidance for my research. His outstanding experimental skill had profound influence on my research. I also thank him to improve the instruments in the lab, which made many of these measurements possible.

I feel grateful to Dr. Steve Eyles for his valuable advice and help when I tried to modify the protein by blocking the two free cysteins.

I would also like to give thanks to Dr Hua Deng, Larry Senak, Dongguang Xiao, Zhongmou Ju and Jianghua Wang for their generous help.

Finally, I would like to thank my parents and my wife, Feng Tan, for their encouragement, patience and support during the course of this work. Without their expectation, this thesis work would not have been proceeded so smoothly.

TABLE OF CONTENTS

Abstract iii
Acknowledgments vi
Table of Contents vii
Abbreviations x
List of Figures xi

Chapter 1 Introduction 1
1.1 General Introduction 1
1.1.1 What is protein folding problem 1
1.1.2 What is the importance of protein folding problem 2
1.2 Molten Globule State 2
1.3 α-Lactalbumin 4
1.4 Techniques Used for Protein Structure Studies 5
1.5 Technique Used in This Study 7
1.6 Principals of Fourier Transformation Infrared Spectroscopy 9
Figure Legends 15

Chapter 2 Methodology and Band Assignment 20
2.1 How to Study 20
2.2 FT-IR Measurement 20
2.3 Spectra Analysis 21
2.3.1 Second derivative 22
2.3.2 Fourier self-deconvolution 22
2.3.3 Double difference spectra 26
2.3.4 Adjustment of sample leakage 27

2.4 Protein Structures and IR Bands 28
2.4.1 Region from 1500 cm^{-1} to 1600 cm^{-1} 28
2.4.2 Region from 1600 cm^{-1} to 1700 cm^{-1} 29
2.5 Band Assignment for Native α-Lactalbumin 32
2.6 Band Assignment for Unfolded α-Lactalbumin 34
Figure Legends 36

Chapter 3 An FT-IR Study of the Complex Melting Behavior of α-Lactalbumin 44
3.1 Abstract 44
3.2 Introduction 44
3.3 Materials and Methods 48
3.4 Results 51
3.5 Discussion 58
Figure Legends 64

Chapter 4 The Melting Behavior of The Acid Form and Apo α-Lactalbumin: Evidence of Separate Melting Behaviors of Helices and β-Structures 71
4.1 Introduction 71
4.2 Materials and Methods 77
4.2.1 Preparation of protein samples 77
4.2.2 Preparation of protein solutions 77
4.2.3 Reversibility and aggregation 78
4.2.4 Instrument and data analysis 79
4.3 Results and Discussion 80
4.3.1 The acid form of α-Lactalbumin 80

4.3.2 The apo form of α-Lactalbumin 82
Figure Legends 90

Chapter 5 The Melting Behavior of Disulfide Link Destabilized α-Lactalbumin 102
5.1 Introduction 102
5.2 Materials and Methods 102
5.2.1 Ellman's method 103
5.2.2 How to trap the 3ss form of α-Lactalbumin 106
5.2.3 Preparation of cam-3ss form 108
5.2.4 Preparation of protein solutions 110
5.3 Results and Discussion 111
5.3.1 The holo cam-3ss form of α-lactalbumin 111
5.3.2 The apo cam 3ss form of α-lactalbumin 114
5.4 Conclusions 117
Figure Legends 118

Chapter 6 The Protein Folding Pathway of α-Lactalbumin 134
6.1 General Thought of Protein Folding 134
6.2 How Does α-Lactalbumin Fold to Its Native State 136
6.2.1 Helical structures are formed first 137
6.2.2 β-structures are formed subsequently 137
6.2.3 Tertiary structures in β-structure region are formed at stage 3 138
6.2.4 Folding of helical domain at stage 139
6.3 Summery 140
References 141

Abbreviations

CD: Circular Dichroism

FTIR: Fourier Transformation Spectroscopy

NMR: Nuclear Magnetic Resonance

α-LA: α–Lactalbumin

BLA: Bovine α-Lactalbumin

MG: Molten Globule

SDS: Sodium Dodecyl Sulfate

PAGE: Polyacrylamide Gel Electrophoresis

DTT: Dithiothreitol

DTNB: Dithiobisnitrobenzoic Acid

TNB: 2-nitro-5-thiobenzoic Acid

CAM-3SS: Three Disulfide Carboxyamidomethylate

MCT: Mercury Cadium Telluride

LIST OF FIGURES

Figures

Figure 1.1	16
Figure 1.2	17
Figure 1.3	18
Figure 1.4	19
Figure 2.1	37
Figure 2.2	38
Figure 2.3	39
Figure 2.4	40
Figure 2.5	41
Figure 2.6	42
Figure 2.7	43
Figure 3.1(a, b, c)	66
Figure 3.2(a, b)	67
Figure 3.3(a, b)	68
Figure 3.4	69
Figure 3.5(a, b)	70
Figure 4.1	92
Figure 4.2(a)	93
Figure 4.2(b)	94
Figure 4.3	95
Figure 4.4(a)	96
Figure 4.4(b)	97
Figure 4.5	98

Figure 4.6 99
Figure 4.7 100
Figure 4.8 101
Figure 5.1 121
Figure 5.2 122
Figure 5.3(a) 123
Figure 5.3(b) 124
Figure 5.4 125
Figure 5.5 126
Figure 5.6 127
Figure 5.7(a) 128
Figure 5.7(b) 129
Figure 5.8 130
Figure 5.9 131
Figure 5.10 132
Figure 5.11 133

Chapter 1 Introduction

1.1 General Introduction

1.1.1 *What is protein folding Problem*

Proteins are large molecules with typical molecular weights of tens of thousands. To be biologically active, protein must adopt specific folded three-dimensional, tertiary structures. Yet the genetic information for the protein specifies only the primary structure, the linear sequence of amino acids in the polypeptide backbone. Many purified proteins can spontaneously refold in vitro after being completely unfolded, so the three-dimensional structure must be determined by the primary structure. How this occurs has come to be known as "the protein folding problem". How protein folds up to its unique structure thus becomes one of the most challenging subjects in molecular biology.

The problem can be broken down into four related questions (Pain, 1994):

1. By what kinetic process or pathway does the protein adopt its native and biologically active folded conformation?
2. What is the physical basis of the stability of the folded conformation?
3. Why does the amino acid sequence determine one particular folding process and resultant three-dimensional structure, instead of others?
4. Given the amino acid sequence of a protein, how can its three-dimensional structure be predicted?

This thesis focus primarily on the first question.

1.1.2 *What is the importance of the protein folding problem*

The molecular details of the folding process are under intense investigation both theoretically and experimentally. This is because the future design of biologically active proteins and peptides must take into account how these biopolymers arrive at their final structures on the one hand. On the other hand, over the past decade, studies of how proteins fold have led to realize the mechanism of some diseases. One of the examples is that the way protein clumps form in the test tube is remarkably similar to how protein form the so-called "amyloid" deposits that are pathological hallmarks of some dozen different diseases --- the best known of which is the common memory disorder Alzheimer's. Abnormal protein folding may also account for a group of mysterious infectious diseases, which include scrapie in sheep, mad cow diseases, and Creutzfeldt-Jacob disease in humans (Taubes, 1996). Given the growing evidences that abnormal protein folding leads to amyloid diseases, researchers have begun to turn their attention to devising potential treatments that work by preventing protein from misfolding. All these factors account for why the study on protein folding becomes one of the hottest research area over the past decade.

1.2 Molten Globule State

A variety of proteins have been observed under certain conditions to exist in stable conformations that are neither fully folded nor fully unfolded.

The fact that these conformations have sufficient similarities suggests that they are different manifestations of a third stable conformational state that has come to be known as the molten globule.

Molten globule has received substantial attention because they have been postulated to be general, early intermediates in protein folding pathway (figure 1.1) (Ptitsyn, 1987; Ptitsyn, 1992; Kuwajima, 1989; Haynie & Freire, 1993). The properties of molten globules include the following:

(i) substantial secondary structures, comparable to that of native protein;

(ii) absence of well-defined tertiary packing;

(iii) lack of a cooperative thermal unfolding transition;

(iv) compactness (Peng & Kim,1994).

Two classes of molten globule are observed experimentally. It is known that a number of proteins (i.e. α-lactalbumin, carbonic anhydrase B, apomyoglobin, cytochrome c, etc), subjected to particular conditions, adopt a thermodynamically stable structure which conforms to these notions. These equilibrium molten globules belong to the first class. The others are observed during the protein folding and therefore they occur as kinetic intermediates in folding. The properties of these two have been shown to be closely similar. The time-resolved NMR studies on bovine α-lactalbumin provided new evidences for the importance of stable molten globule states as general protein folding intermediates (Balbach et al., 1995). Whatever its actual role in folding turns out to be, the studies of the stable molten globules form the basis for much that is known about the kinetic species. These studies have further led to suggestions of a variety of roles for both

the neutral and acid molten globules in the living cell. The molten globule as a functional entity has been found in protein transport, membrane insertion and protein-chaperone interactions.

1.3. α-lactalbumin

This protein presents in the milk whey from most species of mammals. It functions as a modifier protein in lactose galactosyltransferase (Brodbeck et al., 1967). In addition to its physiological roles, α-lactalbumin has been demonstrated to exhibit potent antitumor activity in human mammary carcinoma cell lines (Bano et al., 1985). This protein is relatively small, containing 123 residues. The native state (Fig. 1.2) contains four α-helices and a β-sheet domain which contains a small antiparallel β-sheet and several looplike structures. Four disulfides exist in α-lactalbumin. Among them, the disulfide 6-120 exhibits superreactivity which arises from the geometric strain imposed on the disulfide bond in native α-lactalbumin (Kuwajima, 1990). The strong Ca^{2+} binding ability resides in a typical Ca^{2+}-binding loop in which two peptide carbonyls and three carboxylate groups (Asp-82, Asp-87 and Asp-88) act as ligands(Pardon et al., 1995; Stuart et al., 1986)

α-lactalbumin is one of the most thoroughly studied proteins which can form molten globule state . This protein may be denatured by acid or base, by high temperature, by removing the Ca^{2+} and cleaving the disulfide

connecting cystein 6 and cystein 120, and by intermediate concentrations of Gu.HCl and by perchlorate salts to form states that are not so disordered as that of completely unfolded state in high concentration of Gu.HCl. They are generally thought to be different forms of the same molten globule state.

Of these forms, the acid (A-state) form has probably received the most attention. The α-helical domain of the A-state is largely intact and probably forms the core structure of this conformation. The A-state contains essentially the same helix content as a native α-lactalbumin (Dolgikh et al., 1985). NMR studies of proton exchange and NOE determinations suggest that some parts of the helixes found in α-lactalbumin remain helical in the A-state and are shielded from solvent (Peng & Kim, 1994; Alexandrescu et al.,1993).

A recent study found that a protein, where the β-sheet domain had been dissected away, formed the same topology as the A-state (Peng & Kim, 1994). And most recently, their studies suggest that the β-sheet domain could be formed only in the presence of Ca^{2+} (Wu et al., 1996). It was also reported that α-lactalbumin could adopt molten globule state when one of its four disulfide bonds was cleaved and Ca^{2+} was removed (Ewbank & Creighton, 1991). The thermal denaturation behavior of α-lactalbumin has been extensively studied by CD and calorimetric techniques.

1.4 Techniques Used for Protein Structural Studies

The ultimate goal of structural studies of protein is to gain insight into protein three-dimensional structure at a high resolution level. This can often be accomplished by the application of techniques such as X-ray crystallography or multidimensional nuclear magnetic resonance (NMR) spectroscopy. However, high resolution studies of proteins are not always feasible. For example, crystallographic studies require high-quality single crystals which for many proteins are not available. Furthermore, the question arises as to whether the relatively "static" structure in single crystals adequately represents the protein conformation in vitro and in vivo. NMR offers a somewhat better flexibility in studying protein structure in biological relevant environments. However, NMR is not be easily used to study molten globule because of its large intrinsic time. It can not resolve fluctuating structures. Low resolution spectroscopy is the only possible way to study such fluctuating structures as molten globules.

The practical limitations encountered in high-resolution structural studies of proteins stimulate continual progress in the development and improvement of low-resolution spectroscopic methods which provide global insight into the overall secondary structure of proteins without being able to establish the precise three-dimensional location of individual structural elements. The most popular method to investigate protein secondary structures at low resolution level is to use circular dichroism. Circular dichroism is capable of yielding sensitive helical structures but the correlation between the β-structure as determined by CD versus that determined by X-ray become low. In light of the problems inherent to CD, vibrational spectroscopy have been receiving a great deal of attention.

Raman and IR are types of vibrational spectroscopy widely used. The Raman signals come from scattering light and always mix with fluorescence background. In contrast, IR signals are based on absorption and free from fluorescence disturbance so more suitable to make quantitative analysis (figure 1.3). IR is unique for this purpose for two reasons: one is its small intrinsic time to perform a measurement; the other is its equal sensitivity to α-helix and β-sheet. FT-IR studies of proteins have advanced greatly over the past decade, and now the technique experiences a rapid growth in popularity and providing more and more complimentary information.

1.5 Technique used for this study

We have applied FT-IR spectroscopy to studying structures and temperature melting behavior of the following five forms of α-lactalbumin:

1. The intact form (holo);
2. Low pH form (acid);
3. Ca^{2+} free form (apo);
4. Disulfide bond 6-120 broken and blocked form (holo cam-3ss);
5. Ca^{2+} free cam-3ss form (apo cam-3ss).

The advantage of FT-IR method to study thermal denaturation of α-lactalbumin lies in the fact that the different marker band positions between helices and β-sheet structures make it possible to monitor the behavior of these two domains separately.

How FT-IR spectra give us information of protein structures?

That the IR spectroscopy could provide information on the secondary structure of proteins was first demonstrated by Elliot (1951), and Elliot (1954), who showed that empirical correlation existed between the frequency of the so-called amide I and amide II absorption of a protein and the predominant secondary structural motif within the protein as determined by X-ray diffraction studies. That such an empirical correlation exists is not surprising given the nature of the amide I and II modes.

The amide I absorption contains contributions from the C=O stretching vibration of the amide group (about 80%) with a minor contribution from the C-N stretching vibration, while the amide II absorption appears to be significantly less pure, arising from N-H bending (60%) and C-N stretching (40%) vibration.

Based on these descriptions, the exact frequency of the amide I and II absorption would be predicted to be influenced by the strength of any hydrogen bonds involving amide C=O and N-H groups. In protein, each of the amide groups is involved in a secondary structure of some type: either a helix, an extended sheet, or one of the other secondary structures. Because each of these secondary structure motifs is associated with characteristic hydrogen bonding pattern between amide C=O and N-H groups, it is to be expected that each type of secondary structure will give rise to characteristic amide I absorption. These amide bands are also potentially sensitive to the environment change because different external conditions may have their unique influence on the hydrogen bonding of backbone. It is this separation of amide absorption that underlies the determination of protein secondary

structure by IR spectroscopy. The detailed band assignment will be discussed in chapter 2.

The stability of native protein is strongly dependent on the temperature. At temperature high enough, protein will eventually be unfolded due to the increase of the entropy term ($T\Delta S$) although cold denaturation may happen at low temperature. As a result, changing protein stability with temperature will lead to alteration of the population of folded, unfolded and any intermediates that may emerge. Making FT-IR measurement of protein by increasing temperature, we can monitor the structural alternation and the structures of any possible intermediates that may populate. These intermediates may populate and be important in protein folding pathway. Moreover, the different marker bands of various protein secondary structures make it possible to monitor the transition behavior of a single secondary structure without significant contributions of the other components, thus giving us quantitative information of the changes of different structures. FT-IR spectroscopy is predominately sensitive to protein secondary structures. Therefore it can provide the information about not only transitions but also the detailed structural changes. In this thesis, we report our FT-IR study of heat induced denaturation behavior of α-lactalbumin.

1.6 Principals of Fourier Transformation Infrared Spectroscopy

The design of most interferometers used for infrared spectrometry today is based on that of the two-beam interferometer originally designed by

Michelson in 1891. Many other two-beam interferometers have subsequently been designed that may be more useful for certain specific applications than the Michelson interferometer. Nevertheless, the theory behind all scanning two-beam interferometers is similar.

The Michelson interferometer is a device that can divide a beam of radiation into two paths and then recombine the two beams after a path difference has been introduced. The intensity variations of the beam emerging from the interferometer can be measured as a function of path difference by a detector. The simplest form of Michelson interferometer is shown in figure 1.4. It consists of two mutually perpendicular plan mirrors, one of which can move along an axis that is perpendicular to its plans. The movable mirror is either moved at a constant velocity or is held at equally spaced points for fixed short time periods and rapidly stepped between these points. Between the fixed mirror and the movable mirror is a beamsplitter, there a beam of radiation from an external source can be partially reflected to the fixed mirror. After the beam returns to the beamsplitter, the two beams interfere and are again partially reflected and partially transmitted. Because of the effect of interference, the intensity of each beam passing to the detector depends on the difference in path of the beams in the two arms of interferometer. The variation in the intensity of the beam passing to the detector as a function of the path difference ultimately yields the spectral information in a Fourier transform spectrometer.

To understand the processes occurring in a Michelson interferometer better, let us first consider an idealized situation where a source of monochromatic radiation produces an infinitely narrow, perfectly collimated

beam. We suppose the wavelength of the beam is λ We will assume that the beamsplitter is a nonabsorbent film whose reflectance and transmittance are both exactly 50 %. If the mirror is moved at constant velocity, the signal at the detector will be seen to vary sinusoidally. The intensity of the beam at the detector measured as a function of retardation is given the symbol $I'(\delta)$. It follows that the intensity at any point where $\delta=n\lambda$ is equal to the intensity of the source $I(\gamma)$. At other values of δ, the intensity of the beam at the detector is given by

$$I'(\delta) = 0.5I(\gamma)[1 + \cos(2\pi\delta/\lambda)] \qquad (1.1)$$

It can been seen that $I'(\delta)$ is composed of a constant component equal to $0.5I(\gamma)$, and a modified component equal to $0.5I(\gamma)\cos(2\pi\delta/\lambda)$. Only the second component is important in spectrometric measurements, and it is this modulated component that is generally referred to as the interferogram, $I(\delta)$. The interferogram from a monochromatic source measured with an ideal interferometer is given by the equation

$$I(\delta) = 0.5I(\gamma)\cos(2\pi\delta/\lambda) \qquad (1.2)$$

The amplitude of the interferogram as observed after detection and amplification is proportional not only to the intensity of the source but also to the beamsplitter efficiency, detector response, and amplifier characteristics. Of these factors, only $I(\gamma)$ varies from one measurement to the next for a given system configuration while all the other factors remain constant. Therefore Equation 1.2 may be modified by a single wavenumber dependent correction factor, $H(\gamma)$, to give

$$I(\delta) = 0.5H(\gamma)I(\gamma)\cos(2\pi\delta/\lambda) \qquad (1.3)$$

where 0.5 $H(\gamma)I(\gamma)$ may be set equal to $B(\gamma)$, the single-beam spectral intensity. The simplest equation representing the interferogram is therefore

$$I(\delta) = B(\gamma)\cos(2\pi\delta/\lambda) \qquad (1.4)$$

The parameter $B(\gamma)$ gives the intensity of the source at a wavelength γ as modified by the instrumental characteristics.

When the source is a continuum, the interferogram can be represented by the integral:

$$I(\delta) = \int_{-\infty}^{+\infty} B(\gamma)\cos(\frac{2\pi_C\delta}{\gamma})d\gamma \qquad (1.5)$$

Fourier transform pair, the other being

$$B'(\gamma) = \int_{0}^{+\infty} I'(\delta)\cos(\frac{2\pi_C\delta}{\gamma})d\gamma \qquad (1.6)$$

It may be noted that $I(\delta)$ is an even function, so that equation 1.6 may be rewritten as

$$B(\gamma) = 2\int_{0}^{+\infty} I(\delta)\cos(\frac{2\pi_C\delta}{\gamma})d\gamma \qquad (1.7)$$

Equation 1.7 shows that in theory one could measure the complete spectrum from 0 to $+\infty$ at infinitely high resolution. In reality, the retardation is limited, and it is fairly simple to illustrate conceptually how the resolution of a spectrum measured interferometrically depends on the maximum retardation of the scan. By restricting the maximum retardation of the interferogram to Δ, we are effectively multiplying the complete interferogram by a truncation function, $D(\delta)$, which is infinity between $\delta = -\Delta$ and $+\Delta$, and zero at all other points, that is

$$D(\delta) = 1 \qquad \text{if } -\Delta \leq \delta \leq +\Delta$$
$$D(\delta) = 0 \qquad \text{if } \delta > |\Delta|$$

It can be shown that Fourier transform of the product of two functions is the convolution of the FT of each function. The effect of multiplying $I(\delta)$ by boxcar function $D(\delta)$ is to yield a spectrum on Fourier transformation that is the convolution of the FT of $I(\delta)$ measured with an infinitely long retardation and the FT of $I(\delta)$ is the true spectrum, $B(\gamma)$, while the FT of $D(\delta)$, $f(\gamma)$, is given by

$$f(\gamma) = [\, 2\Delta\sin(2\pi\Delta/\lambda)] \,/\, (2\pi\Delta/\lambda) = 2\Delta\,\mathrm{sinc}(2\pi\Delta/\lambda) \qquad (1.8)$$

The intersection points of this function are located at $n/2\Delta$, obviously the resolution of the spectra are determined by $1/2\Delta$, in reverse proportion to the maximum retardation Δ.

The limitation of the maximum retardation introduces not only lower resolution but also side lobe which may give arise to small band (figure)

when convoluting with real spectra. If instead of using the boxcar truncation function D(δ), we introduce some other functions such as triangle function, the amplitude of the side lobes can be considerably reduced from that of the side lobes for the sinc function. Suppression of the magnitude of these oscillations is known as *apodization*. In this study, all interferogram are modified by a Blackman-Harris 3-term apodization.

When the sample is inserted in the optical path, the interferogram thus obtained, I'(δ), is different from I(δ) because of additional absorption of sample. The absorbance of the sample, therefore, is given by

$$A=\mathrm{Log}[B(\gamma)/B'(\gamma)] \qquad (1.9)$$

where $$B'(\gamma)=2\int_0^{+\infty} I'(\delta)\cos(\frac{2\pi_C\delta}{\gamma})d\gamma$$

FT-IR spectra have no influence from the fluorescence background because IR spectra are based on absorption rather than scattering in Raman. Therefore it is more suitable to use IR spectra to quantitatively study the protein structures. However, it is feasible but not straightforward to this end. In the chapter 2, I will introduce the methodology of this FT-IR study in details. The band assignment, partly based on our study and partly based on the work of others, will also be discussed in chapter 2. The results of this investigation of the intact α-lactalbumin and the modified forms will be reported and discussed in chapter 3, 4 and 5 respectively.

Figure Legends

Figure 1.1 Schematic illustration of protein folding pathway.

Figure 1.2 Two-domain structures of α-lactalbumin. The larger structural domain contains the four α-helices (A-D), and the smaller domain contains two strands of β-sheet. The cysteine residues forming four disulfide bonds and asparatate side chains involved in binding of a calcium ion at the domain interfaces are shown explicitly.

Figure 1.3 The energy diagram of photon-molecule interaction.

Figure 1.4 FT-IR experiment setup.

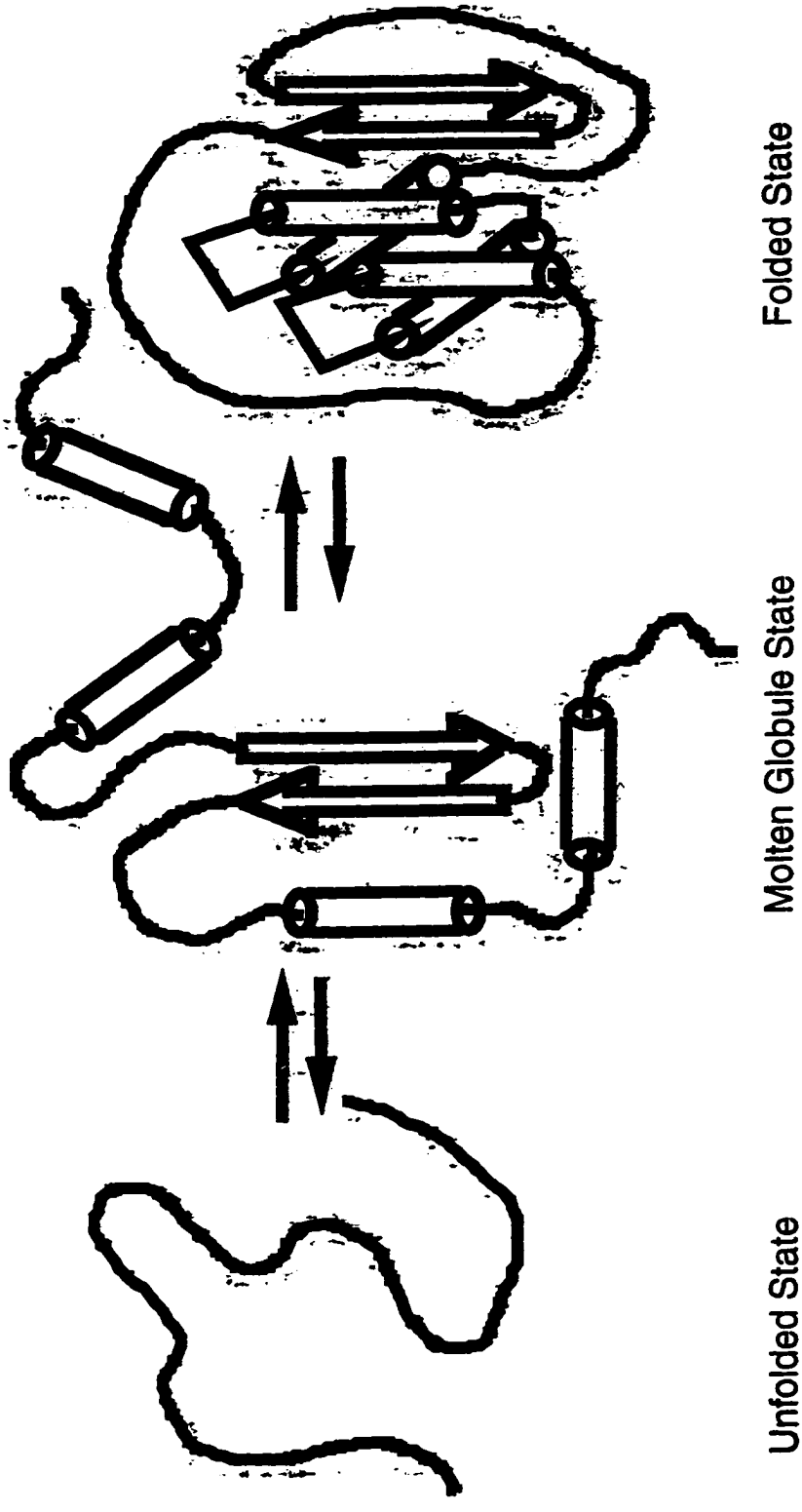

Figure 1.1

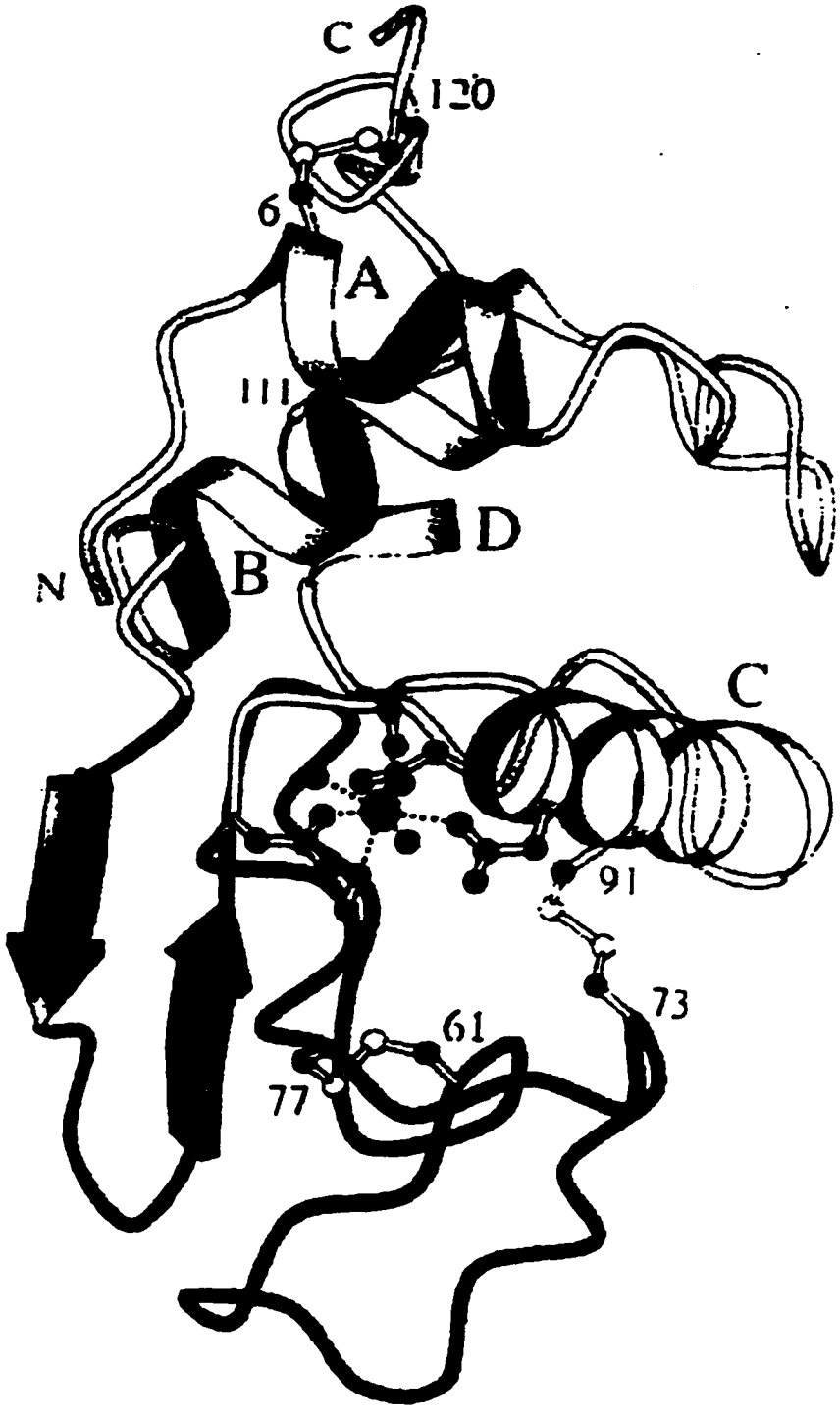

Figure 1.2

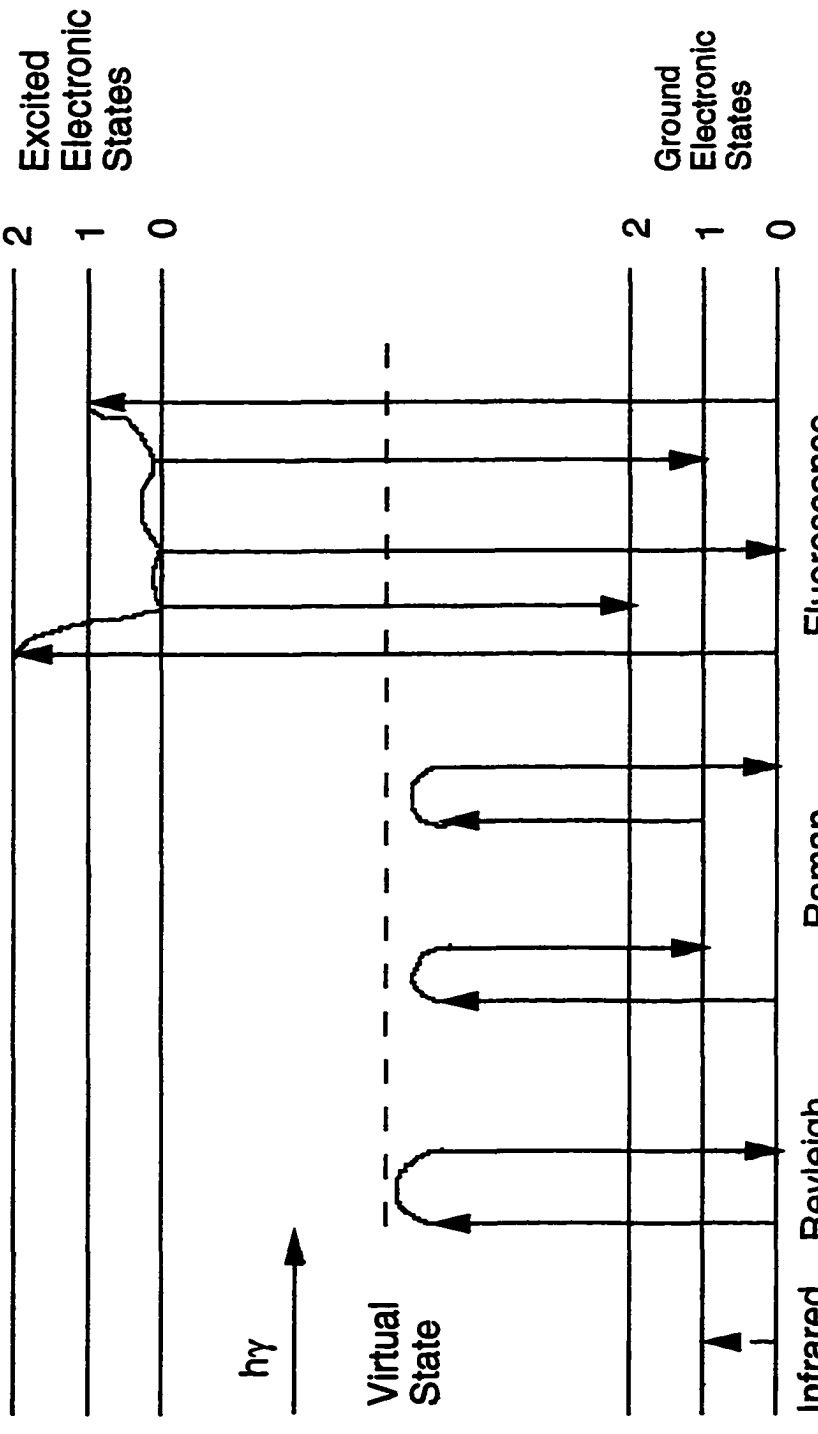

Figure 1.3

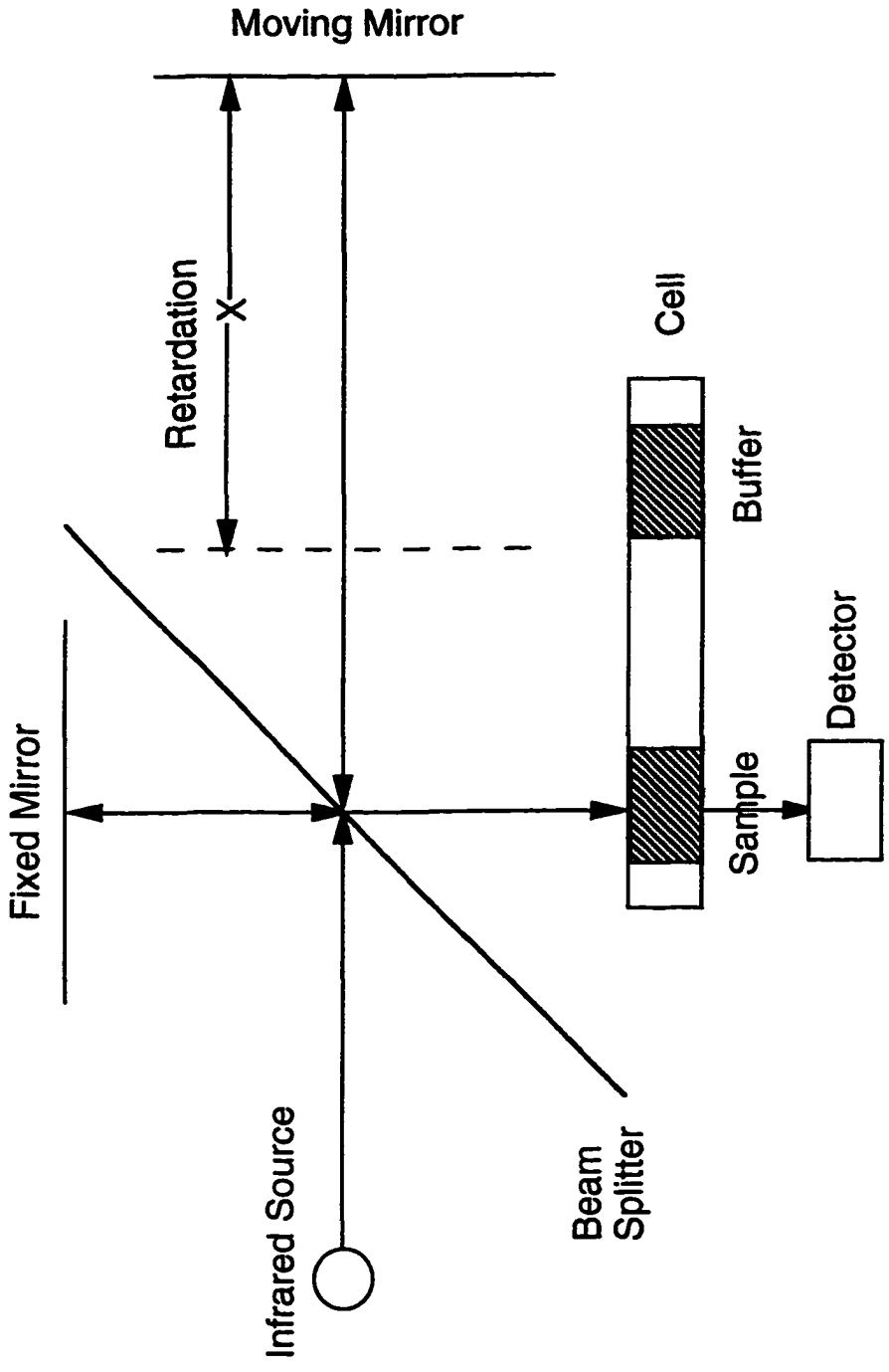

Figure 1.4

Chapter 2 Methodology and Band Assignment

2.1 How to Study

We have used FT-IR spectroscopy to study protein structure changes during its heat denaturing process. Prior to this, some studies have been performed via Raman spectroscopy. Although theoretically speaking Raman spectroscopy should have similar sensitivity to protein secondary structures, the strong florescence background greatly decreases the signal to noise ratio, so that the spectra have to be over smoothed to eliminate the background noise. FT-IR spectra do not have florescence problem and more important, the sample is loaded in a "sandwich" cell (Figure 2.1) rather than an open Raman cell. In this case, it is possible to seal the sample inside without leakage and change of thickness.

2.2 FTIR Measurement

The tendency to aggregate when proteins are denatured allows the measurement only at low concentration. This, together with a strong H_2O absorption band in amide I region, makes an IR study of this protein complicated. In our experiment, several measures were taken to circumvent this problem. First, D_2O was introduced to replace H_2O. In this case, the strong absorption band at 1642 cm^{-1} in H_2O is shifted down to around 1200 cm^{-1} in D_2O, thus leaving the amide I region clear to be used for protein. It follows that thicker spacer can be used to enhance protein signal. Second, data of sample and buffer were collected alternatively to eliminate water vapor contribution to resultant spectra as much as possible.

2.3 Spectra Analysis

Infrared spectroscopy, with the advent of Fourier-transform spectrometers and resolution-enhancement (band-narrowing) algorithms, has become a widely used method for the examination of protein secondary structure in solution. Most infrared studies of protein conformation focus on absorption in the amide I (designated amide I' in deuterated peptides and proteins) region (1620-1700 cm^{-1}) which arise primarily from stretching vibrations of the backbone C=O groups (Miyazawa & Blout, 1961) (Figure 2.2). The frequency of these vibrations has been shown to be sensitive to the molecular geometry and hydrogen bonding characteristics of the peptide backbone (Prestrelski et al., 1991a;Jackson & Mantsch, 1995). Specific secondary structure gives rise to bands that consistently appear in just a narrow portion of the amide I' region (Byler & Susi, 1986). However, for most polypeptides and proteins, the separation between these component bands is frequently less than their inherent bandwidths. Thus, one typically observes only a signal, undifferentiated composite amide I band which both is quite broad and often appears featureless (Prestrelski et al., 1991). Figure 2.3 shows a set of the original amide I band of α-lactalbumin at various temperature. What we can see from these spectra is the gradual shift of the amide I bands. Because these bandwidths are inherently large, increasing the instrumental resolution is no use in this case. Thus, mathematical methods termed resolution enhancement or band-narrowing techniques, including derivative spectroscopy (Susi & Byler, 1983) and Fourier self-deconvolution (Byler & Susi, 1986), have been applied to visualizing the individual amide I components in protein spectra.

2.3.1 Second Derivative

Calculation of spectral derivative is often used to aid in the visualization of overlapping absorption. Figure 2.4 shows the second derivative spectra at elevated temperatures. They are useful to discern the band position of highly overlapped spectra. The changes of the second derivative spectra do not have linear relation to the amplitude of the corresponding bands in the original spectra. So they are not able to provide quantitative information for us. However, the qualitative results can be drawn based on second derivative spectra. The alteration of the amplitude in second derivative spectra stands for the real change of the corresponding secondary structure component. However, derivation suffers from the fact that relative integrated intensities are not maintained. Furthermore, significant edge effects are possible in derivative spectra.(Moffatt & Mantsch, 1992). Moreover, if the spectrum has a significant slope at the edges of the region to be subjected to derivation, distortions will be introduced at the edges of the derivative spectrum. This is easily avoided by choosing a wider spectral region than is desired for analysis and ignoring any feature at edges of this extended region (Jackson & Mantsch, 1995). In this thesis, all the bands are processed through both derivative and Fourier self-deconvolution (FSD) method. Only those bands appearing in both spectra are assigned in order to avoid artifacts due to data processing.

2.3.2 Fourier Self-deconvolution

Another widely used mathematical methods for resolution enhancement is Fourier self-deconvolution (Kauppinen et al., 1981). Any

IR absorption can be considered to arise from the convolution of a delta function that has position but no width and a Lorenzian that has width but no position to produce a Lorenzian with both position and width. In the Fourier domain, this is expressed as the multiplication of the Fourier transform of the delta function (a cosine) with the Fourier transform of the Lorenzian (a decaying exponential, the rate of decay of which is determined by the width of the Lorenzian) to produce an exponentially decaying cosine. The wider the Lorenzian, the more rapid the rate of decay. In theory, therefore, it is possible to reduce the IR bands to delta functions that have no width but maintain their frequency characteristics by deconvolving the correct Lorenzian from the absorption profile. This is achieved by multiplying the Fourier transform of the absorption band (our exponentially decaying cosine) by the correct increasing exponential to regenerate the corresponding cosine. The inverse Fourier transform than give the delta function. The general case (Kauppinen et al., 1981) of the relationships between a spectrum $E(\gamma)$in the wavenumber domain, and its interferogram I(x) are given by

$$E(\gamma) = \int I(x)\exp(i2\pi\gamma x)dx = \xi\{I(x)\} \qquad (2.1)$$

And

$$I(x) = \int E(\gamma)\exp(-i2\pi\gamma x)d\gamma = \xi^{-1}\{E(\gamma)\} \qquad (2.2)$$

where $\xi\{\}$ is the Fourier transform, $\xi^{-1}\{\}$ is the inverse Fourier transform, and x has units of centimeters.

Any experimental spectrum, $E(\gamma)$, can be expressed as a convolution of a lineshape function, $G(\gamma)$, and a spectrum, $E'(\gamma)$, that is

$$E(\gamma) = G(\gamma) * E'(\gamma) = \int G(\gamma') E'(\gamma - \gamma')d\gamma' \qquad (2.3)$$

where * indicates the convolution operation.

In order to deconvolute $G(\gamma)$ from $E(\gamma)$ we take the inverse Fourier transform of both sides of Eq.(2.3), giving

$$I(x) = \xi^{-1} \{G(\gamma)\} \bullet I'(x) \qquad (2.4)$$

and the interferogram corresponding to the deconvoluted spectrum is given by

$$I'(x) = [\ 1/\xi^{-1}\{G(\gamma)\}] \bullet I(x) \qquad (2.5)$$

That is, the deconvolution operation in Fourier transform space requires a particular form of apodization of the interferogram. $E'(\gamma)$ is then simply obtained by taking the Fourier transform of $I'(x)$.

In practice we never produce the delta function as we are usually dealing with many decaying cosines superimposed on each other, each of which is decaying at a different rate. Rather, what is attempted is to simply reduce the rate of decay of the underlying cosines by multiplication with an increasing exponential and so reduce the width of the corresponding absorption. However, the choice of the correct increasing exponential is

subjective. If the deconvolution parameters are chosen such that the rate of increase of the exponential corresponds to band width greater than the width of the absorption being studied, they will result in the sidelobes at the edges of the absorption bands. In this study, we carefully select the parameters by reference of other studies. The band width of the lineshape function ranges from 25 cm^{-1} to 30 cm^{-1}. Figure 2.5 shows the deconvolved spectra at elevated temperature. It should be noted that previous FTIR study of α-lactalbumin by Prestrelski used band width of 36 cm^{-1} to deconvolve the amide I spectra. Compared to this, the band width we used here are much smaller. The correspondence of the band positions as visualized by both FSD and second derivative spectra further ensures the correctness of these resolution enhancement methods.

Furthermore, the amide I band includes many subbands with different bandwidth and band shape. However, in the FSD process, every subband is treated as having same bandwidth and shape, resulting in a deformed deconvolved spectrum. As a consequence, any curve fitting methods based on deconvolved spectra which are used to quantitatively make comparison of various subbands are rootless and should be avoided.

In addition to the above caveats, it should be remembered that FSD and derivative methods also reduce the width of water vapor absorption and enhance noise, producing very sharp peaks with even minimal deconvolution. Noise and water vapor can quickly become a problem in resolution enhanced spectra if the spectra have low signal to noise ratio and/or high contribution from water vapor. For this reason, in this thesis all resolution enhancement were performed on the original

spectra with multiplying factor 1.0 which is able to keep water vapor contribution minimum, and 26 repetition of 32 scans are averaged for each of the two cells installed in the shuttle for all IR spectra to eliminate any possibly detectable deconvolution of noise.

2.3.3 Double Difference Spectra

Resolution enhancement methods enable us to discern the positions of the bands. However, they are hardly provide us with quantitative information about proteins during their heat denaturing processes such as transition curves. Double difference spectra (Figure 2.6) are based on the original spectra without any mathematical processing. Therefore, double difference spectra can be used for this purpose. However, due to strong overlap of the different structural bands, it is difficult to obtain specific structural transitions directly based on double difference spectra.

The other kind of difference spectra comes from the deconvoluted spectra. Since in FDS process all bands are deconvoluted by a single Lorenzian function with the same parameter (band width), and the intrinsic band width for various secondary structures are different, it is not suitable to investigate the relative amount of various structures quantitatively based on the deconvolved spectra. For this reason, comparison of different structure components based on curve fitting of deconvolved spectra is strongly discouraged. In fact, it is not clear whether all protein secondary structures give rise to the same band shape, or to what extent environmental effects are important in determining band shape. However, for quantitative derived from any single position which is

deformed to the same extent, the deformation introduced by mathematical process has little effect on the results. In these studies, we managed to obtain transition curves by FDS processed spectra. However, this application is strictly limited to the spectra of the apo and apo cam-3ss forms which have to be measured in AgCl windows because fringes inhibit us to make analysis by normal difference spectra. The difference deconvolved spectra at various temperature are plotted in figure 2.7.

2.3.4 Adjustment of Sample Leakage

Without the presence of the high vacuum oil, it has been demonstrated that sample leakage happens above 65 ^{o}C. The sealed cell as shown in figure 2.1 prevents the sample leakage effectively. However, we can not make sure there is no sample leakage at higher temperatures. Sometimes the sample leakage does exist in an unpredictable manner, especially at high temperature close to 100 ^{o}C. Even if the leakage at high temperature is prevented, it is possible to have thickness changes. In this extremely hot condition, the thickness of the sample film is determined not only by the fixed thickness of the spacer, but also by the thickness of the high vacuum oil. This oil tends to expand at high temperature, resulting in the change of thickness of the sample film. If only one of the film has this thickness change or leakage, we are able to reduce the corresponding spectra to those that have not the thickness change or leakage according to the reference spectra that do not have this change. If the sample leakage or thickness change happens at the buffer compartment, no special methodology should be used. However, if the leakage or thickness change happens at the sample compartment, the following procedure can be used to

generate the resultant spectra without the influence of the sample leakage or thickness change:

1. Subtract the protein spectra from the buffer spectra.
2. Adjust the subtraction coefficient until the baseline between 1750 and 2000 cm^{-1} become flat.
3. Reverse the spectra to be the positive spectra.

The worst thing that may happen is when the two films change their thickness at the same time.

2.4 Protein Structures and IR Bands

2.4.1 Region from 1400 - 1600 cm^{-1}

This region contains the amide II' band, the HOD bending mode, and side-chain contributions. It can be seen from figure 2.3 that a dominant band between 1400 cm^{-1} and 1500 cm^{-1} appear in the IR spectrum of protein. This band is formed by a strong overlap of amide II' band and HOD bending mode. In IR spectroscopy the extent of hydrogen-deuterium exchange can be monitored directly by checking the changes in the amide II band (1550 cm^{-1}). Upon exposure of a peptide to D_2O, this band is shifted to 1450 cm^{-1}. The amide II band is dominated by N-H bending vibration and isotopic substitution of the peptide bond N-H to N-D results in this large shift (100 cm^{-1}). However, as the result of strong overlap, this composite band has little use to provide information of protein structures because the HOD bending mode and their amplitudes have similar value. The band around 1516 cm^{-1} is present in all spectra and is assigned to tyrosine side-chain. This band is found to be little changed with

temperature. Another band near 1580 cm^{-1} (figure 2.4 & 2.5) arises from the carboxylate group (Chirgadze et al., 1975; Venyaminov & Kalnin, 1990). This might also be explained by the contributions from two amino acids, glutamic acid and asparic acid, as well as by minor absorption bands of side chains around 1600 cm^{-1} Indeed, several strong overlapping bands may have contributions to this region. In some case, the spectra show some bands around and above 1700 cm^{-1}. This may be due to COOD groups (Chirgadze et al., 1975; Casal et al., 1988). This band usually appears when protein solution is at low pH due to protonated carboxylate groups (Stokkum et al., 1995). The amide II vibrations of some unexchanged peptide groups can also contribute to this region.

2.4.2 1600 cm^{-1}- 1700 cm^{-1} Range

Some sidechain vibrations have some contributions to this region. However, the bands from these vibrations are usually limited to the region between 1600 cm^{-1} to 1620 cm^{-1}. The region between 1610 cm^{-1} and 1700 cm^{-1} contains mainly contributions of the amide I' band. It is formed by a complex vibration mode which is dominated by the peptide group C=O stretch with minor contribution from the C-N stretching vibration (Figure 2.2). This band is quite sensitive to protein secondary structure (Susi & Byler, 1986; Jackson & Mantsch, 1995)

The dihedral angles of polypeptide chain determine the chain geometry, which dictate the length and direction of hydrogen bonds involving amide C=O and N-H group. Variation in length and direction of hydrogen bonds result in the strength of the hydrogen bond for different

secondary structures, which in turn produces characteristic amide I frequencies. The stronger the hydrogen bond involving the amide C=O, the lower the electron density in the C=O group and the lower the amide I absorption appears. By this theory, one can predict the lowest amide I frequency to occur for extended polypeptide chains. In such extended chains, intramolecular hydrogen bonding is not possible. However, the extended nature of the chains allow very close alignment of neighboring chains, which favors the formation of extremely strong intermolecular hydrogen bonding. The formation of these very strong hydrogen bonds would be expected to produce a correspondingly low amide I maximum. If the dihedral angles are changed such that the formation of intramolecular hydrogen bonds is possible with the polypeptide chains still in an extended state, the classic antiparallel β-sheet is formed. Steric constraints in this intramolecular interaction mean that the strength of the intramolecular hydrogen bonds stabilizing the β-sheet are not so strong as the intermolecular hydrogen bonds stabilizing the extended aggregate, and the amide I frequency is expected to increase. For α-helix, the C=O group of residue n is positioned so as to be able to form a linear hydrogen bond with the N-H group of residue n+4. The length of the hydrogen bond formed in the α-helix will be slightly longer than that in an antiparallel β-sheet, and the resulting amide I' frequency will be further increased. Actually, the backbone of the linear polypeptide chain consists of a repeated sequence of three atoms of each residue in the chain the amide N, the C^{α} and the carbonyl C (2.6).

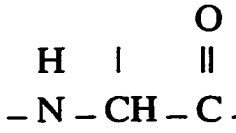

(2.6)

In principle, rotation could occur about any of the three bonds of each residue of polypeptide backbone, but peptide bond appears to have partial double-bonded character due to its resonance structure equation (2.7).

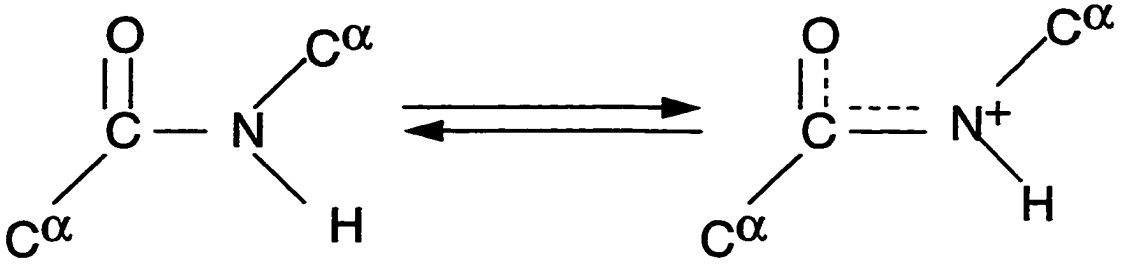

(2.7)

The peptide bonds appears to have approximately 40 percent double-bonded character. Consequently, rotation of this bond is restricted, and six atoms depicted in equation 2.7 have strong tendency to be coplanar. Any rotation exerted on the partial double bonds, which is the case in the protein when secondary structures are formed, may push electron out of the C-N partial double bond to the carbonyl bond. As a result, higher electron density in the C=O double bond will be resulted. It follows that there will have higher amide I frequency for those portions of polypeptide backbone which undergo torsion to a higher degree. Obviously, intermolecular β-sheet has less backbone torsion so has the lowest frequency of amide I. Intramolecular β-structure also undergoes little torsion except for the components connecting the strands, so intramolecular β-structure gives rise to higher frequency than that of intermolecular β-structure. Helical structures receive even more strain on their polypeptide backbone than that of β-structures, so have higher amide I frequency than those of extended structures. Other factors, such as the hydrogen bonding formed between

C=O group and water molecules, also have influence on the band positions of amide I. Since various secondary structures have different but unique conformation, they will give different amide I bands. FT-IR study of conformation of proteins and polypeptides has received much attention over the past decade (Surewicz et al., 1993).

Many empirical conclusions have been obtained by comparing the amide I band with their X-ray structures (Surewicz et al., 1993; Haris et al., 1995; Jackson & Mantsch, 1995). These studies show that β-structure usually exhibits bands at low frequency, ranging from 1620 to 1637 cm^{-1} in D_2O, and aggregation stuff demonstrates the bands between 1610 to 1620 cm^{-1} in the same solvent. The bands between 1650 and 1660 cm^{-1} are attributable to the α-helices. Turn structures usually show amide I bands at high frequencies above 1660 cm^{-1} It is revealed that random structures usually show bands between 1640 to 1650 cm^{-1} in D_2O. Although much effort has been made to assign the amide I bands to various secondary structure components, it is still not completely clear exactly which bands correspond to which component. Some times the same amide I bands may correspond to different secondary structure component. for example, it was found some helical structure show band at low frequency between 1630 and 1640 cm^{-1} which overlap with the bands assigned to the extended conformation. Consequently, there is no reliable assignment of amide I bands to secondary structures at present. The band assignment should be considered case by case, depending upon the protein studied, solvent environment, temperature and whether the protein is denatured.

2.5 Band Assignment of Native α-lactalbumin

Five bands, 1629 cm^{-1}, 1638 cm^{-1}, 1653 cm^{-1}, 1663 cm^{-1} and 1675 cm^{-1} are always associated with the native state (Figure 2.4 & 2.5). Among these, the shoulder around 1629 cm^{-1} is widely regarded as the contribution of β-sheet, and the peak around 1653 cm^{-1} comes from α-helices in hydrophobic environment. The band at 1638 cm^{-1} was assigned to be 3_{10} helix by Perstrelskl (Prestrelski et al., 1991b). Indeed, it is proposed that the 3_{10} helices in other proteins also give rise to the band at 1638 cm^{-1} (Martinez & Millhauser, 1995; Holzbaur et al., 1996). α-helices may also show a band at same position due to special water carbonyl interaction. It is thought that in the native protein a helical structure on the surface of protein faces two environments. One side of helix closely contacts with the water molecules while the other side is buried inside protein and faces hydrophobic environment. The side of helix in hydrophobic environment gives rise to the usual bands from 1650 to 1660 cm^{-1} which is the marker band of α-helix. On the other hand, the hydrogen bonding formed between water molecule and backbone carbonyl on the opposite face draws electron out of the C=O double bond, consequently decreases the bond order and shifts down the amide I frequency. Therefore, both 3_{10} helix and solvated α-helix may contribute to the band at 1638 cm^{-1}. As a result, we assign this band to the helical structure rather than 3_{10} helix or solvated helix. Turn structures usually show additional bands at high frequency which may be 1663 cm^{-1} and 1675 cm^{-1} in this case. It should be noted that the band at 1675 cm^{-1} may also come from high frequency of β-structures which arise as byproduct of low frequency of β-structures (Holzbaur et al., 1996).

The band around 1618 cm^{-1} is most likely caused by side chain vibration. It always appears in the native form of LA but disappears when protein is denatured. This suggests that this band is only associated with the side chain vibration in the environment of folded protein. Although intermolecular β-sheet aggregation band is also located in this region, the band of aggregation should be strong and sharp and has a weak band around 1684 cm^{-1} also (Holzbaur et al., 1996).

Although accurate and reliable band assignment can not be realized completely, we can at least pinpoint some bands as the markers of some kinds of structures or domains. For the IR spectrum of native α-lactalbumin, the band at 1629 cm^{-1} represent the structure of β-sheet, the band located at 1638 cm^{-1} come from helical structure, and the band at 1653 cm^{-1} is the marker band of dry helix. The alteration of the amplitude of the band at 1629 cm^{-1} reflects the behavior of β-sheet domain, while the changes of 1638 cm^{-1} and 1653 cm^{-1} exhibit the behavior of helical domain. So, it is feasible to study the thermal denaturation behaviors of β-sheet domain and helical domain separately by monitoring the changes of their marker bands.

2.6 Band Assignment for Unfolded α-lactalbumin

At temperature high enough, each form of α-lactalbumin is denatured. All denatured structures at high temperature show two bands. One of them is between 1645 cm^{-1} and 1649 cm^{-1} (figure 2.4 &2.5) which is widely thought to be a marker band of random structure of native protein in D_2O. Therefore, the band at this region indicates that random structure

dominates in this high temperature denatured protein However, we can not eliminate the possibility that some regular structures exist in the heat denatured protein. Actually, it is reported that for a small number of proteins known to be largely α-helical the major amide I component is shifted to wavenumbers somewhat below 1650 cm^{-1} (Trewhella et al., 1989; Jackson et al., 1991). Moreover, the secondary structures of α-lactalbumin at high temperature have been found to contain a lot of helical structure as judged by CD (Dolgikh et al., 1985). Therefore, it is possible that some solvated helical structure at high temperature also gives contribution to this band. As the consequence, the band from 1645 to 1650 cm^{-1} is contribution from disordered structure plus a minor contribution from solvated helix. The band at 1675 cm^{-1} in heat denatured form is assigned to be the marker band of turn structures.

As temperature increases, the band at 1618 cm^{-1} shown in the spectrum of each form of native LA decrease while the band at 1612 cm^{-1} become stronger and stronger. We assume the new band at 1612 cm^{-1}, which has been assigned to be the vibration of tyrosin sidechain, represents the same structure component with marker band at 1618 cm^{-1} in native protein. It is most likely that the downshift of this band is caused by different environment to which the side chain is exposed after the protein is denatured. One explanation is that this involves H-D exchange happened after the hydrophobic cluster region collapse which gives well protection from H-D exchange in the environment of native protein.

Figure Legends

Figure 2.1 The cell used in the FT-IR measurement. The high vacuum grease is applied to the surface of the spacer to prevent the sample or buffer from leakage.

Figure 2.2 The normal mode designed as the amide I mode of the peptide linkage.

Figure 2.3 The original spectra of the holo form of α-lactalbumin at low and high temperature.

Figure 2.4 The second derivative spectra of the holo form of α-lactalbumin at different temperatures.

Figure 2.5 The deconvolved spectra of the holo form of α-lactalbumin at various temperatures.

Figure 2.6 Double difference spectra of the holo form of α-lactalbumin. The spectra are used to generate transition curve quantitatively.

Figure 2.7 The deconvolved double difference spectra of the holo form of α-lactalbumin at different temperatures. The spectra are generated by subtracting the deconvolved spectra from that at 5.2 °C.

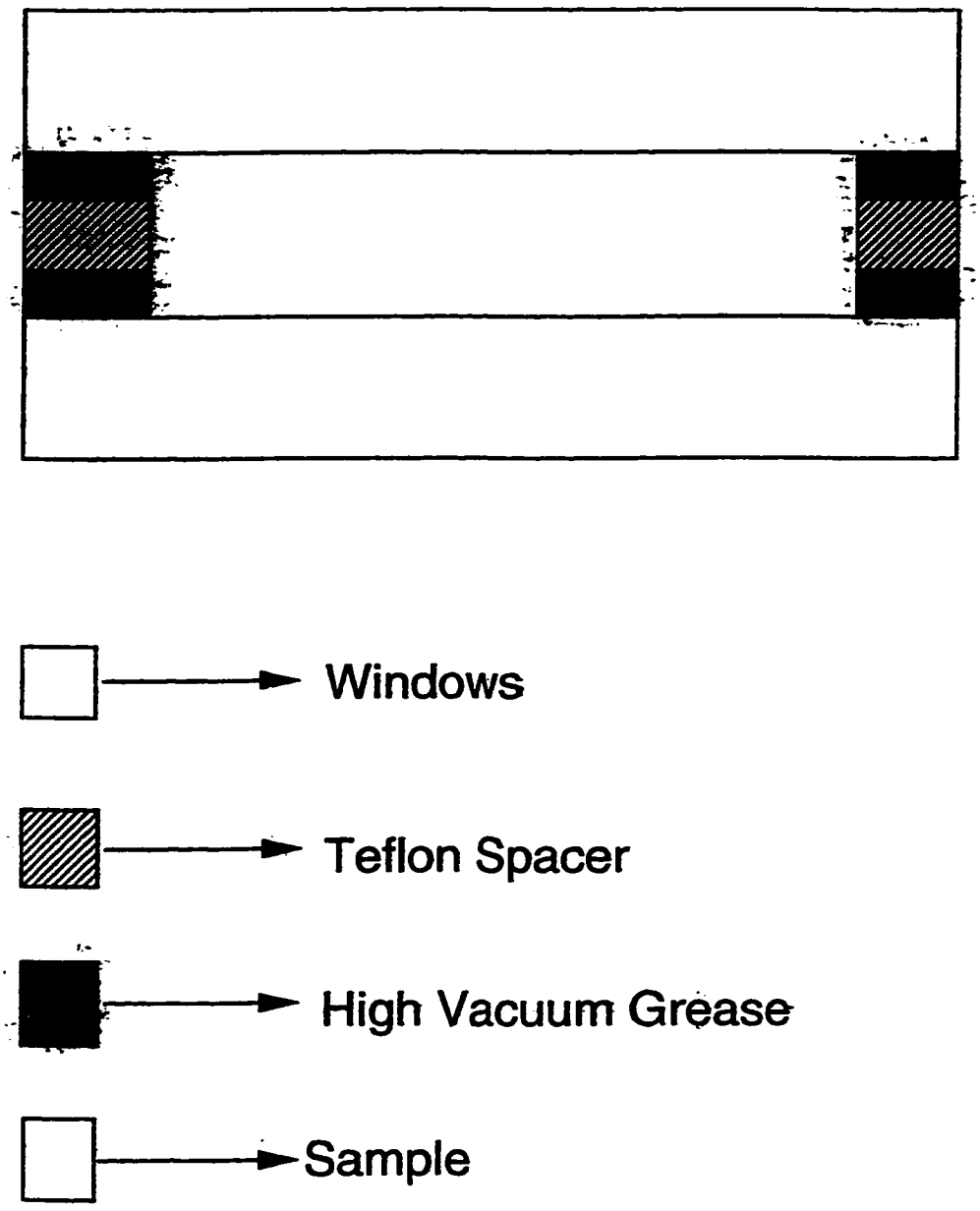

Figure 2.1

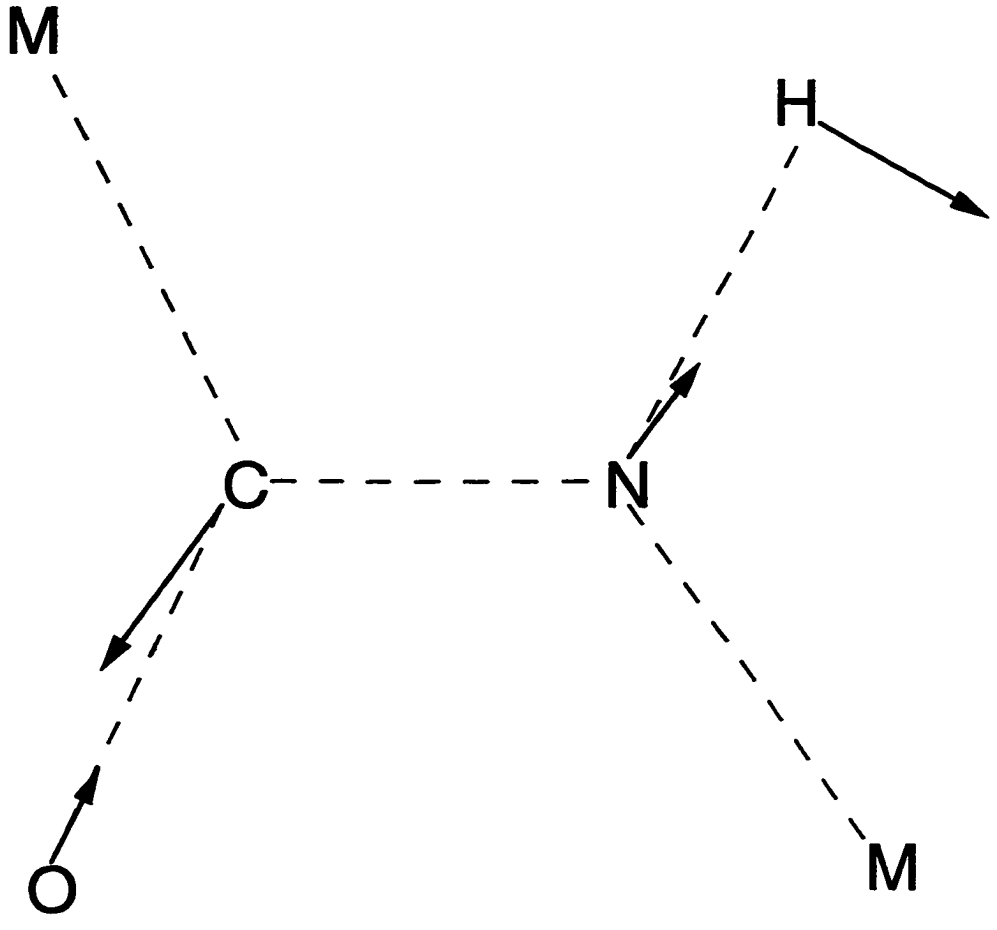

Figure 2.2

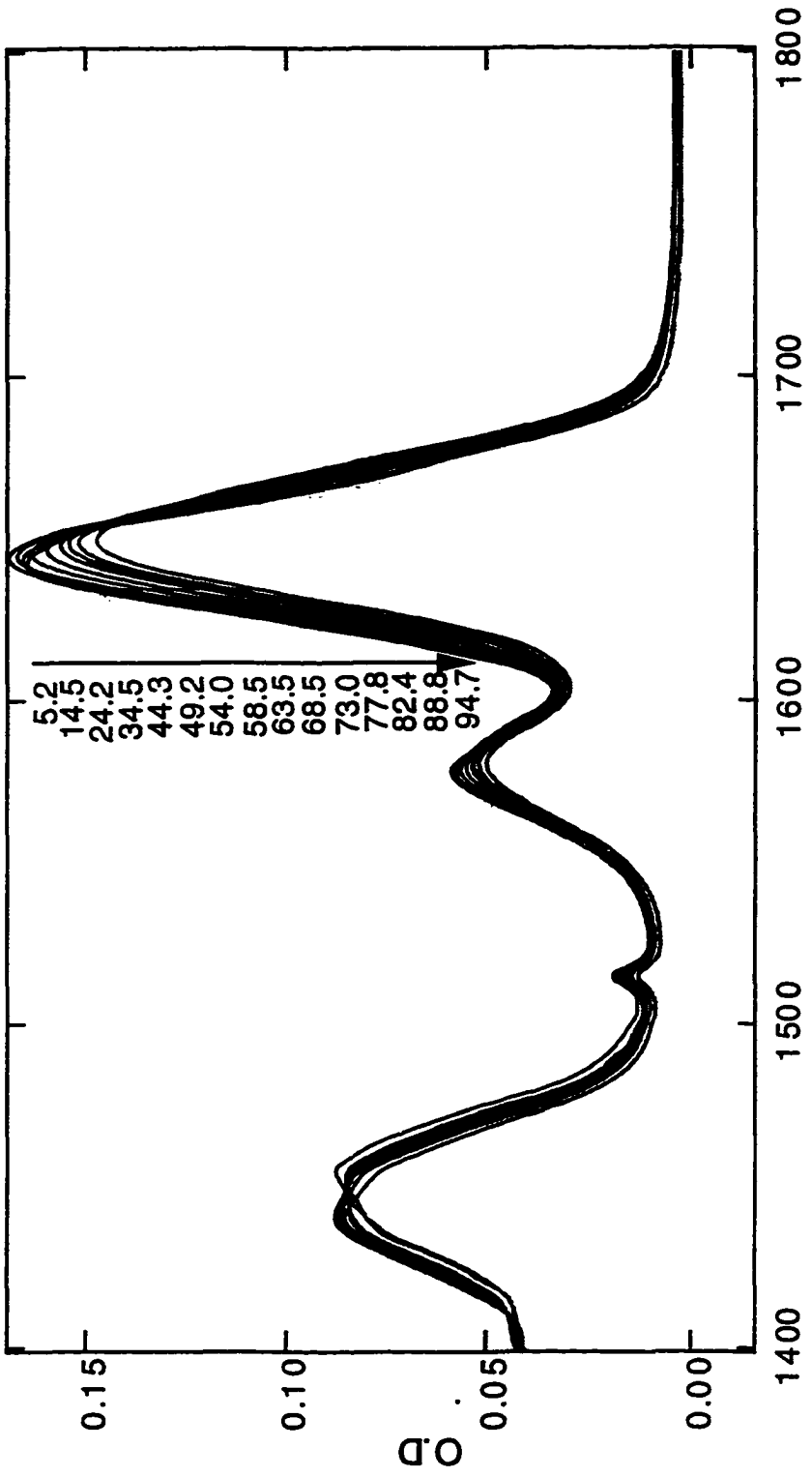

Figure 2.3

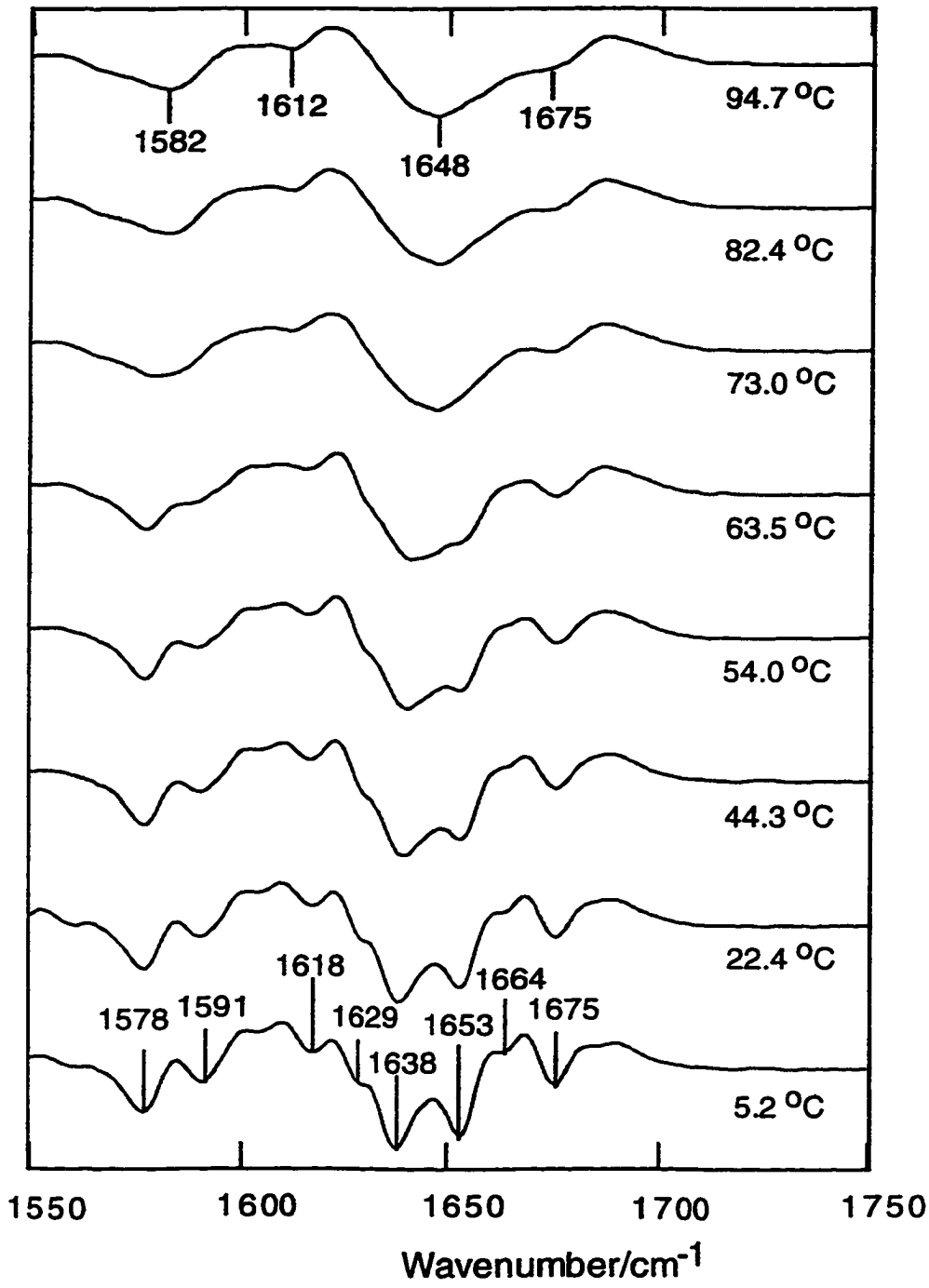

Figure 2.4

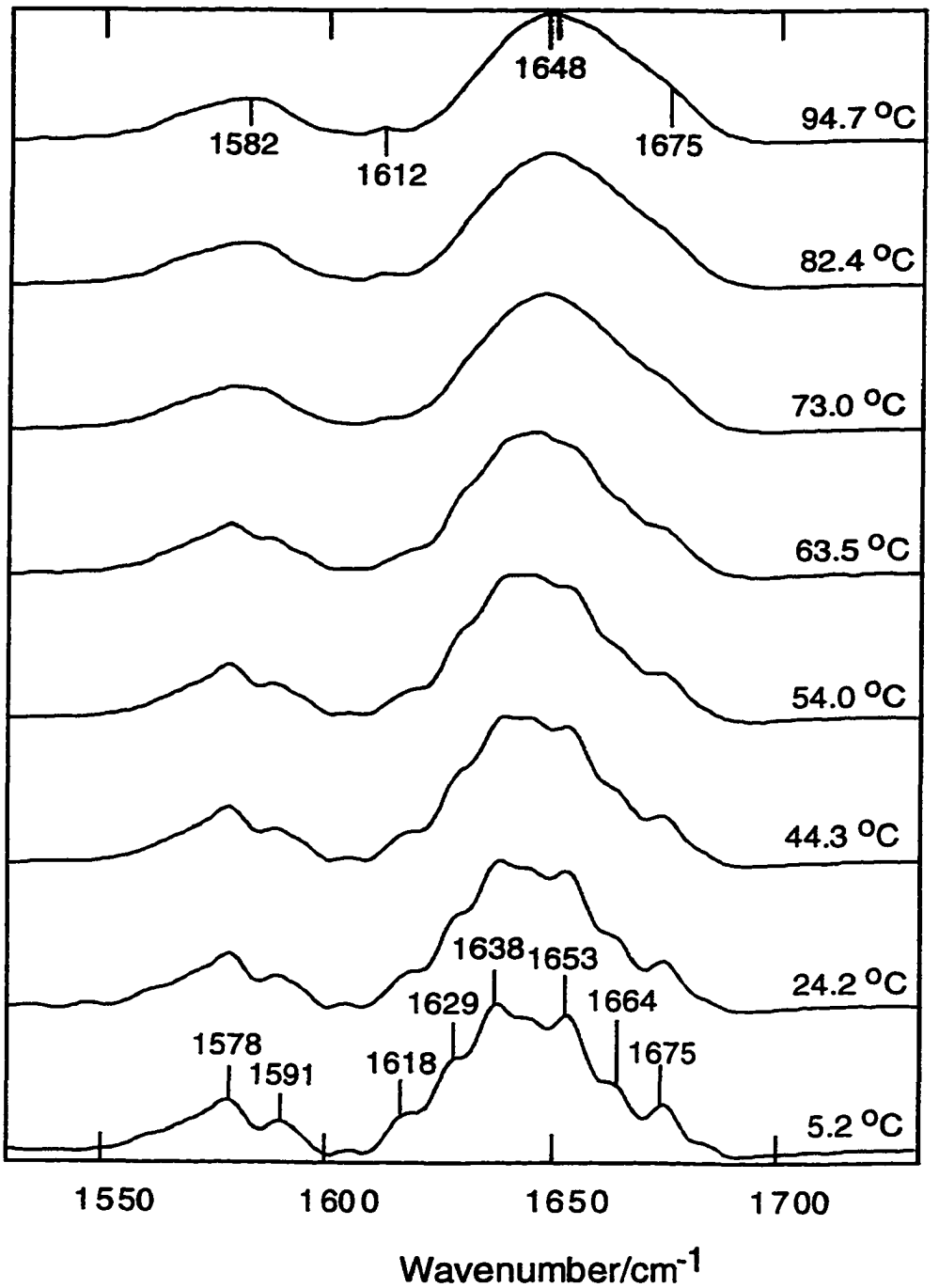

Figure 2.5

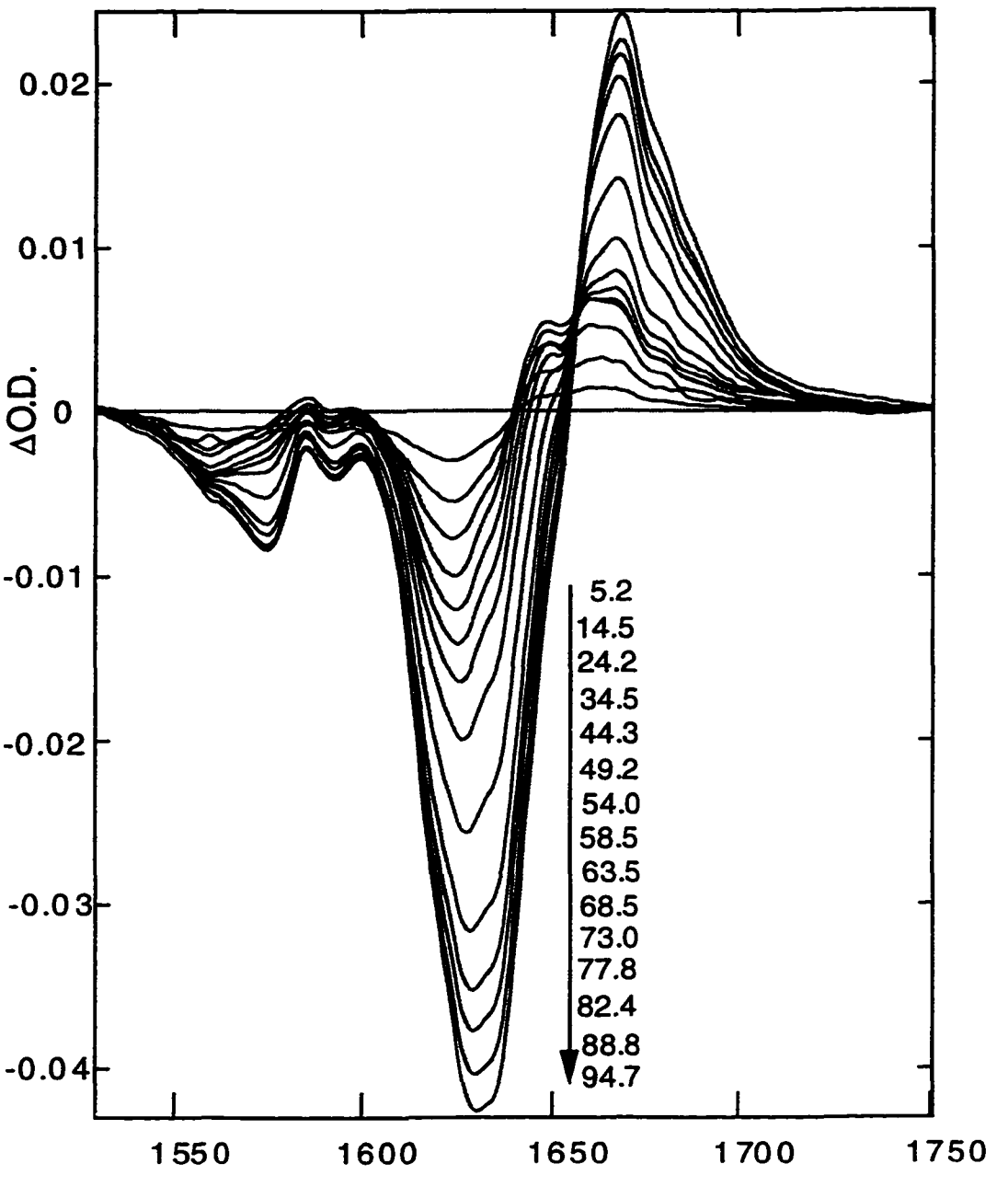

Figure 2.6

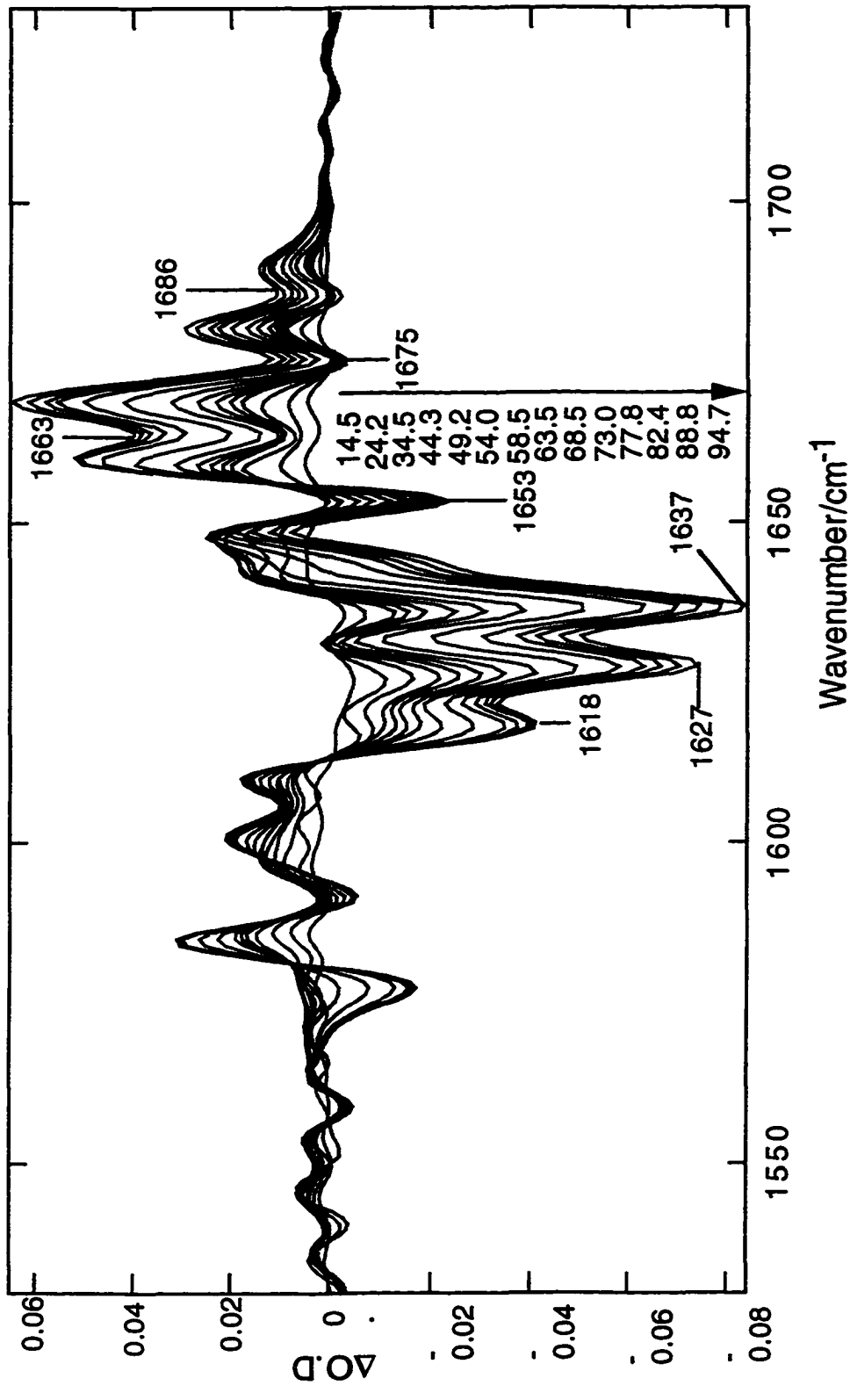

Figure 2.7

Chapter 3 An FTIR Study of the Complex Melting Behavior of α-Lactalbumin

3.1 Abstract

We have studied the thermal denaturation of holo α-lactalbumin (α-LA) using FTIR spectroscopy by monitoring the absorbance of protein bands in the secondary structure sensitive amide I region. In agreement with results obtained by other techniques, a major cooperative melting transition is observed between 60 and 80 °C. This main transition is found to involve predominantly the unfolding of helical structures. Addition of excess Ca^{2+} ions raises the T_m of the cooperative melting transition but does not change the protein substructures involved in the transition. In addition to the main transition, there are at least two other distinct melting processes. One of them is gradual, independent of excess Ca^{2+}, and occurs throughout the measured temperature range below the major cooperative transition. This melting process involves denaturation of α-LA's β-hairpin. The other melting process is affected by the addition of excess Ca^{2+} and involves the denaturation of helical structures. In absence of excess calcium, this transition, occurring between 45 to 60 °C, strongly overlaps with the major cooperative melting. Our results indicate that the β-hairpin of α-LA is not directly stabilized by the bound calcium ion present in the holo protein and melts independently from the rest of the protein.

3.2 Introduction

α-Lactalbumin (α-LA) is a small globular protein containing 123 residues that consists of two domains connected by a small bridge section (Acharya et al., 1989; Acharya et al., 1991). The α-domain is made up of only helical structures (both α- and 3_{10}-helices). The β-domain includes a double-stranded β-hairpin and some helical structure (Hendrix et al., 1996; Wu et al., 1996). The structure of α-LA is stabilized by four disulfide cross-links. Two of them are in the α-domain, one is in the β-domain, and one is a part of the interdomain bridge. A distinctive feature of the β-domain is a Ca^{2+} binding site which plays an important structural role (Kuwajima et al., 1986; Stuart et al., 1986). In absence of intrinsic bound Ca^{2+} ion (the apo protein), the protein is destabilized and melts at a much lower temperature (the temperature decrease is 20-40 °C, depending upon salt and its concentration) than holo α-LA (Kuwajima et al., 1986; Griko et al., 1994). Holo α-LA can exist in three forms in equilibrium: in native, in unfolded, and in the form which properties are somewhat intermediate with respect to the other two (see Kuwajima, 1989 and Ptitsyn, 1992 for references). The last form has been named a molten globule. The balance of these three forms depends upon conditions: buffer salt and its concentration, abundance of calcium, pH, temperature, and denaturant concentration. The molten globule is believed to resemble an intermediate on the protein folding pathway (Kuwajima, 1989; Ptitsyn, 1992; Kim & Baldwin, 1990; Christensen & Pain, 1991; Arai & Kuwajima, 1996).

Because of these features, α-LA has been widely researched with regards to protein structure and thermodynamics and in protein folding studies (Kuwajima, 1989; Ptitsyn, 1992). Whilst in earlier denaturation work holo α-LA was treated as a whole, recent research on protein with

partially reduced disulfides and its mutants lacking some of disulfides have shown that the α- and β-domains can fold independently under some conditions (Acharya et al., 1989; Acharya et al., 1991). The domains behave differently even on the level of a molten globule. Thus, in the acid destabilized form of α-LA, the α-domain remains in a native-like topology while the β-domain is largely unstructured (Wu et al., 1995). However, under native conditions, the behavior of unmodified protein appears to undergo a highly cooperative denaturation process as shown by equilibrium (Griko et al., 1994; Privalov, 1996) and kinetic (Balbach et al., 1995) folding studies. To investigate the controversy between the structural independence of domains and cooperative behavior of protein molecule as a whole, folding studies are needed probing selectively the substructures of the protein. When such a study was carried out by means of NMR for apo α-LA, the results suggested that the β-hairpin appears earlier than the rest of the protein structure (Balbach et al., 1996).

A number of studies have investigated the thermal unfolding/folding of holo α-LA (Kuwajima et al., 1986; Griko et al., 1994; Dolgikh et al., 1985; Permyakov et al., 1985; Vanderheeren et al., 1994; Vanderheeren et al., 1996). As judged by calorimetry, CD, and NMR spectroscopy, holo a-LA undergoes a cooperative transition with a T_m of around 65 °C. The presence of excess Ca^{2+} stabilizes the holo protein and shifts the transition 10 °C to higher temperatures (Kuwajima et al., 1986; Vanderheeren et al., 1996). The detailed study of the temperature-denatured state had proved that it is compact, rich with secondary structure, and similar to the other intermediate states of holo α-LA (Dolgikh et al., 1985; Dolgikh et al.,

1981). The extensive study of temperature-induced denaturation of holo α-LA has shown a complexity of melting which includes several transitions (Vanderheeren et al., 1994). Previous interpretation of this complex melting has assumed a coexistence of the three forms of holo α-LA in the transition region: holo-native, holo-melted, and apo-melted forms (Vanderheeren et al., 1996). However, there is very limited information on the specific structural nature of the various forms.

In this paper, we report a thermal denaturation study of intact α-lactalbumin by FTIR spectroscopy. Vibrational spectroscopy can monitor separately substructures within the intact protein and also be sensitive to fast interchanging forms. It has been shown that helices, β-structure, and disordered backbone could be determined separately from the IR absorbance spectrum of α-LA in amide I region (Prestrelski et al., 1991). Therefore, IR spectroscopy can report the separate melting behavior of these elements of secondary structure. In agreement with previous studies, it is found that holo α-LA undergoes a major cooperative transition between 60 and 80 °C with T_m depending on calcium concentration. Besides this main transition, however, there are at least two other melting processes. One of them is a gradual process, independent of excess Ca^{2+}, and which occurs throughout the low temperatures prior to the major cooperative melting and includes mostly the denaturation of β-hairpin structure. Hence, our results indicate that the sole β-hairpin of holo α-LA melts independently from the rest of the protein. The second minor melting process depends upon the concentration of extrinsic calcium and involves the helical structures of holo α-LA. When no excess calcium is added, the process strongly overlaps with

the major cooperative melting. A previous FTIR thermal melting study of α-LA has been performed (Stokkum et al., 1995); however, the protein aggregated at high temperatures. The results presented here are free of aggregation products even at the highest temperatures, presumably because of the lower concentrations used in our study.

3.3 Materials and Methods

Bovine α-lactalbumin (Type I) was purchased from Sigma (St. Louis, MO) and was further purified with gel filtration on Sephadex G-75 in 0.1 M Tris buffer, pH 8.1 at 5 °C. Then, it was dialyzed against deionized water, lyophilized and stored at -80 °C. The sample thus obtained was homogeneous on polyacrylamide gel electrophoresis in the presence of SDS. This procedure does not remove the calcium ion that is normally bound to the Sigma protein. Hence, all measurements reported herein are on the holo protein. Protein concentration was determined by optical absorbance at 280 nm using an extinction coefficient of $E_{1\%}$= 20.9 cm^{-1}. α-LA concentrations of 8-10 mg/ml were used for IR measurements. The reported pH* values are uncorrected pH-meter readings at room temperature. All other chemicals were purchased from Sigma and were of the highest available purity.

The sample solutions were made in D_2O with 4 mM sodium cacodylate buffer (pH* 6.8) containing 10 mM KCl. pH* was adjusted by DCl and NaOD. To facilitate H-D exchange, the protein sample was incubated in D_2O at 55 °C for two hours. Prior to the IR measurements, the protein

solutions were equilibrated with the reference solvent on a Sephadex G-25 column. Both protein and buffer samples were collected from the same elution to ensure balanced HDO in both the reference and protein solutions. The sample aliquots after the column were used to control its pH* and concentration.

At the high concentrations required for the IR study, it is important to insure that the observed transitions are both reversible and that the samples are free from aggregation products. Reversibility was verified by determining the melting curve as a function of increasing temperature, holding a high temperature for a fixed period, and then performing a rescan of the melting curve toward lower temperatures. Only data from runs verified to be reversible are presented herein. IR absorption in the amide I' (the prime denotes deuterated peptide linkage) is quite sensitive to the formation of aggregates with marker bands at 1623 (strong) and 1680 (weak) cm^{-1} typical of intermolecular β-structure showing up. It was found that prolonged exposure of the holo α-LA to a high temperature (above 80 and 70 °C in the absence and the presence of 10 mM $CaCl_2$ respectively) resulted in irreversible denaturation (see also Kuwajima et al., 1986). The appearance of the irreversible fraction correlated with the characteristic bands at 1623 (strong) and 1680 (weak) cm^{-1} Only the spectra free of the aggregation features were used for the analysis.

IR absorbance spectra were measured by an IFS-66 Fourier-transform spectrometer (Bruker Instruments, Inc., Billerica, MA) using an MCT detector. Both reference and sample solutions were simultaneously loaded

into a thermostated dual cell shuttle accessory. CaF_2 sandwich cells with 56 μm Teflon spacers were used. To prevent sample leakage at high temperature, thin smears of inert silicon grease on the spacer were used. No influence of the grease on data was found at least below 65 °C where control measurements in the absence of the grease were possible. A two-position sample shuttle was used to alternate between the sample and buffer positions; this procedure substantially decrease the spectral contribution of residual water vapor after subtraction. 26 repetitions of 32 scans were averaged for the each of the two cells. Spectra were collected with 2 cm^{-1} resolution, and a Blackman-Harris 3-term apodization was applied. Temperature, determined by a BAT-12 thermometer with a type IT-18 thermocouple microprobe attached directly to the cell surface (Physitemp Instruments, Inc., Clifton, NJ), was controlled with a Model 1167 bath circulator (VWR Scientific, S. Plainfield, NJ).

OPUS 2.0 (Bruker Instruments, Inc.) and Grams/386 (Galactic Industries Corp., Salem, NH) software was used for data collection and analysis. Solvent background spectrum was subtracted from each protein solution spectrum. As the sample and reference cells were assembled separately, their pathlengths were not completely equal (the difference was within 5%). To correct for this, the solvent spectrum was multiplied by a correction factor determined by requiring a baseline flat between 1750 cm^{-1} and 2000 cm^{-1} and by an accurate subtraction of D_2O absorption bands at 3840 cm^{-1} of solution and reference spectra (Venyaminov et al., 1996). No correction was introduced in solvent subtraction for the spectra intended for

deconvolution and derivation to keep the residual water vapor background minimal.

The positions of band components in the amide I' region were determined by using both the second-derivatives and deconvolved spectra. The second derivative spectra were calculated using the Savitzky-Golay algorithm (with 4th order polynome on 19 data point window which corresponds approximately to FWHH=20 cm^{-1} for our data sets). Deconvolution, based on the method of Griffiths and Pariente (Griffiths & Pariente, 1986), was performed between 1530 and 1730 cm^{-1} with FWHH=25 cm^{-1} A linear baseline was subtracted prior to deconvolution to ensure zero absorption at the ends of the spectral interval.

3.4 Results

Infrared absorbance spectra of holo α-LA at several temperatures are presented in the Figure 1a. The region between 1610 and 1700 cm^{-1} contains mainly contributions of the amide I' band. It is formed by a complex vibrational mode which is dominated by the peptide group C=O stretch (about 80%) with a minor contribution from the C-N stretching vibration. This band is sensitive to protein secondary structure (Susi & Byler, 1986; Jackson & Mantsch, 1995). The absorbance between 1540-1620 cm^{-1} is due to side chain vibrations of aromatic groups as well as the asymmetric stretching mode of COO^- groups (Susi & Byler, 1986). The amide II vibrations of some unexchanged peptide groups can also contribute

to this region. The intrinsic bandwidths of the amide I' band components are often greater than a separation between neighboring bands. In this case, resolution enhancement techniques, such as derivation and deconvolution, have been shown to be useful in making assignments (Arrondo et al., 1993). The second derivatives and deconvolved spectra are presented in Figures 1b and 1c, respectively, and components at 1617, 1629, 1638, 1645, 1654, 1664, 1676, and 1686 cm^{-1} are clearly observed.

The measured spectra of native holo α-LA below 45 °C are similar to earlier studies (Prestrelski et al., 1991; Prestrelski et al., 1991) except for differences between 1645 and 1668 cm^{-1} Although the samples of the previous studies contained excess calcium ions, this is not the source of the discrepancy because the IR absorbance spectra of native holo α-LA contain the same components (although with different relative intensities) in the absence of extrinsic Ca^{2+} and in presence of 10 mM of $CaCl_2$ (compare the low temperature spectra in Figures 1 and 2). We believe that the small differences between the current study and previous results are due to incomplete deuterium exchange in the previous work. This is consistent with the observation of time dependent IR changes in those studies (Prestrelski et al., 1991; Prestrelski et al., 1991). In our case, deutero-exchange at an elevated temperature was performed before the addition of excess Ca^{2+} to the protein solution. However, in (Prestrelski et al., 1991; Prestrelski et al., 1991) the lyophilized protein was directly dissolved in the Ca^{2+}-containing buffer which stabilizes the protein and decelerates an H-D exchange.

According to previous assignments between band position and secondary structure (Prestrelski et al., 1991; Prestrelski et al., 1991), the bands at 1638 and 1654 cm^{-1} correspond to 3_{10}- and α-helices respectively, the 1629 and 1675 cm^{-1} bands to the low and high frequency components of β-sheet structure, the 1668, 1675, and 1686 cm^{-1} peaks to unfolded structures, and the component at 1645 cm^{-1} to the disordered part of the polypeptide backbone. It is also possible that part of the intensity of the 1638 cm^{-1} band is due to α-helical structure exposed to solvent since it is known that a band at 1635-1645 cm^{-1} is observed for model polypeptide α-helices and in destabilized α-helical proteins (see Chirgadze et al., 1974 and references therein). However, the spectrum of these so-called "solvated" helices is generally characterized by a rather wide band, and they exhibit very gradual melting dependence with low cooperativity (Martinez et al., 1995). In the case of holo α-LA, neither second derivative nor deconvolved spectra show any difference between the widths of 1638 and 1654 cm^{-1} bands, and, moreover, the major change in cooperative melting (see below) is found to come from the 1638 cm^{-1} component. Therefore, most, if not all, of the intensity from the 1638 cm^{-1} component arises from 3_{10}-helix in α-LA.

The amide I' band of the α-LA at 78 °C (Figure 3.1) is essentially featureless, even after deconvolution, and is dominated by a wide band centered near 1648 cm^{-1}. Only a small band near 1674 cm^{-1} is otherwise evident in the second derivative and deconvolved spectra. Similar wide spectra with maximum at 1642-1650 cm^{-1} and a shoulder at higher frequencies were found for several proteins that have been temperature

denatured (see Fabian & Mantsch, 1995 and references therein) and disordered polypeptides (Martinez & Millhauser, 1995). Such a spectrum does not mean that the temperature denatured protein is structureless because fluctuating elements of secondary structure may result into wide components which cannot be detected with derivation or deconvolution. For example, considerable helicity and a small but tightly packed 'core' of residues was detected by means of enhanced equilibrium and kinetics studies of the acid apoMb-E form of apomyoglobin, and this form has very similar IR absorbance spectrum to the high temperature spectrum of holo α-LA (R. Gilmanshin, R. H. Callender, R. B. Dyer, in preparation). Therefore, although the comparison of the spectra measured at different temperatures (Figure 1) shows that the decrease of intensity of the secondary structure components is accompanied by a concomitant intensity increase of the disordered structure bands, we believe it cannot be concluded that there is no secondary structure in the melted form of holo α-LA as previously suggested (Dolgikh et al., 1985; Dolgikh et al., 1981).

The temperature dependencies of IR absorbance at different wavenumbers for holo α-LA are presented on the Figure 3.3 without (3.3a) and with (3.3b) excess calcium. The wavenumbers corresponding to the minima of the second derivative were chosen because the changes in composition of the corresponding secondary structure components are dominant at these frequencies. The major sigmoidal transition of holo α-LA in Fig. 3.3a is obvious between 60 and 80 °C with T_M near 66-69 °C. A more accurate determination of the T_m is complicated by non-linear changes starting before but overlapping the sigmoidal transition. A similar

but slightly lower value of the T_m (62-67 °C) has been reported previously (Kuwajima et al., 1986; Griko et al., 1994; Dolgikh et al., 1985; Vanderheeren et al., 1996). This apparent increase of the melting temperature is not due to some excess calcium that is present in the solution because of solubility of the IR cell CaF_2 windows since the solubility of CaF_2 is very low (<0.2 mM). The difference in T_m is almost certainly from a stabilization of the native form in the presence of the D_2O environment (Makhatadze et al., 1995; Parker & Clarke, 1997).

Three melting regions can be identified from the data of Figure 3.3: a linear melting region (from 5-45 °C); a non-linear melting region or pre-transition region (from 45-60 °C); and the major sigmoidal transition region (60-80 °C). The three regions are especially obvious in the melting curve measured at 1664 cm^{-1} (see also Fig. 3.4) where the pre-transition region exhibits a change in sign opposite to both the linear melting and sigmoidal denaturation transition changes. Thus, the observed changes in IR absorbance originate from some protein structure transformation rather than from nonspecific temperature dependence of spectral parameters. At 1654 cm^{-1}, which is close to the isosbestic point of the main denaturation transition, the pre-transition effect shows up as a slope change of the dependence at 45°C. The IR absorbance spectra at the temperatures separating the melting regions are presented in Fig. 1a.

The addition of excess $CaCl_2$ (10 mM) produces two obvious effects on the melting behavior of holo α-LA (Fig. 3.3b and 3.4). First, the T_m is shifted to higher temperature 70 °C, as previously observed (Vanderheeren,

et al., 1996; Kuwajima et al., 1986). The second effect is the disappearance of the changes that take place in the pre-transitional melting region. The baseline is linear through the whole temperature range below the sigmoidal melting transition.

Figure 3.5 plots the spectral difference between the high temperature point and the low temperature point, divided by the temperature change to reduce the presented effect to changes per degree centigrade, for the linear and the non-linear pre-transition regions (Fig. 3.5a), and the sigmoidal region (Fig. 3.5b). The results from runs with and without excess Ca^{2+} ions are shown. This method of presentation elucidates the details of the spectral changes with temperature.

The linear region is characterized by several sharp negative bands in the difference spectrum of panel 3.5a. The most intense band is at 1625 cm^{-1} corresponding to the band found at 1629 cm^{-1} in the low temperature α-LA spectrum. Other weaker bands are located at 1635, 1653, and 1676 cm^{-1} (corresponding to the 1638, 1654, and 1676 cm^{-1} bands). The intensity of these bands decrease with increasing temperature and their intensities are traded for the wider disordered bands at 1648 and 1673 cm^{-1} characteristic of disordered structure. The apparent displacements of the difference spectrum bands from their positions found in the amide I' absorbance spectra (see Figs. 3.1 and 3.2) are most probably due to the fact that in the difference spectrum they overlap with the steep wings of disordered structure band of opposite sign. According to previous assignments, the observed changes in the difference spectrum show that

substantial melting of β-structure occurs with a smaller decrease of helical content. The spectral changes within the linear region are quantitatively the same in presence and absence of additional extrinsic calcium. Hence, it can be concluded that additional Ca^{2+} ion(s) (apart from the Ca^{2+} ion of the holo protein) does not stabilize the substructure which is melted at low temperatures.

In the pre-transition region (dotted line, Figure 3.5a), both the β-structure (band at 1629 cm^{-1}) and substantially larger amounts of helices (see minima at 1635 and 1653 cm^{-1} on the difference spectrum) are melted. These helices are contained in a substructure which is stabilized by additional protein-bound Ca^{2+} ion(s) because the addition of 10 mM $CaCl_2$ shifts this pre-transitional melting to higher temperatures and the spectral changes are the same throughout all the temperatures below the major cooperative melting (compare the spectral differences corresponding to the linear regions on Figure 3.5a).

In the cooperative melting temperature region (sigmoidal transition, Figure 3.5b), the major change in the difference spectrum is loss of signal at 1635 cm^{-1} Hence, the major structure elements disrupted within the cooperative transition are 3_{10}-helices and/or solvated a-helices. Small negative shoulders can also be found at 1629, 1654, and 1676 cm^{-1}, indicating some melting of β-sheet, native a-helix and turns. These small changes may be due to overlapping of the cooperative transition with the linear melting process, at least partially. It is possible that substantially more of the native helix melts in the cooperative transition than is shown by

the IR results. The marker position of native a-helix at 1654 cm^{-1} is close to the position of the maximum (ca. 1648 cm^{-1}) of absorbance spectrum of melted protein (Fig. 3.1). Therefore, it is possible that decrease at 1654 cm^{-1} with temperature is matched by increase of a disordered structure absorbance. The denaturation spectral effects within the cooperative melting transition are the same both in presence and absence of excess calcium. Hence, the addition of excess $CaCl_2$ only shifts the transition temperature but does not change the protein substructures involved in the transition.

Unfortunately, the thermodynamic parameters of the melting cannot be determined accurately from the IR data. In the presence of additional $CaCl_2$, a progressive aggregation begins at high temperatures before the end of the transition which hinders an accurate determination of the high temperature baseline. If no extra Ca^{2+} is added, the non-linear pre-transition process overlaps with the sigmoidal transition, and this results in non-linear van't Hoff plots. However, for the sigmoidal transition as monitored at 1627 cm^{-1} (the effects of the non-linear transitions here are minimal because the participating bands are at higher wavenumbers), an estimation of 230 kJ/mol could be obtained for the transition enthalpy. This is smaller than the values of 250 kJ/mol[41] or 295 kJ/mol (Griko et al., 1994) obtained by scanning calorimetry in similar conditions in H_2O. However, a small decrease of melting enthalpy is expected for the melting in D_2O (Makhatadze et al., 1995).

3.5 Discussion

Our results indicate that holo α-LA melting includes at least three different processes. One, a cooperative melting transition with a T_m at 62-67 °C, has been observed in previous studies (Kuwajima et al., 1986; Griko et al., 1994; Dolgikh et al., 1985; Vanderheeren et al., 1996). In agreement with these studies, the T_m of this transition is raised by the addition of excess calcium and involves mostly the melting of helices. An accurate estimation of how much helical structure melts is not possible due to the strong overlapping of their negative going bands upon melting with the positive going bands from denatured polypeptide chain (see also Results).

In addition, between 5-45 °C, a gradual melting of the holo protein in a Ca^{2+}-independent process is also observed. Its quasi-linear temperature dependence shows low (if any) cooperativity in this melting process (Privalov, 1996). According to our data, in combination with the published assignments of amide-I' bands to secondary structure, the observed spectral changes are attributed to the loss of β-structure. This non-cooperative melting process has been reported previously from the results of other techniques (see Balbach et al., 1996 and references therein), and it was proposed that this transition represents some unfolding of the α-domain (Privalov, 1996). However, our results show that the gradual melting involves mostly β-structure and, hence, the β-domain which contains the only β-structure (the b-hairpin) of holo α-LA.

It is not simple to estimate what proportion of the β-structure melts gradually prior the major transition because its amide-I' band (1629 cm^{-1}) overlaps strongly with the side chain (1618 cm^{-1}), helical (1638 cm^{-1}), and

disordered structure (1648 cm^{-1}) bands. As an estimate, we take the absorbance at 1625 cm^{-1} to be a measure of the amount of β-structure because this is the frequency of the maximal effect in the linear temperature region (cf. Fig. 3.5a) and because the overlap of the helical and disordered structure bands is comparatively small. Further, we assume that the β-hairpin (residues 40-50 of α-LA) is completely intact at 5.2 °C and is basically melted at 95.3 °C (the lowest and highest temperatures of our measurements). In this case, the total absorbance change between 5.2 and 94.7 °C is 41 mOD at 1625 cm^{-1}. In the gradual melting region (from 5.5 to 63.1 °C using the longer range in the presence of 10 mM $CaCl_2$), the total change in intensity at 1625 cm^{-1} is 19 mOD. The former range includes the melting of β-sheet structure as well as other structure(s) whereas the latter has to do only with the melting of β-structure. Hence, at least 46% of the β-structure has melted non-cooperatively. The actual proportion is almost certainly larger because of additional absorbance at 1625 cm^{-1} due to the overlapping of neighbor bands.

A third melting process is also observed that takes place at intermediate temperatures, 45-60 °C, just prior to the cooperative transition ('pre-transitional process'). This process involves a substantial decrease of helical substructures (components at 1638 and 1654 cm^{-1}). Contrary to the β-structure loss from 5-45 °C, this process is sensitive to the presence of excess Ca^{2+}, like the cooperative melting process. Also like the cooperative melting process, the pre-transitional melting involves the melting of helices.

In summary, the results suggest that the β-domain of holo α-LA contains two substructures that melt independently from each other. One melts gradually, i.e. non-cooperatively, and involves the β-hairpin of the β-domain. Since the β-domain contains the structurally important Ca^{2+} binding site, it seems clear that the β-domain includes also another substructure, at least partially. The melting of the second substructure is involved in one or both of the other two transitions, because both of them are influenced by the presence of excess Ca^{2+} ions. That the two melting processes occur independently of each other and one process is dependent on excess calcium ions while the other does not is not unreasonable given the β-domain structure of α-LA. The β-hairpin of the β-domain does not include residues in direct contact with the Ca^{2+} ion (Stuart et al., 1986; Acharya et al., 1989); hence, it seems possible that the β-hairpin of the β-domain could melt independently from holo α-LA's Ca^{2+}-binding domain. The Ca^{2+}-binding site is formed by the 3_{10}-helix G in the β-domain (residues 76-82) and α-helix C (86-99) which is assigned either to the α- (Wu et al., 1996) or β-domain (Hendrix et al., 1996) by different authors. Hence, the structure of the protein also is consistent with the melting of helices that are observed in the calcium dependent processes. Our results do not address directly whether or not helices of the a-domain melt in the two calcium dependent processes, but we believe that it is likely that they do given the sigmoidal nature of the cooperative melting process. In any case, an important result from this investigation is that the melting of α-LA occurs in substructures that are not in a one to one identity with its domains as defined by its crystallographic structure. Such heterogeous melting behavior has also been found in apomyoglobin (Gilmanshin et al., 1997).

The complex melting behavior of α-LA has been studied previously using calorimetry and near-UV circular dichroism (Vanderheeren et al., 1996). The proposed model explained the melting complexity due to the co-existence of two denatured forms: with (holo-denatured) and without (apo-denatured) a Ca^{2+} ion at the calcium binding site. The latter apo-denatured form was assumed more disordered than the former one. It was estimated that the change of free energy accompanying Ca^{2+} release from native structure was large; hence, such a step would more likely occur subsequent to formation of the holo-denatured form. The addition of extra $CaCl_2$ increases the relative proportion of the holo-denatured form at lower temperatures which allowed the authors (Vanderheeren et al., 1996) to explain the apparent high temperature shift of the denaturation transition. According to this model (Vanderheeren et al., 1996), it is possible to speculate that the pre-transitional calcium-dependent melting at 45-60 °C found here is the result of the production of the holo-denatured form. The observed major transition results from the further transformation of the holo-denatured form into the apo-form. In this case, the presence of extra 10 mM $CaCl_2$ should increase the proportion of the holo-denatured form after the first transition, shifting calcium ion release to higher temperature and concomitant further denaturation. However, this implies that pre-transitional melting would show up in the IR melting curves with or without the addition of excess calcium except for a change of amplitude (since calcium presumably affects the proportion of holo-denatured to apo-denatured forms). This is not observed since the first Ca^{2+}-dependent melting transitions have different signs in absence and presence of extra

calcium (Fig. 3.4). Hence, the model of Vanderheeren and co-workers (Vanderheeren et al., 1996) does not fit our data very well, although it may apply to the major cooperative melting. In this case, another explanation for the pre-transitional melting is necessary.

There are two possibilities. The pre-transition calcium-dependent melting at 45-60 °C may be a result of a different process that involves a second Ca^{2+}-binding site. Indeed, previous studies of α-LA have indicated a second Ca^{2+}-binding site. We note that a second binding site that undergoes calcium release before the major melting transition can also explain the difference of the results obtained by Vanderheeren et al. (Vanderheeren et al., 1996) in analysis of their CD and calorimetric data. The second possibility is the release of Ca^{2+} ion from native α-LA at high temperature prior to the major cooperative melting. In this case, the pre-transitional melting would involve an equilibrium between unmelted holo α-LA and apo denatured α-LA since it is known that α-LA without Ca^{2+} melts at temperatures lower than what observed in the pre-transitional region. This model for the thermal denaturated holo α-LA would imply that the main transition involves the melting of helices involved in calcium-binding. This would explain why the pre-transition melting disappears in the presence of excess $CaCl_2$.

Figure Legends

Figure 3.1. α-Lactalbumin IR absorbance spectra (a), their second derivatives (b), and deconvolved spectra (c) at different temperatures. The protein concentration was 8.0 mg/ml. The spectra are presented at the temperatures corresponding to the borders of the intervals with different melting behavior (see text and Figure 3.4).

Figure 3.2. The second derivative (a) and deconvolved spectra (b) in the amide I' region of α-lactalbumin in the presence of 10 mM of $CaCl_2$ at 5.5 °C and at 77.4 °C. The protein concentration is 9.5 mg/ml.

Figure 3.3. The temperature dependences of α-lactalbumin IR absorbance at 1628, 1638, 1654, 1664, and 1676 cm^{-1}, without extra calcium (a) and in the presence of 10 mM $CaCl_2$ (b).

Figure 3.4 The dependences measured at 1664 cm^{-1} shown in figure 3.3 are superimposed for clarification. The data measured with 10 mM $CaCl_2$ are divided by 1.2 to compensate for the concentration difference. The dashed lines show the linear baselines of the melting transition without extra calcium. The arrows show temperatures at which the spectra presented at Figure 3.1 were measured.

Figure 3.5. Difference spectra of α-lactalbumin in the amide I' region reduced to per degree centigrade for different temperature intervals: prior (a) and within (b) the major melting transition. Panel (a): linear melting

regime without extra calcium (bold line, calculated for the 44.3 - 5.2C °C interval) and in the presence of 10 mM $CaCl_2$ (dashed line, 58.4 - 5.5 °C); pre-transition non-linear melting without extra calcium (dotted line, 58.9 - 44.3°C). Panel (b): major melting transition without extra calcium (bold line, 77.8 - 58.9 °C) and in the presence of 10mM $CaCl_2$ (dashed line, 77.4 - 58.4 °C). The spectrum at lower temperature was subtracted from a higher temperature spectrum. The spectra with excess Ca^{2+} are divided by 1.2 to compensate for the concentration difference.

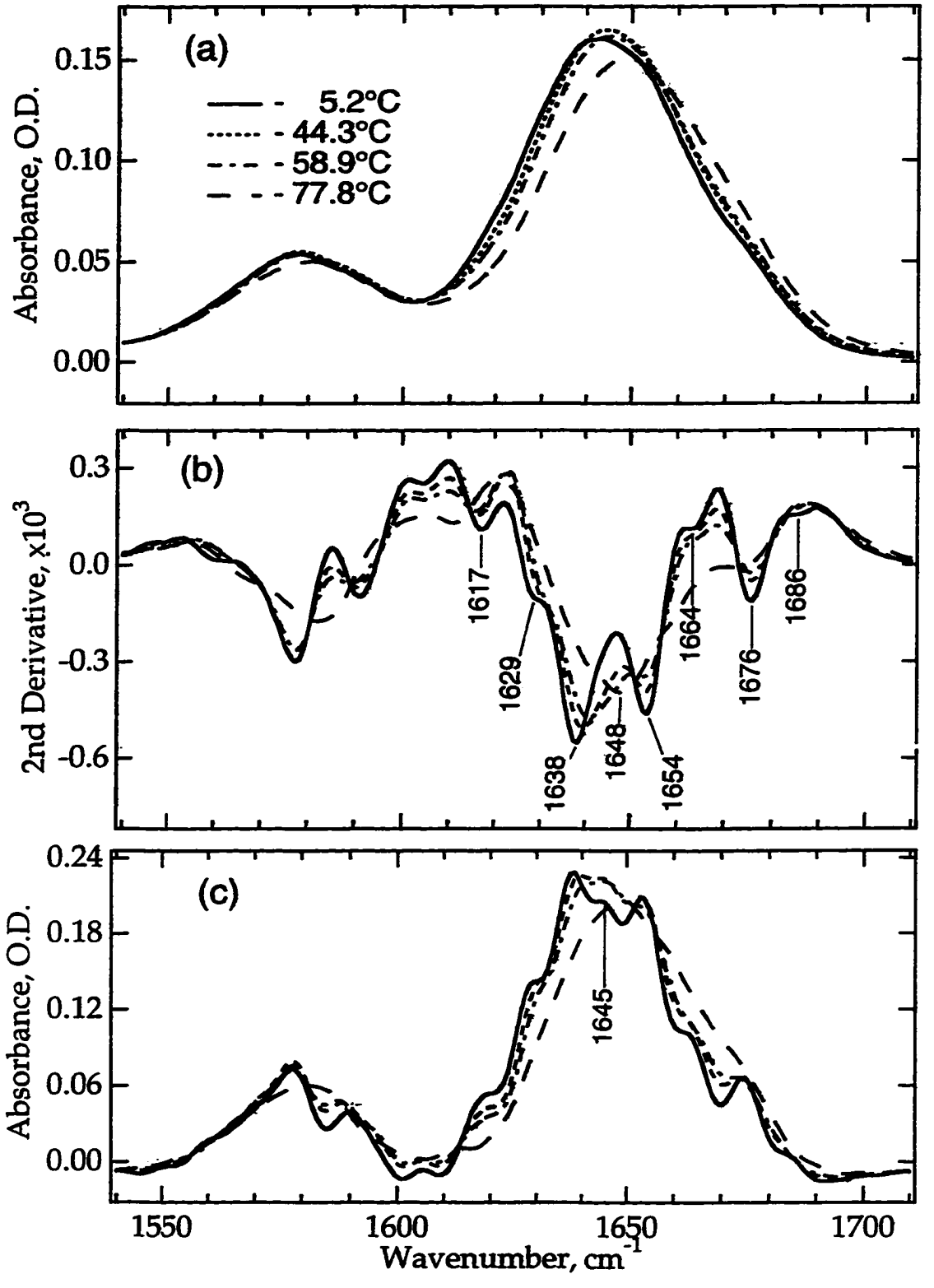

Figure 3.1

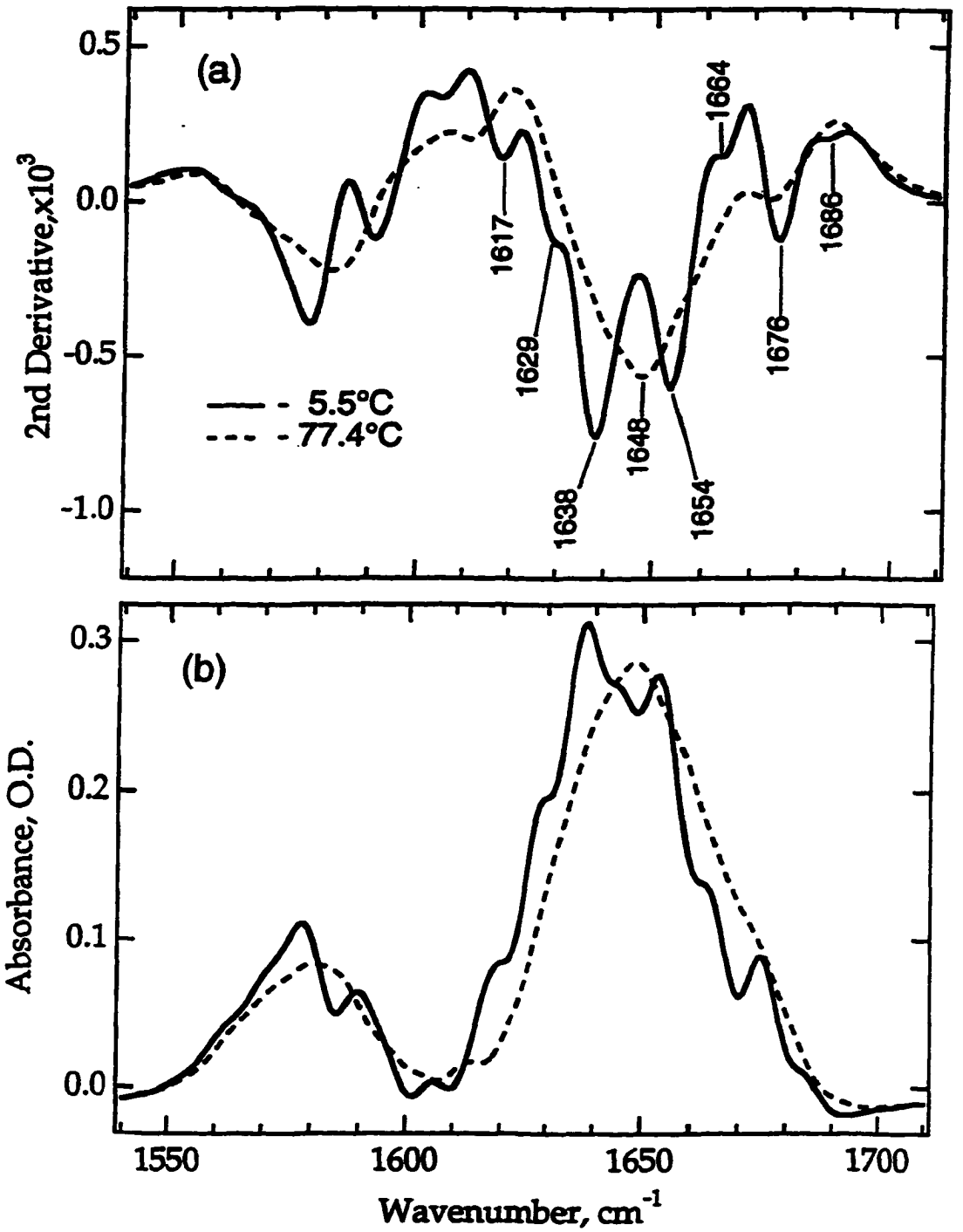

Figure 3.2

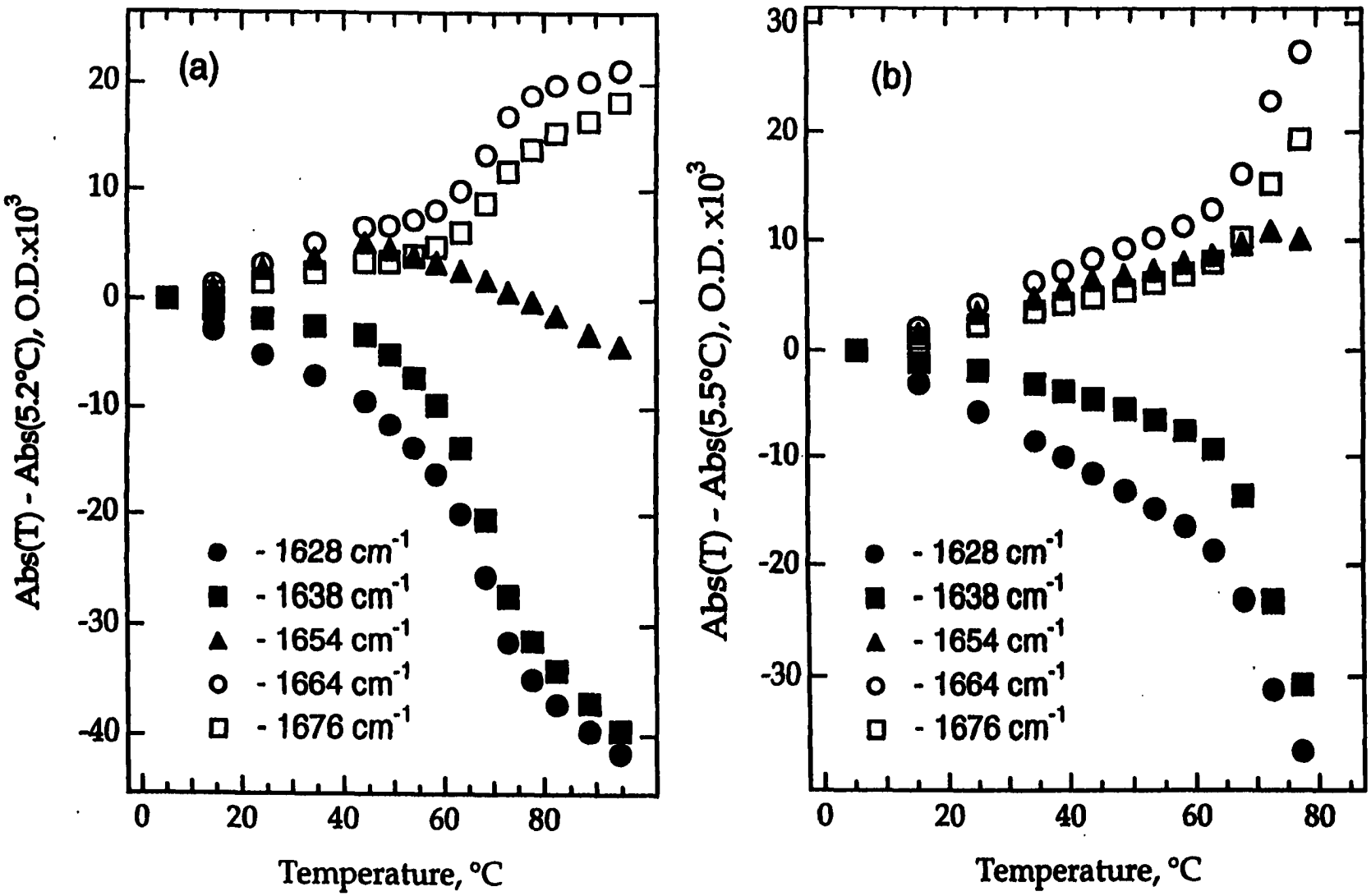

Figure 3.3

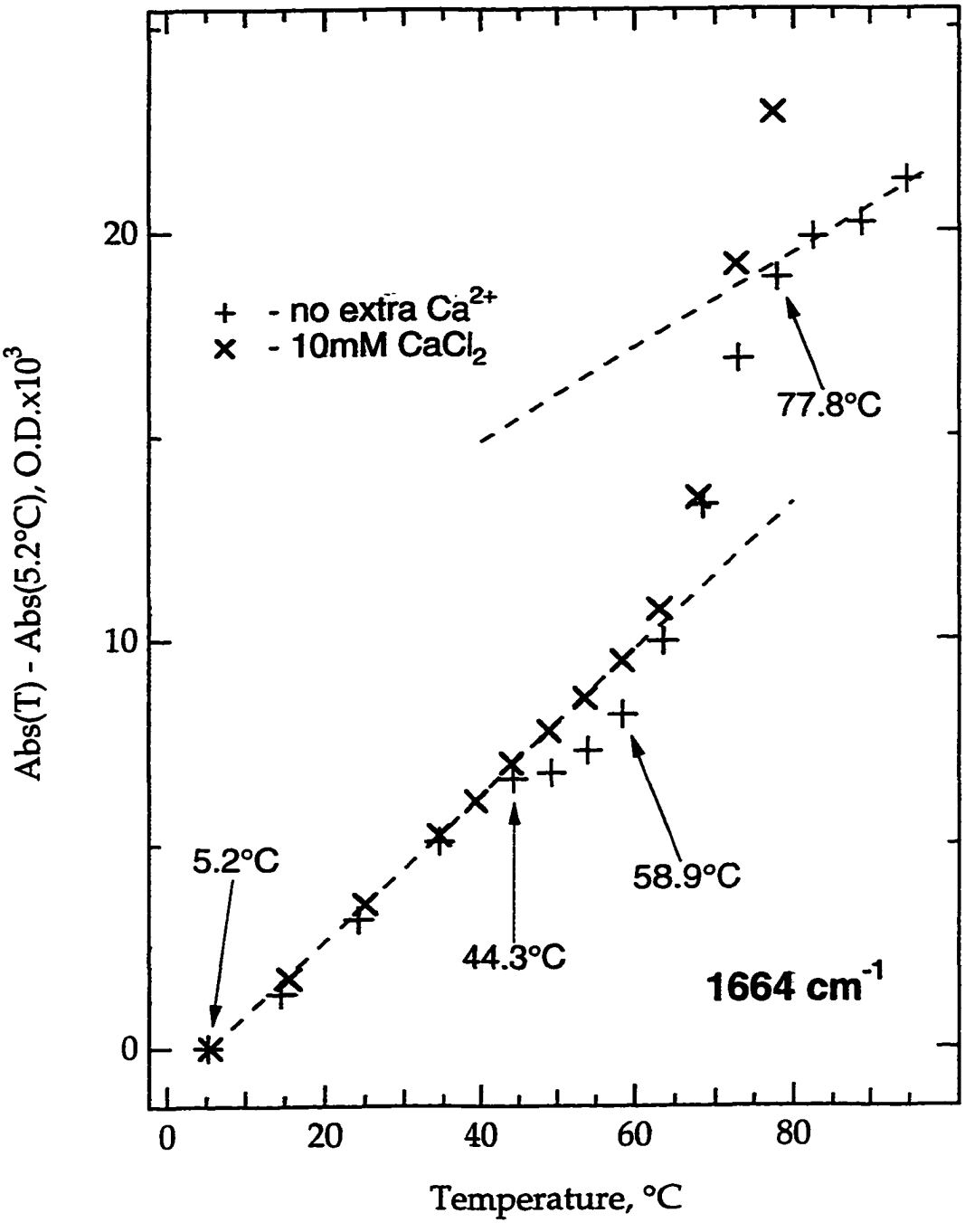

Figure 3.4

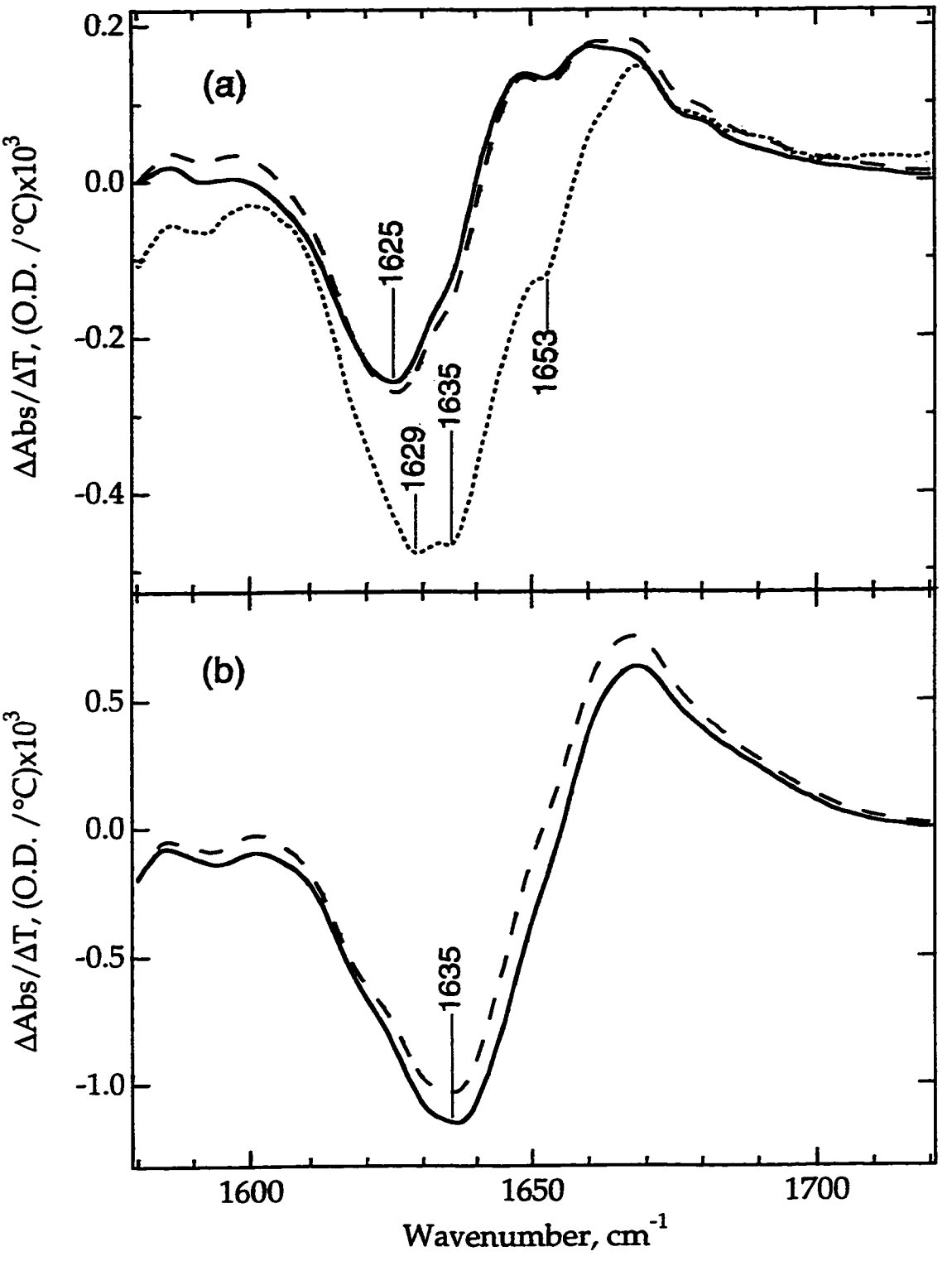

Figure 3.5

Chapter 4 The Melting Behavior of the Acid Form and Apo α-Lactalbumin: Evidence of Separate Melting Behaviors of Helices and β-Structures

4.1 Introduction

α-lactalbumin, as a typical model protein to investigate protein folding problem, has been paid great attention over past two decades. In 1981, α-lactalbumin was found to adopt some intermediate conformation between native and unfolded protein (Dolgikh et al., 1981), leading to the notion of molten globule states. This intermediate state demonstrates almost intact secondary structure components while loosing most of its tertiary interaction (Dolgikh et al., 1981; Dolgikh et al., 1985). It has been proposed to be the general intermediate in protein folding pathway. Since then, α-lactalbumin has becoming one of the most popular proteins to be used to study the molten globule state.

Two kinds of molten globule exist. The first kind of molten globule is postulated to exist in the protein folding pathway and, hence, would play an important role in the folding process. The second kind of molten globule exists in equilibrium and is formed under some extreme conditions. Kinetic molten globules only exist in a transit period, so are difficult to be caught experimentally. On the contrary, equilibrium molten globules can be made in the test tube in a very inexpensive way and, theoretically, can be kept in that state forever. For this reason, much effort has been made to investigate the equilibrium molten globule. However, the question arises as whether

the equilibrium molten globules adopt the same conformations as those in kinetic molten globules. When equilibrium molten globules represent kinetic molten globules, they are of obvious importance for investigation. Some researchers believe that the pathway equilibrium molten globules are often the result of misfolded protein. Others think the equilibrium molten globules basically have the same conformation as those populated in kinetic intermediates. For α-lactalbumin, direct NMR observation of a transient folding intermediate provides new evidence for the importance of molten globules as general intermediates in protein folding (Roder, 1995). In this thesis, all the conclusions drawn from the equilibrium study will be applied to the kinetic molten globules.

Molten globules are found to demonstrate various features in different proteins. Even for the same protein, several kinds of molten globules may exist. Some times, the terminology premolten globule is used to discern their differences. Experimental evidence has been found that a wide range of partially folded but compact states exist, the structure of which can vary from being highly disordered to being highly ordered (Dobinson, 1994; Ptitsyn, 1992). Among the lysozyme-α-lactalbumin family of proteins, the α-lactalbumins studied so far can be characterized as rather highly disordered molten globules (Ptitsyn, 1992; Baum et al., 1989; Chyan et al., 1993). Equine lysozyme represents a more ordered state with a well-defined hydrophobic core (Morozova et al., 1995). Other proteins under appropriate conditions can, however, form partially folded states that are significantly more native-like overall than that of equine lysozymes, while still

maintaining features characteristic of molten globule behavior in at least some regions of their structures (Dobson, 1994; Morozova et al., 1995).

The acid (A-state) form of α-lactalbumin is well known to adopt a molten globule state (Dolgikh et al., 1981) and has probably received most attention. Hydrogen exchange experiment shows the β-sheet domain of the acid form has little protection against H-D exchange while the helical domain at least partially keeps the protection against the exchange (Chyan et al., 1993). This provides us with a clue that in the acid form β-sheet domain is largely denatured while the helical domain may have some core region intact.

A large number of denaturation studies have also been done on the apo form of α-lactalbumin. As a distinct feature of α-LA, the ligand Ca^{2+} may play an important role on the protein stability. If Ca^{2+} does contribute to protein stability, the question arises as whether it stabilizes the two domains of α-LA to the same extent or preferably stabilizes one of them. Since the ligand binding site of α-LA largely involves the amino acid side chains and backbone carbonyls in β-structure domain, the function of the Ca^{2+} was traditionally thought to be on the β-sheet. Most people tend to believe that the ion Ca^{2+} directly relates to the folding of the β-sheet domain. That is, upon removal of this ligand, the β-sheet domain may be denatured, while the metal ion has little effect on the folding and stability of the helical domain. Many experiments are designed to address this question, but these are unsuccessfule.

Recently Peng and Kim (Peng & Kim, 1994) addressed this issue. They designed and constructed a signal chain, recombinant model of the α-helical domain of α-LA. This α-domain consists of residues 1-39 and 81-123 of human α-LA, connected by a short linker of three glycines (the distance between the carbonyl of Gln 39 and the amide of Leu 81 is 7 Å in the crystal structure of α-LA. Cys 91, which forms an interdomain disulfide bond, is changed to Ala to avoid unwanted thiol-disulfide reactions. In total, this α-domain has 86 amino acids, including an N-terminal methionine as a result of expression in *Escherichia coil.*

Their studies indicate that, on the one hand, the helical domain thus formed lacks extensive and specific sidechain packing. On the other hand, this domain has the same tertiary fold and secondary structures as that in intact α-LA (Peng & Kim, 1994). These characteristics exit even in room temperature. As we have shown in chapter 3, the helical domain of intact α-LA remains folded below the major transition temperature (T_m around 65 ^oC). This suggests that the folding of the helical domain needs some external factors. These external factors could be either β-sheet domain or calcium ion or both since the differences between dissected helical domain and the helical domain in intact protein lie in whether the β-sheet domain and calcium ion are present.

In another study of α-LA, Peng and Kim (Wu et al., 1996) removed the disulfide bond inside the β-sheet domain and disulfide bond linking β-sheet and helical domain, resulting in a denatured β-sheet domain. Thermal denaturation study of this modified protein exhibited no sigmoidal transition

no matter whether calcium was present. This proves that Ca^{2+} could not be the only external factor to facilitate the folding of helical domain. The other factor, β-sheet domain must have some contributions. In a separate study (Wu et al., 1996), the disulfide bonds located in the helical domain were specifically removed by site-mutation of corresponding cysteins while the SS bonds in β-sheet domain and the interdomain bridge were kept intact. In the absence of Ca^{2+}, the thermal denaturation behavior of this protein shows no sigmoidal transition. But in the presence of calcium ions, a cooperative transition which involves some denaturation is found. Peng and Kim thought this denatured part of structure belongs to the folded β-sheet domain. If their thoughts are correct, the results indicate that the folding of β-sheet needs binding of calcium ion, and β-structure domain could be folded while the helical domain still lacks well folded tertiary structures. Based on these facts, they suggest that initial formation of the molten globule yield a species in which the α-helical domain is native-like while the β-sheet domain is predominantly unfolded, and subsequently a locking step requiring organization of the β-sheet domain and calcium binding in α-LA yields the unique native structure (Wu et al., 1996).

However, the technique they used to monitor the structure changes is circular dicroism. As we have mentioned before, CD is not sensitive to β-sheet enough, and its near UV signal have some effect on the far UV CD. Any changes in near UV CD could have contribution to the far UV, and the disturbance to the far UV brought about by near UV signal may have comparable amplitude of real signal diminution from β-sheet. This makes the claim of β-structure changes based on only far UV CD questionable,

especially for the α-lactalbumin in which just a small portion of β-sheet presents (Prestrelski et al., 1991a; Prestrelski et al., 1991b). Compared to this, FT-IR spectroscopy is able to provide complementary information since unlike CD, the amide I region of IR absorption has similar sensitivity to β-structure and helical structure separately.

A kinetic NMR study (Balbach et al., 1996) was also done on the apo form which exhibits a very slow folding process. This 2-D NMR study suggested that the mainchain in the β-structure region adopts native environment earlier than the other region.

Most recently (Veprintsev et al., 1997), the heat denaturing studies of the apo form of α-lactalbumin performed by various techniques demonstrate that there are two transitions with midpoints at 25-30 degree and 15-20 degree. So it was hence proposed that another intermediate exists between the native state and the classic intermediate state which is long be regarded as having same conformation as equilibrium molten globule (Veprintsev et al., 1997). This intermediate has the basic characteristics of the molten globule but should have a distinctly different structure from that of classic molten globule. The detailed differences were not reported due to the limitation of the experimental techniques which are insensitive to either secondary structures or β-structure.

In this chapter, we will report our heat denaturing study of destabilized forms of α-lactalbumin. The first one is the acid form. It has been widely known that the acid form of α-lactalbumin adopts molten

globule state, so it is a reference of molten globule state. The second one is the apo form which has the ligand calcium ion removed. We will observe two transitions of the apo form, which actually are associated with denaturation of separate domain.

4.2 Materials and Methods

4.2.1 Preparation of Protein Samples

Bovine α-lactalbumin was purchased from Sigma and was further purified with gel filtration on Sephadex G-75 in 0.1 mM Tris buffer at pH 8.1. The purified protein was dialyzed against deionized water, lyophilized and stored at -80 ^{o}C. Its concentration was determined spectrophotometrically using an extinction coefficient at 280 nm of $E_{1\%}$= 20.9 cm^{-1}. Ca^{2+} was removed by addition of EDTA in excess to protein. Bovine α-LA concentrations of 3 to 8 mg/ml were used for IR measurement. All sample solutions were made in D_2O. Reported pH* values were direct reading of pH-meter.

4.2.2 Preparation of Protein Solutions

The apo bovine α-LA and the was made by depositing same volume of 10 mM EDTA solution after adjusting pH*. As mentioned before, no specific buffer was present in the protein solution to avoid pH shifts at high temperature due to the buffer. Protein itself acts as a buffer in this case. There is little change of pH coming from protein. Actually a lot of heat

denaturation studies on α-LA were done without the presence of buffer, such as Dolgikh et al. (Dolgikh et al., 1981). Before FT-IR measurement, the protein solutions were equilibrated with the reference to a sephadex G-25 column. Both protein and buffer samples were collected from the same elution to ensure balanced HDO present in buffer and protein solutions. All the above processes were done in the cold room of 5 °C. For the apo form of protein, the sample was in the presence of 10 μM EDTA to eliminate possible Ca^{2+} contamination. Sample aliquots after the column were used to determine the pH* and concentration. The pH value of the protein in D_2O was adjusted by DCl and NaOD.

4.2.3 Reversibility and aggregation

Aggregation was monitored on the one hand, by the band between 1615 and 1623 cm^{-1}, where a strong and sharp band usually shows up in this region with a concommitant weak band at 1680 ~ 1684 cm^{-1} when intermolecular aggregation is formed. On the other hand, melting reversibility is also used to check for the possible aggregation (see chapter 3). Reversibility was checked by lowering the temperature of the sample to that below transition temperature in the fastest way. This was realized by the second circulator with the temperature set to the target. The reversibility is analyzed not only by absorption spectrum but also by second derivative spectrum. It was found that the heat denaturation of the acid form is reversible at experimental concentrations. For the apo form, most of the protein molecules are reversible, but we still found a small portion of them are apparently not reversible. Noting that the time constant of the refolding

of the apo form is about 8 minutes (Balbach et al., 1996) at 3 °C, we may explain this "irreversibility" of the protein molecules actually is due to this slow refolding mechanism in comparison with fast cooling process (within 2 minutes). In particular, the refolding kinetics may be extremely slow at high temperature. In addition, protein may aggregate if exposed to high temperature environment for a long time (Kuwajima et al., 1986)..Based on the above discussion, we believe the apo form did not form aggregates during the transitions to any extent.

4.2.4 Instrument and data analysis

IR spectra were acquired on a Bruker IFS-66 Fourier-Transform Infrared Spectrometer using MCT detector. A demountable liquid flow sample shuttle accessory with two cells and 56 μm Teflon spacers was used. AgCl windows were used for apo and apo CAM-3SS forms (chapter 5), while CaF_2 windows were used for the other forms. The sample chamber was continuously purged with dry nitrogen gas. Data were collected with the aperture open to 3 mm setting. The two position sample shuttle was set to alternate between sample and buffer positions to eliminate the residual water vapor contribution after subtraction. 32 scans were collected, coadded and apodized with Blackman-Harris 3-term and 2 cm^{-1} resolution for each position and each repetition. Data of 26 repetition were collected and averaged to get each spectrum. The OPUS 2.0 and Grams/386 softwares were used for data collection and analysis. The positions of band components in the amide I' region were determined by using second-derivative which was obtained by Savitsky-Golay algorithm. The transition curves were derived from double difference spectra. Deconvolution, based on the method of Griffiths and Pariente (Griffiths & Pariente, 1986),

was performed between 1530 and 1730 cm^{-1} with FWHH=25 cm^{-1}. A linear baseline was subtracted prior to deconvolution to ensure zero absorption at the ends of the spectral interval.

4.3 Results and Discussion

4.3.1 The acid form of α-lactalbumin

The study of the acid form of α–LA by CD was made over twenty years ago (Dolgikh et al., 1981). The strong maker bands for helical structures in far UV CD made people believe that the acid form have almost same amount of secondary structures as that in native protein. And the disappearance of the near UV CD indicates the acid form still does not form tertiary structures (Dolgikh et al., 1981). The concept of molten globule is largely rooted from the study of this form.

The second derivative spectra of the acid form at 5, 35 and 85 °C are displayed in figure 4.1. At 35 °C, we can see the dominate and broad band at 1648 cm^{-1}. The bands between 1640 and 1650 cm^{-1} in D_2O are attributable to the contribution of random structures and solvated helices. The fluctuation of these denatured component explains why the bands are broad. Since a large amount of helical structures is detected by CD (Dolgikh et al., 1981; Dolgikh et al., 1985), we believe there are a lot of solvated helical structures contributing to this band in the IR. Because these random and solvated helical structures have broad bands and close marker band positions, we can not separate them from each other.

The second derivative spectrum at temperature 5 °C also shows a weak band around 1638 cm^{-1}. This band is assigned to be the contribution from 3_{10} helices in the native α-LA. Observation of this band suggests that the acid form may have some regular helical structures at low temperature. As the temperature elevates, this regular structures are denatured. Compared to the native α-LA, the second derivative spectra do not show the band at 1629 cm^{-1} at all experimental temperatures. This band has been assigned to be the marker band of β-sheet in α-LA (Prestrelski et al., 1991a; Prestrelski et al., 1991b). However, we can not eliminate the possibility of the existance of the β-structure. Highly fluctuating β-structure may give rise to a broad band which is not able to be detected by the second derivative analysis. Indeed the double difference spectra shown in figure 4.2b) indicates a red shifted spectrum minima at low temperature compared to those at high temperatures which may relate to a band at 1629 cm^{-1}. Nevertheless, little folded β-structures exists in the acid form. This is consistent with the results based on hydrogen exchange experiment which show that the mainchain region corresponding the β-structure in the native α-LA exhibit little protection from hydrogen exchange (Chyan et al., 1993), suggesting denatured β-structure. The spectra at high temperatures are pretty similar to the high temperature spectra of the holo form (see chapter 3).

Figure 4.2 plots the absorbance spectra (figure 4.2a) and double difference spectra (figure 4.2b) of the acid form at various temperatures. The decrease at low frequency and increase at high frequency at elevated

temperature is similar to that of the holo form (see chapter 3), suggesting unfolding of the secondary structures.

The transition curve obtained from figure 4.2b is shown in figure 4.3. No transition with sigmoidal pattern can be found in figure 4.3. Only a gradual melting process happens. This suggests that no tertiary structures are melted in the acid form. The gradual melting behavior can be explained by the unfolding of the solvated helical structures. This is consistent with the recent CD measurement of α-LA which indicates little helical structure at high temperature (Hendrix et al., 1996).

4.3.2 The apo form of α-lactalbumin

The question arises as to whether the calcium ion plays a crucial role on cooperativity. Preliminary studies on the apo form of α-LA indicated there are two transitions in the range 15-20 ^{o}C and 25-30 ^{o}C respectively, suggesting an intermediate different from the classic molten globule (Veprintsev et al., 1997).

An FTIR study of the apo form of α-LA in CaF_2 window has been reported (Prestrelski et al., 1991a). A previous report of an infrared examination of Ca^{2+}-binding proteins checked for the possible contamination from CaF_2 windows (Trewhella et al., 1989). This study found no protein bound calcium using atomic absorption spectroscopy. We performed a thermal denaturation study of the apo form using CaF_2 windows. However, our results indicate that there is a problem in the study

of Ca^{2+} free α-LA when CaF_2 windows are used. α-LA does bind calcium ion from the windows and shifts the transition temperature up to around 50 °C, even with the presence of 10 mM EDTA (data not shown). Previous investigation of thermal denaturing behavior of the apo form by the calorimetric method has demonstrated that the major transition is located around 30 °C (Dolgikh et.al., 1981), significantly lower than 50 °C. We believe this upshift is caused by the binding of calcium ion from the FTIR windows.

Indeed, the calcium ion dissolved in the sample solution is easily bound to the apo form of α-LA due to the protein's strong binding site whose binding constant reaches the order of 10^8 - 10^9 M^{-1} (Berliner & Johnson, 1988). The CaF_2 window, in this case, plays an very important role by providing the sample solution with Ca^{2+}, especially at high temperature which facilitates the dissolving process as shown below.

$$CaF_2 + \text{apo-BLA} \longleftrightarrow Ca^{2+} + 2F^- + \text{apo-BLA} \longleftrightarrow \text{holo-BLA} + 2F^- \qquad (4.7)$$

The strong binding constant makes the equilibrium move to the right. The presence of EDTA does not affect the result. In this case, the dissolved calcium ions preferably bind to EDTA molecules until saturation. However, more and more calcium in windows is dissolved. The total concentration of Ca^{2+} in the sample solution keeps constant. After this, α-LA binds to the calcium, thus no actual apo form is reached.

To avoid this problem, we replaced the CaF_2 windows by AgCl windows which are not only transparent in the amide I region but also insoluble in water. The denaturation study on the apo form did not show evidence of binding. All the experiments were performed under dark to prevent the potential reaction of the AgCl with light.

The amide I' absorption spectra at different temperatures are displayed in figure 4.4a, and the double difference spectra are plotted in figure 4.4b. Apparently, based on double difference spectra (figure 4.4b), two sigmoidal transitions are found in the experimental temperature rang (figure 4.5). The first transition is around 20 ^{o}C, and the second transition is around 40 ^{o}C. Both transitions display weak sigmoidal character compared to that of the holo forms. The similar results have been reported before when α-LA was studied in H_2O (Veprintsev et al., 1997). They reported that transition temperatures of the apo form of α-LA in H_2O monitored by CD, calorimetric method and fluorescence are not consistent. They gave different transition temperatures, 15-20 and 25-30 ^{o}C. The difference can be adjusted by two different solvents. They thought this is due to two transitions of the apo form. But no detailed structure changes were determined.

The apo form of α-LA remains native at low temperature (5 ^{o}C) as shown from the second derivative spectra (Figure 4.6). The basic pattern of the second derivative spectra of this low temperature form is identical with that of the corresponding holo form. As temperature elevates, the amplitude of the bands at 1638 and 1653 cm^{-1} decreases at the first transition region

shown in figure 4.6 while that of the band at 1629 cm^{-1} increases as seen from the second derivative spectra. This may be interpreted as a melting of helical structures and increasing β-structures. However, the conclusions based on the amplitude changes of the second derivative spectra can not be trusted with 100% confidence. These spectra are sensitive to the sharpness of the real bands and may not accurately reflect the real changes. It should be noted that a band at 1681 cm^{-1} also increase as a byproduct of the band at 1629 cm^{-1}. These two bands are widely believed to come from the contribution of antiparallar β-sheet. Therefore, we think the simultaneous changes of these two bands can hardly be explained as coincidence. It is possible that more β-sheet is formed while the helical domain is denatured.

As temperature continues to increase, the bands at 1629 cm^{-1} and 1681 cm^{-1} begin to diminish and finally disappear completely. The second derivative spectra of the apo α-LA at high temperature are reduced to those of the holo forms, suggesting that high temperature forms tend to have same structural features. The decease of the bands at 1629 and 1681 cm^{-1} is obviously due to the unfolding of the β-structure. Moreover, the temperature range of this change is located in the second transition region as shown in figure 4.5, indicating that the second transition is closely related to the unfolding of β-sheet.

Figure 4.7 displays the double difference deconvolved spectra of the apo form of α-LA. In this figure, the high temperature deconvolved spectrum is subtracted from the corresponding spectra of 5 ^{o}C and 27 ^{o}C. Compared to that of 27 ^{o}C, the difference spectrum of 5^{o}C exhibits lower

amplitude for the band at 1629 cm^{-1} and higher amplitude for the band at 1638 cm^{-1}, suggesting that the protein at 27 ^{o}C has less unstructured helical domain and more β-sheet. The cooperative presence of the band at 1681 cm^{-1} with that at 1629 cm^{-1} provide us with further evidence that the band at 1629 cm^{-1} come from the contribution of β-structure. These are consistent with the results drawn from the second derivative spectra.

The transition curve based on the double difference deconvolved spectra (figure 4.7) are plotted in figure 4.8. They clearly show two transitions. The first one involves the increase of β-sheet and decrease of helical structures with middle transition temperature around 20 ^{o}C while the second one only relates to the denaturation of β-sheet with T_m around 40 ^{o}C.

These infer that some of β-sheet component is formed through the first transition, and all are unstructured via the second transition. In contrast, the helical domain is denatured through first transition. It is unclear whether the denatured helical domain contains some solvated helical structure based on FTIR experiment. It is also hard to conclude whether the helical domain is denatured partly or completely after the first transition since the two transitions are so overlapped that no pure intermediate can be reached.

Compared to these, the results obtained by calorimetric method give the peak with the maximum ranging from 28 ^{o}C to 41 ^{o}C, depending on the concentration of Tris buffer (Griko et al., 1994). Actually, Tris has 0.02 pk_a

change per degree. It was also reported that EDTA could shift the transition temperature of the apo form (Kronman & Bratcher, 1983). In our experiment, no Tris was presented. The reason that 10 μM EDTA is present is to eliminate the possible calcium contamination. The apo form of α-LA maintains substantial near UV CD spectrum which is weaker than the holo form anyway. Creighton has proposed that about 20% of the apo form of α-LA at room temperature is in the molten globule state with the assumption of the coexistence of native and molten globule states at this temperature (Ewbank & Creighton, 1993(b)). However, our study indicates that the apo form of α-LA at room temperature is a mixture of native protein and an intermediate which is different from the classic molten globule. The second derivative spectra of the acid form of α-LA at low and high temperatures are displayed in figure 4.1. No evidence of β-sheet is present even at low temperature, and this is consistent with the result from H-D exchange experiment (Chyan et al., 1993).

Interestingly, the protein dissection study of α-LA by Kim and his colleagues showed the β-sheet domain could fold without helical domain but could not fold without Ca^{2+} (Wu et al., 1996). Our intact protein study of the apo form by FTIR demonstrates a β-sheet rich intermediate with at least partially denatured helical domain. If this resembles the structure of an intermediate that is present in protein folding pathway, it seems to suggest β-sheet domain can be formed without Ca^{2+}.

Our results are supported by the most recent thermal denaturation studies. It was found that the transition temperature of the apo α-LA ranges

from 25 to 30 °C when monitored by fluorescence emission maximum and quantum yield, but the T_m ranges from 15 to 20 °C if near UV CD at 270 nm or differential scanning microcalorimetry method was used (Veprintsev et al., 1997). The reason for the different results obtained from previous studies (Dolgikh et al., 1981; Dolgikh et al., 1985) is not clear. Veprintsev et al. further proposed that there is an intermediate different from classic molten globule. Although the transition temperatures they found are somewhat lower than those we found by FTIR, the different solvent (H_2O and D_2O) used may explain this difference. The T_m of proteins in D_2O are generally larger than that in H_2O.

Another experiment was performed to investigate the folding behavior of α-lactalbumin when the acid form of α-LA underwent a pH jump by fast mixing process. The apo α-LA refolds to its native state after pH jumps from 2.0 to 7.0 at 3 °C (Balbach et al., 1996). Since the apo form of α-LA refolds much slower than the holo form, 2D NMR was used to monitor the folding at individual residues. Interestingly, compared to the time constant found by fluorescence method (Balbach et al., 1995), the time constants for the individual secondary structure elements found by this experiment are all within one standard deviation of the mean, with the exception of that for the β-sheet region between residues 40 and 50. They propose that this β-sheet region may achieve a native-like structure in its main chain before other regions. However, the small number of the probes and low signal-to-noise ratio makes suggestions that the conclusion is premature (Balbach et al., 1996).

It should be noted that fluorescence spectroscopy is only sensitive to the tertiary structural changes while both FTIR and two dimensional NMR are sensitive to the alternation in mainchain regions. This explains well why the other techniques have difficulties to find this intermediate with β-structure. In addition, the intermediate of the apo form found here have some difference with that found by Kim (Wu et al., 1996). As mentioned before, they found some regular structures are formed when calcium ion is present because a transition is associated with CD signal changes. Therefore, what they found may include some well established tertiary interaction in β-sheet domain. Without the presence of Ca^{2+}, they can find nothing because no tertiary structure is formed. This does not in anyway mean that the protein is unfolded, indeed the β-structure may be formed but lack tertiary structure, and this partially folded protein can not be seen other than FTIR and 2-D NMR spectroscopy which can detect the changes of main chain region.

Figure Legends

Figure 4.1 The second derivative spectra of the acid form in the amide I' region at 5 °C, 35 °C and 85 °C. The spectra are obtained from the corresponding absorbance spectra shown in 4.2a. The protein was dissolved in 50 mM KCl in D_2O at pH* 2.0. The protein concentration is 8.0 mg/ml .

Figure 4.2 The amide I' absorbance spectra of the acid form a) and the double difference spectra b). The double difference spectra are generated by subtracting the absorbance spectrum at 5 °C shown in a) from those at other temperatures.

Figure 4.3 The temperature dependence of the IR absorbance spectra in the amide I' region. The curves are obtained from double difference spectra shown in figure 4.2b). The transition curves monitored by 1638 and 1669 cm^{-1} are displayed.

Figure 4.4 The apo α-LA absorbance spectra in the amide I' region a) and the double difference spectra b). To generate b) the absorbance spectrum at 95 °C was deducted from the absorbance spectra at the other temperatures.

Figure 4.5 The transition curve obtained from the double difference spectra of the apo form of α-LA (see figure 4.4b) in the presence of 10 mM KCl in D_2O at pH* 6.9. The absorbance difference shown is calculated by subtracting the spectra minima from the spectra maxima in the double

difference spectra (figure 4.4b). The protein concentration of 8.2 mg/ml was used for the measurement.

Figure 4.6 The second derivative spectra of the apo form of α-LA at 5 °C, 35 °C and 80 °C. The corresponding spectra were generated from the absorbance spectra shown in figure 4.3a.

Figure 4.7 The deconvolved double difference spectra of the apo form α-LA at 5 °C and 35 °C. The spectra were obtained by subtracting the deconvoled absorbance spectrum at 95 °C from the corresponding spectra at 5 °C and 35 °C. The larger amplitude of the band at 1629 cm^{-1} and the lower amplitude of the bands at 1637 and 1653 cm^{-1} at 35 °C compared to that at 5 °C suggest that the helical domain is unstructured before the β-sheet domain.

Figure 4.8 The transition curves obtained from the bands at 1629 and 1637 cm^{-1} in the deconvolved double difference spectra. The curves indicate that the denaturation of the helical structures happens around the first transition (about 20 °C) while the melting of the β-structure happens through the second transition (about 40 °C).

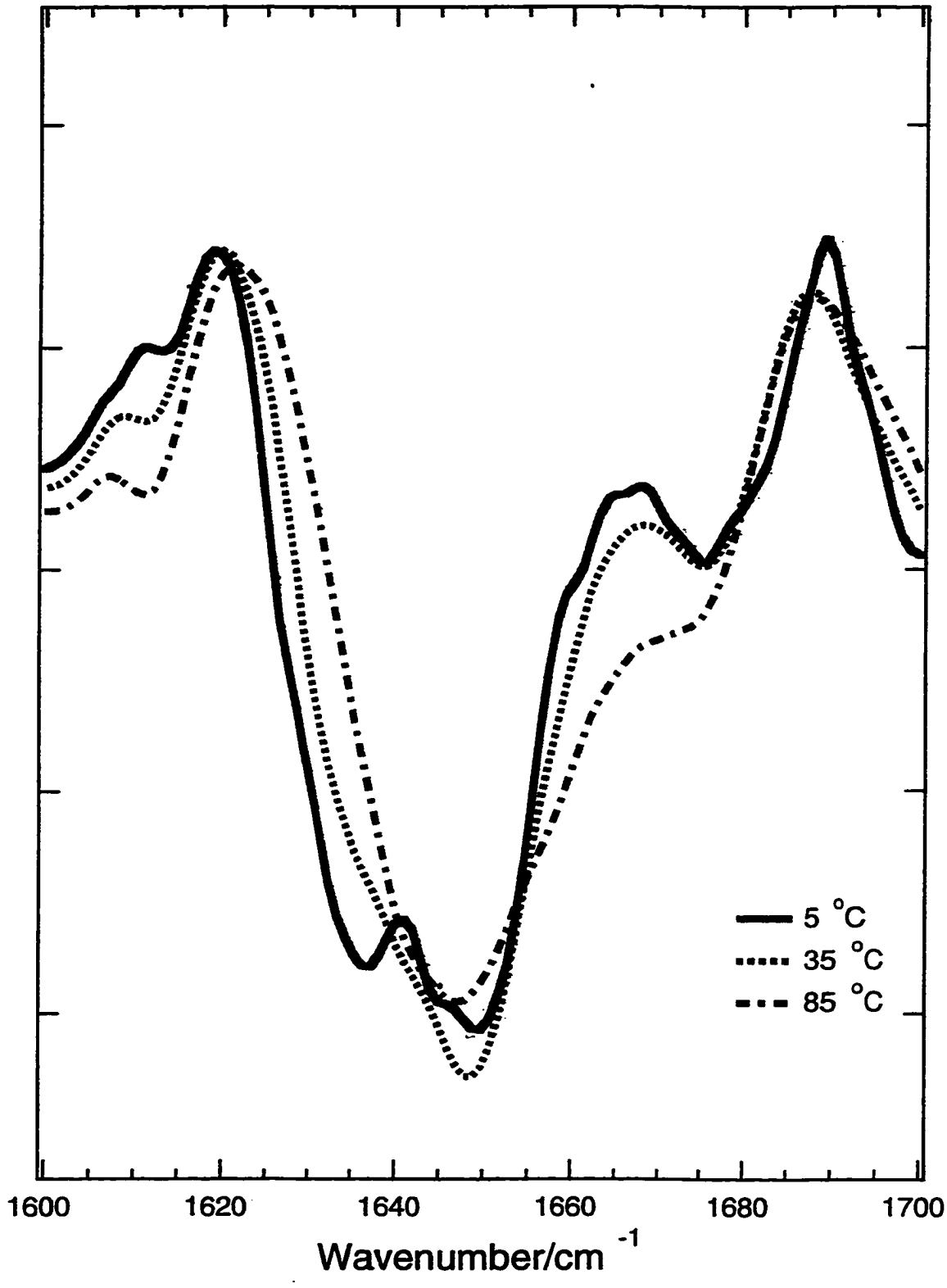

Figure 4.1

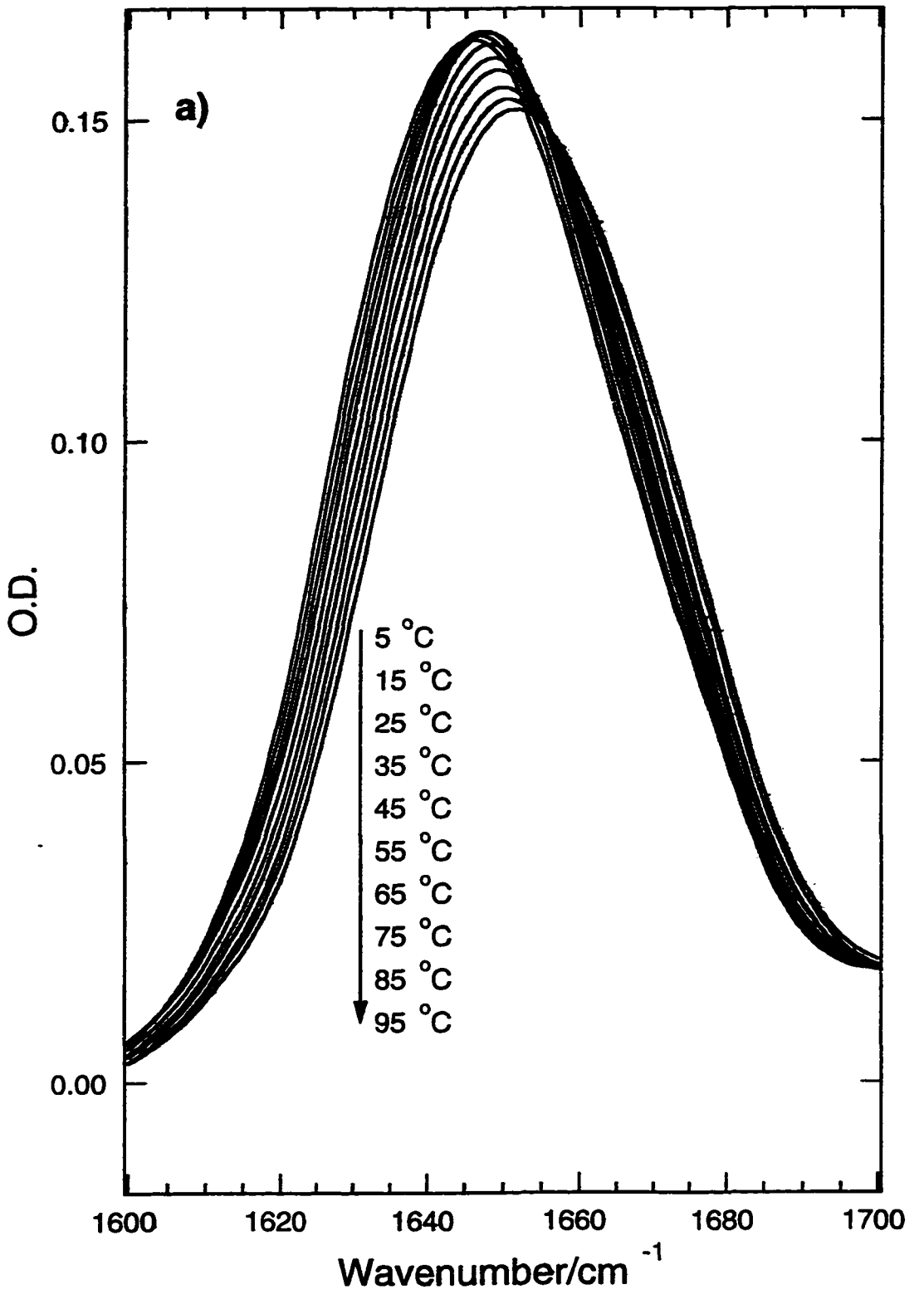

Figure 4.2a

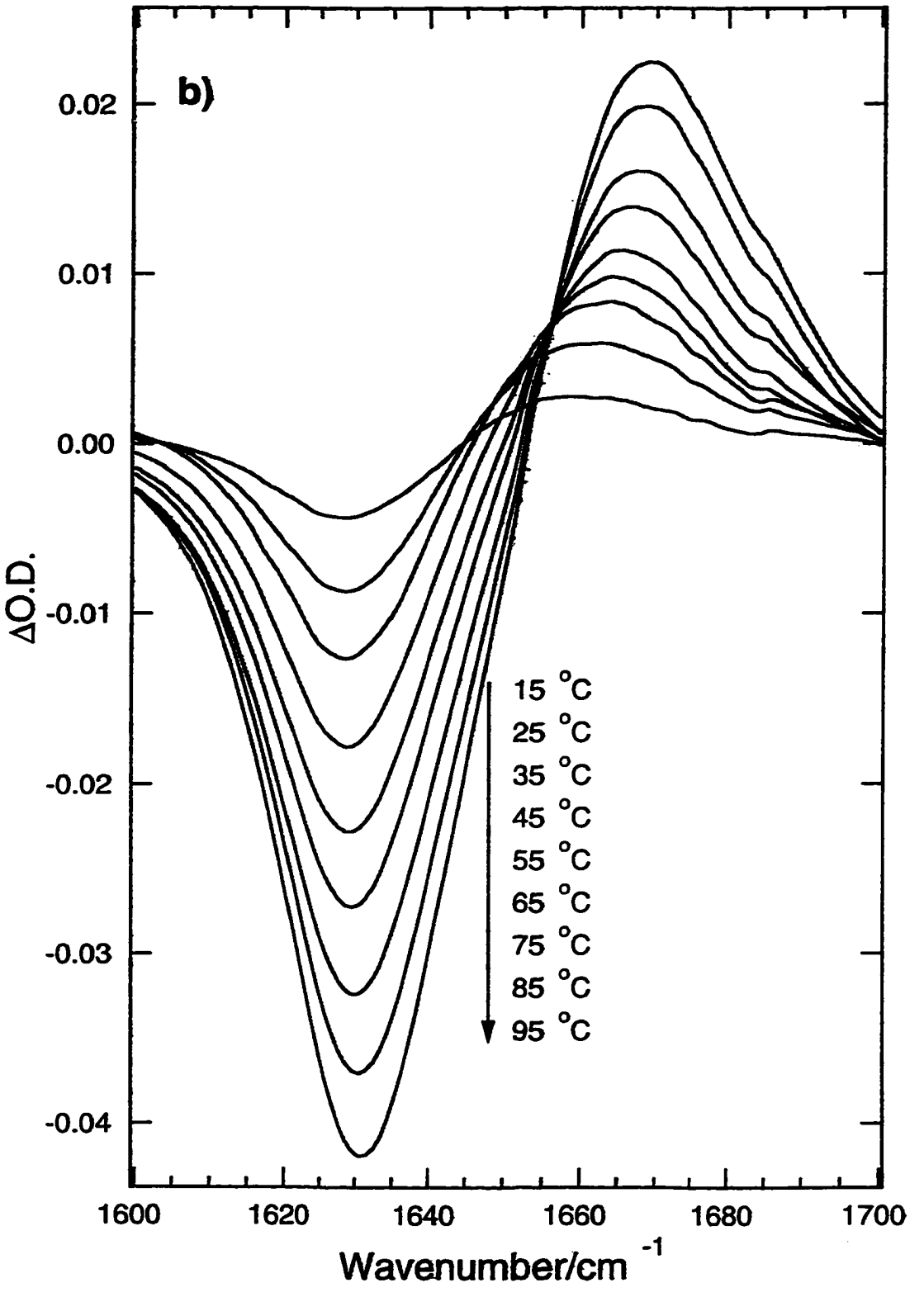

Figure 4.2b

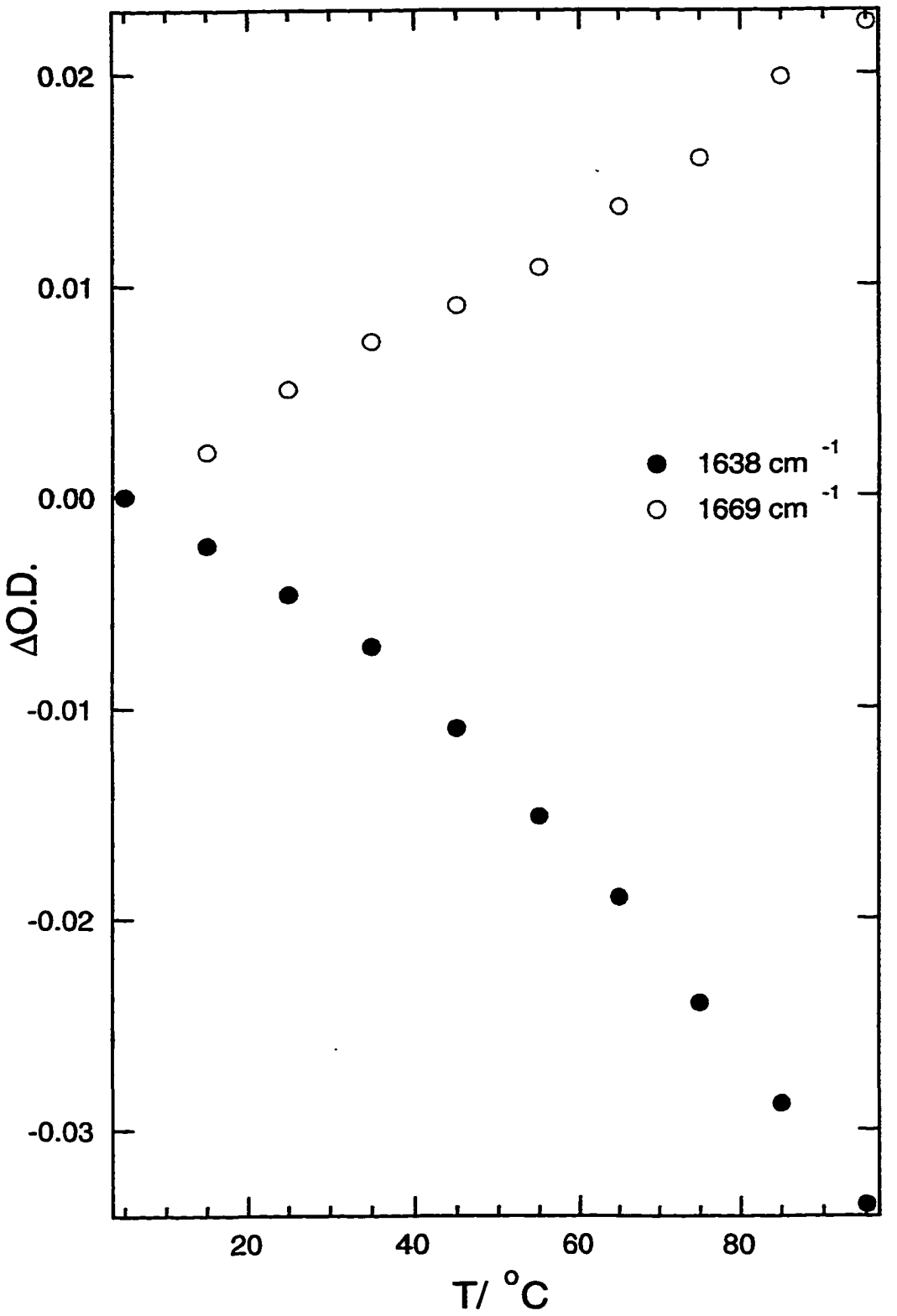

Figure 4.3

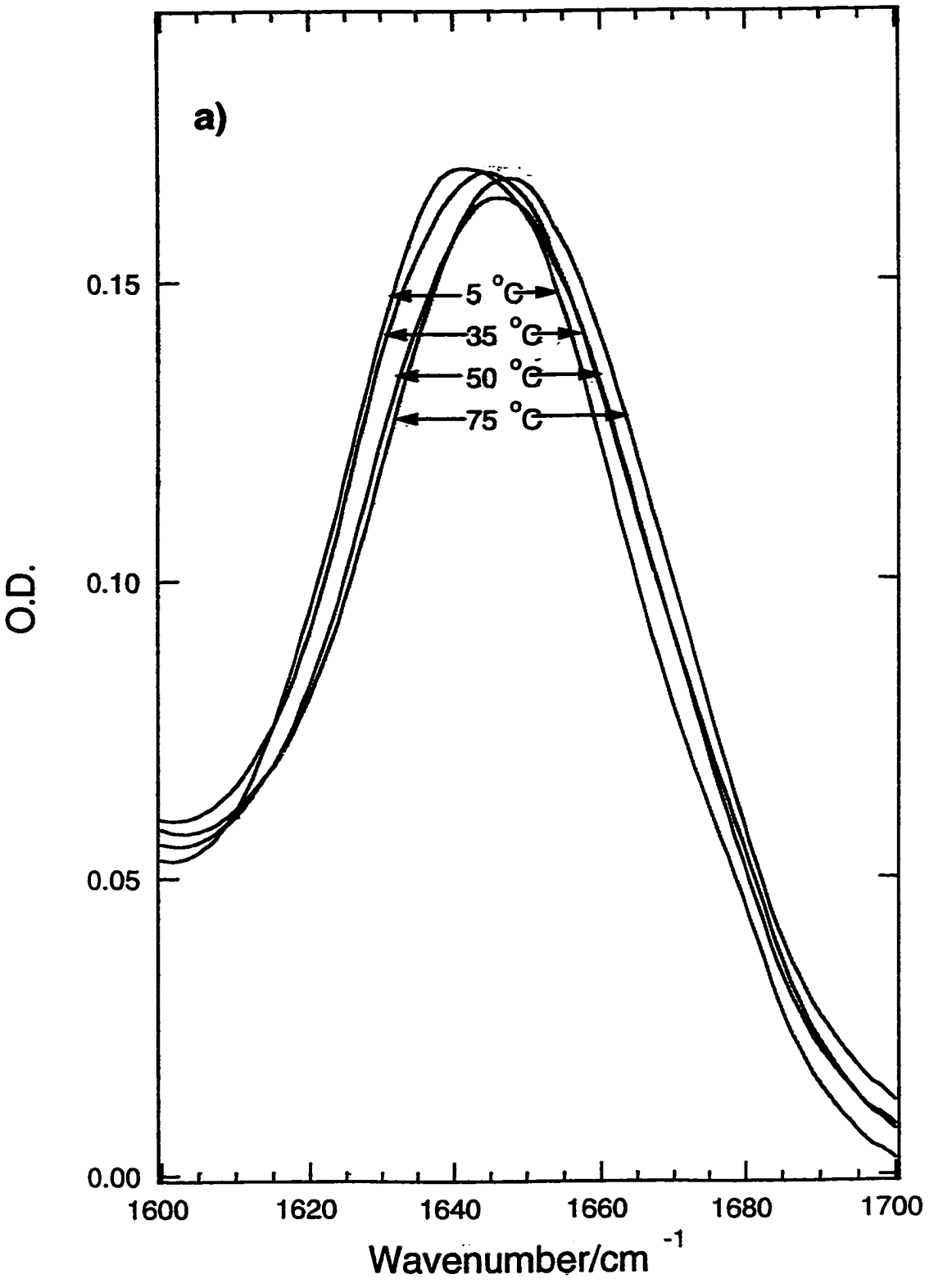

Figure 4.4a

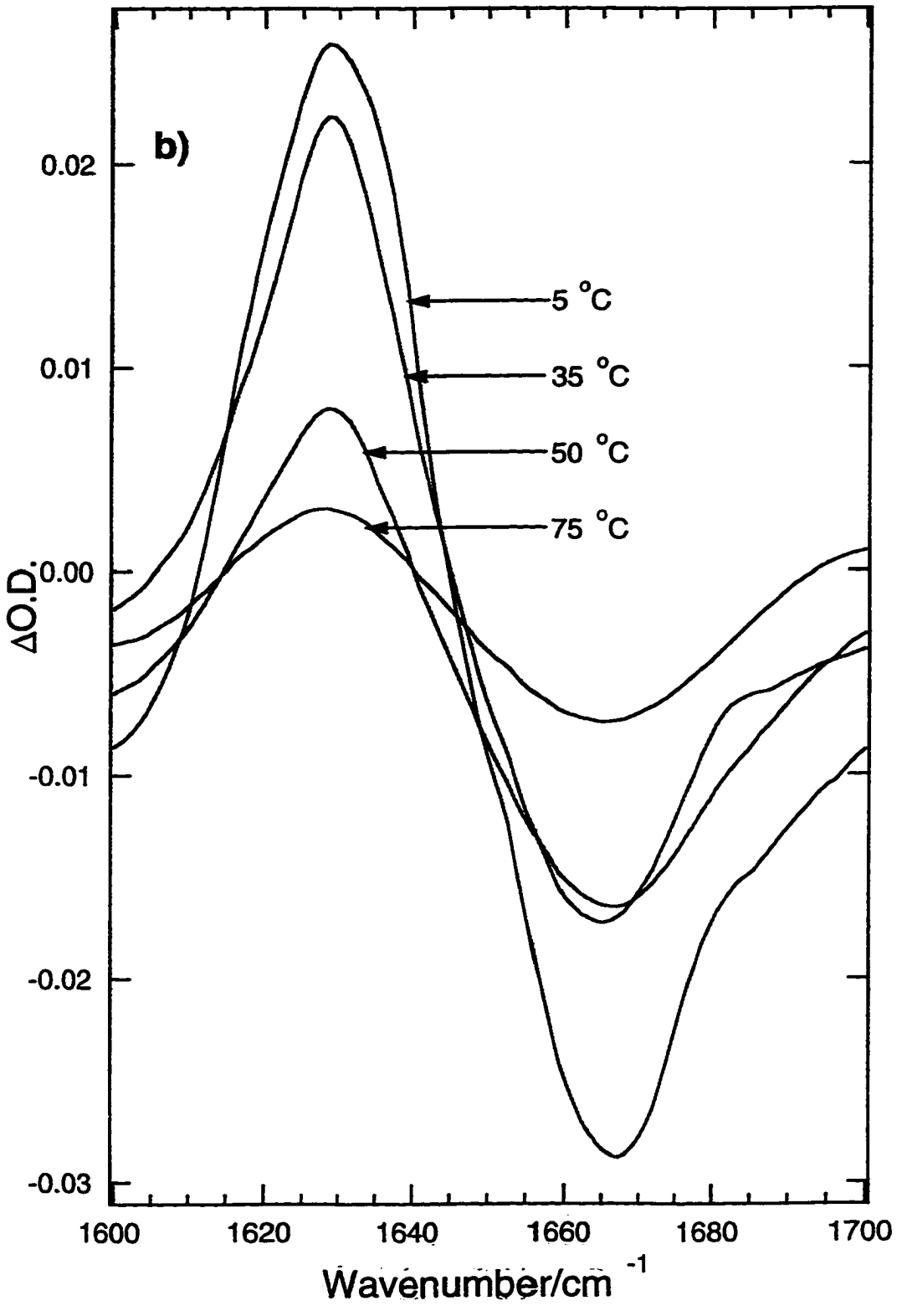

Figure 4.4b

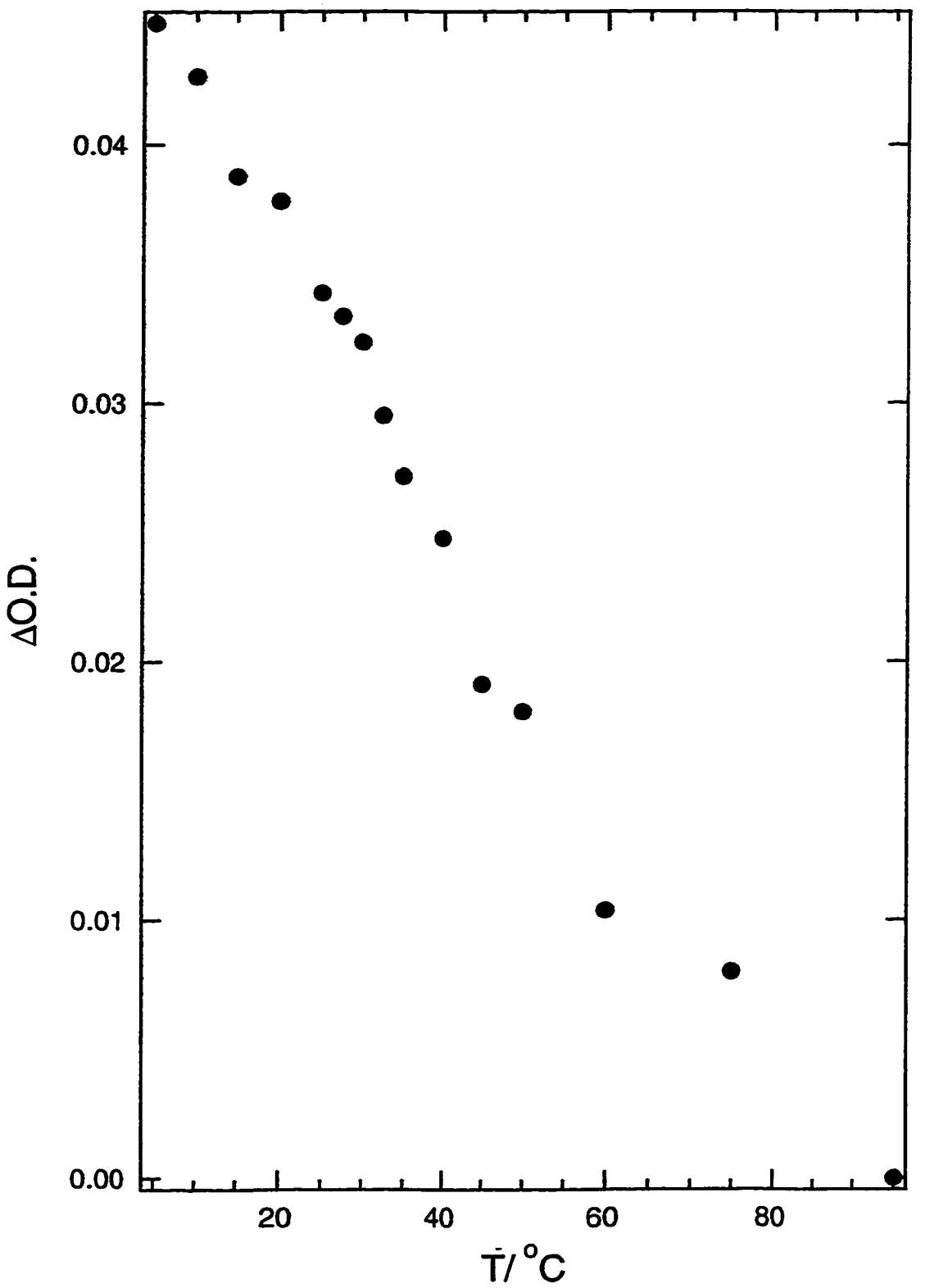

Figure 4.5

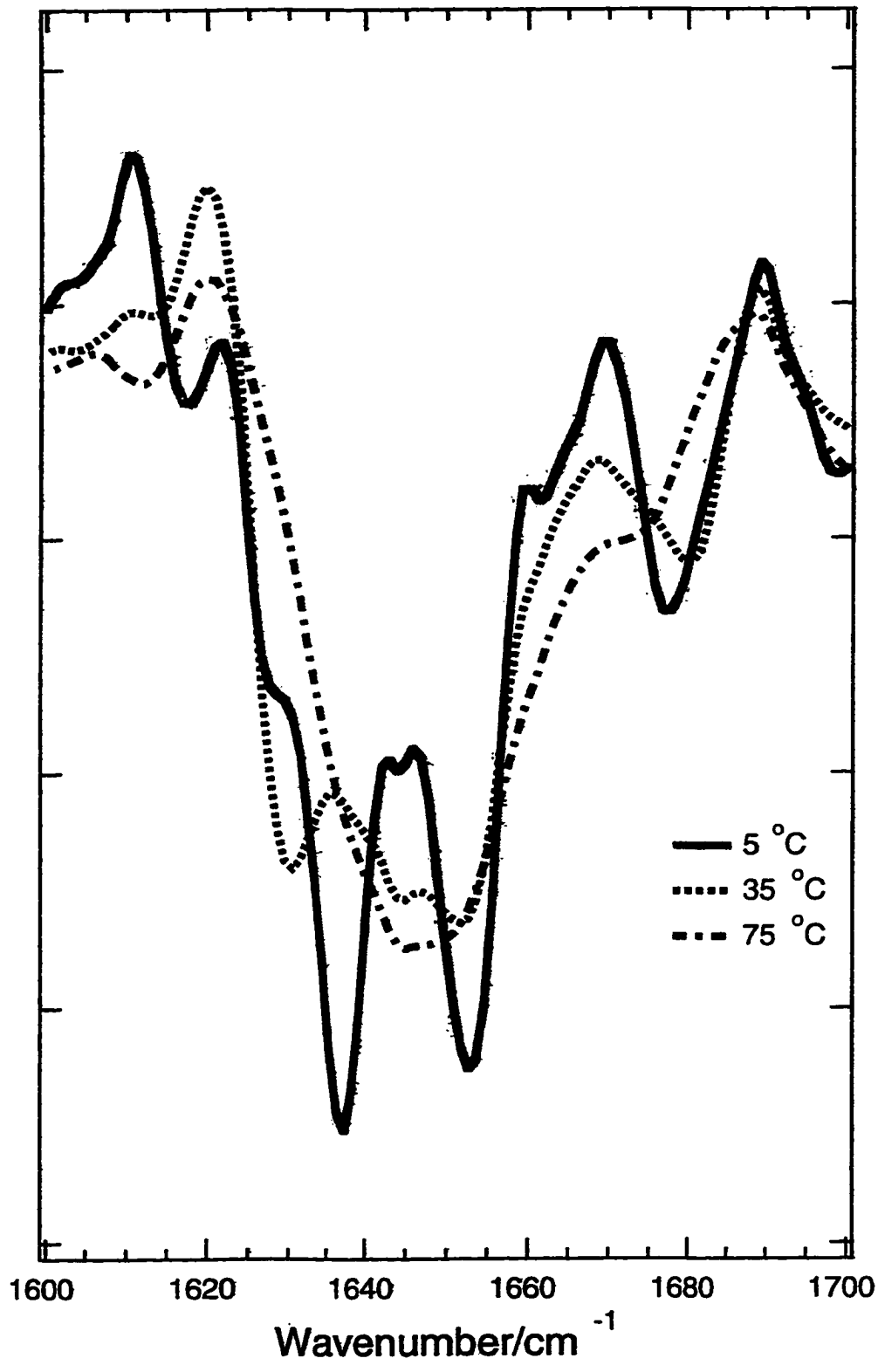

Figure 4.6

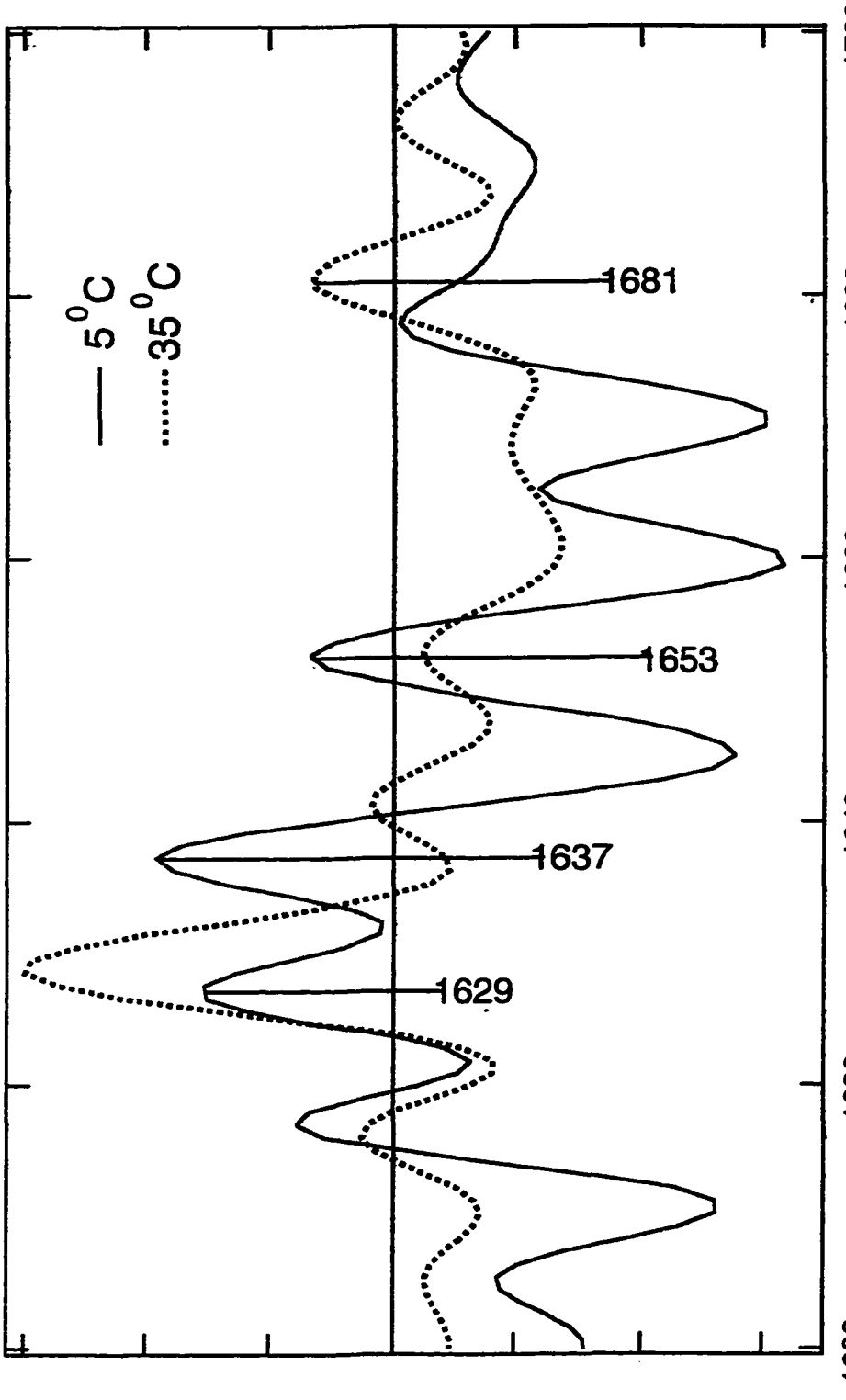

Figure 4.7

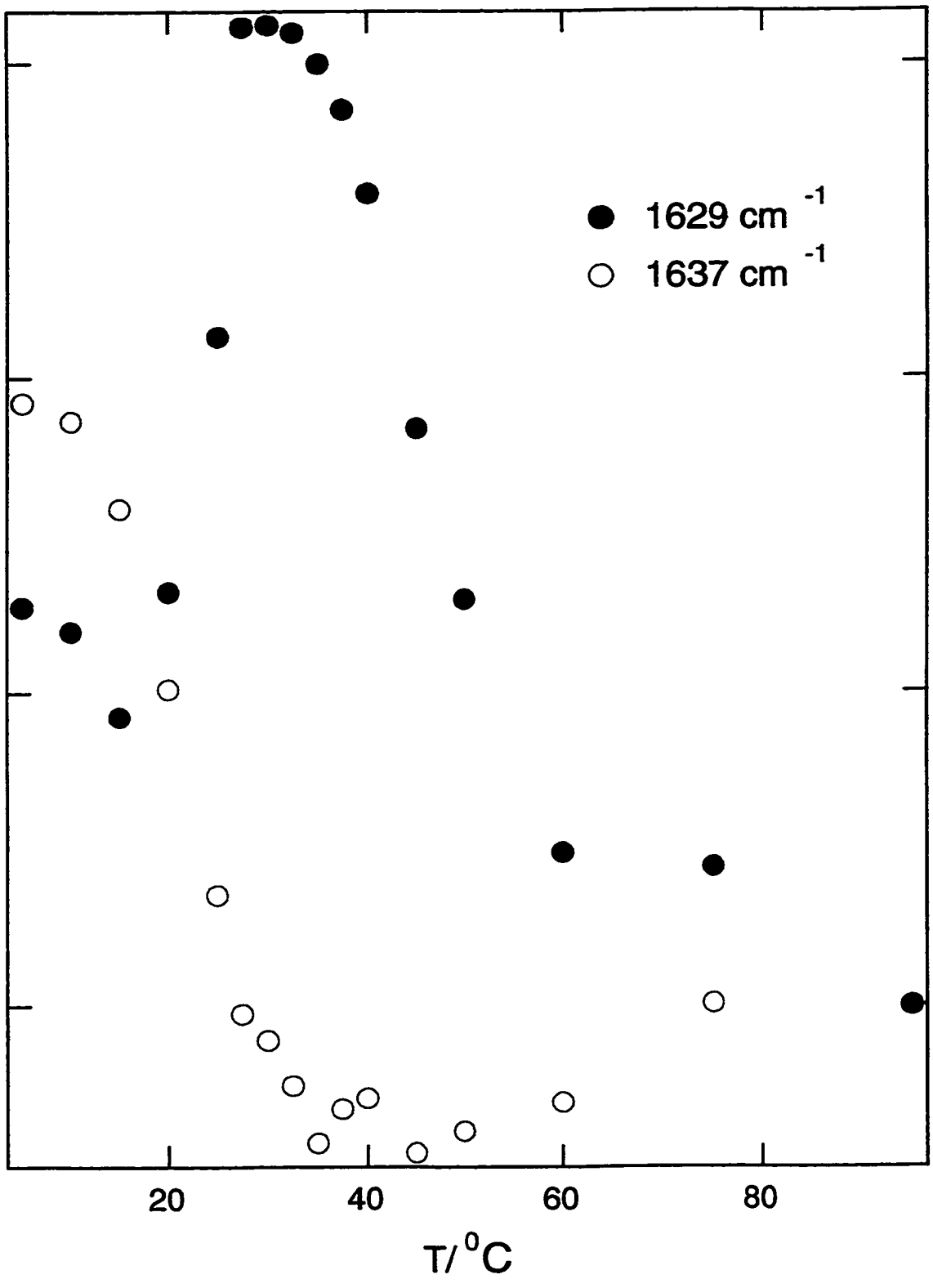

Figure 4.8

Chapter 5 The Melting Behavior of Disulfide Link Destabilized α-Lactalbumin

5.1 Introduction

An appealing feature of α-lactalbumin is the suppereactivity of its 6-120 disulfide bond, presumably caused by local geometry strain (Kuwajima et al., 1990). It is obvious that the function of this disulfide bond is to bring about the stability of the entire protein. The broken 6-120 disulfide linkage will increase the entropy of unfolded state, thus decreasing the unfolding energy and destabilize the native protein. The broken disulfide bond of 6-120, together with removal of the bound calcium ion, leads to a molten globule state at room temperature while α-lactalbumin with only 6-120 bond removed keeps its native state (Ewbank & Creighton, 1991).

In this chapter, we report a heat denaturation study of two forms of α-lactalbumin with disulfide bridge 6-120 removed, the holo 3ss form and the apo 3ss form. In addition, the cystein 6 and 120 are specifically blocked. The reasons are discussed in details in the following sections. We will observe that the two transitions of the apo form actually are associated with separate domain denaturation. The apo 3ss form basically has the same behavior as the apo form except that one transition is shifted out of the experimental temperature range due to the destabilized domain caused by the broken 6-120 disulfide bond.

5.2 Materials and Methods

5.2.1 Ellman's Method

The superreactivity of the disulfide bond 6-120 gives us opportunity to specifically cleave this bridge while keeping other SS bonds intact. DTT is a strong reductant and was used to cleave the SS 6-120 in this study. However, the extent of the bond being cut is time dependent, concentration dependent and temperature dependent. We should first mix the protein with DTT at fixed concentration and temperature but, at later times, to check how long it need for the 6-120 bond to be cleaved completely. To this end, first we should figure out how to separate the DTT from the protein. Second, we need to design an effective and accurate method to measure the free cysteins remaining in each protein. The protein can be easily separated from DTT quickly by passage a small G-25 sephadex. We use Ellman's method to reach the second goal.

In 1959, Ellman introduced a reagent, 5,5'-dithiobis (2-nitrobenzoic acid) (DTNB), which has found extensive use in the estimation of free thiol groups in native and denatured proteins. The procedure is based on the reaction of the thiol with DTNB to give the mixed disulfide and 2-nitro-5-thiobenzoic acid (TNB) which is quantified by the absorbance of the dianion (TNB^{2-}) at 412 nm (Eq. 5.1) (see Riddles et al., 1979).

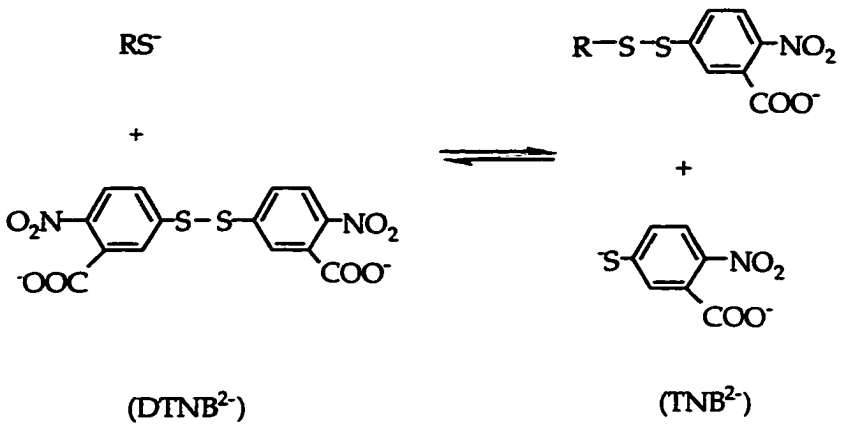

$(DTNB^{2-})$ (TNB^{2-})

(5.1)

In the case that large excessive DTNB is added to the reduced protein, all the thiol groups react with DTNB (Equ 5.2), thus the absorption coefficient will be given by the following equation (Equ. 5.3):

$$ArSSAr + RS^{-} \longrightarrow ArS^{-} + ArSSR + ArSSAr\,(exess) \tag{5.2}$$

$$\varepsilon 412(TNB^{2-}) = \frac{\Delta A - A_{ArSSR} + (ArSSAr - ArSSAr(excess))}{[RS^{-}]} \tag{5.3}$$

where ΔA is the difference between the final absorbance at 412 nm and that of the DTNB initially, appropriately corrected for dilution. It follows that

$$\frac{\Delta A}{[cysteine]} = \varepsilon 412(TNB2-) + \varepsilon 412(ArSSR) - \varepsilon 412(ArSSAr)$$

$$= \text{constant} \tag{5.4}$$

The constant value given by equation 5.3 can be obtained by plotting the ΔA against the concentration of cystein. We calibrate this constant by measuring the concentration of thiol group of various known concentration.

The slope we got in the linear region (Figure 5.1), 14,045 $M^{-1}cm^{-1}$, corresponds to the constant value expressed in equation 5.4.

In the real measurement, 400 µl DTNB is deposited in an absorption cell. 200 µl protein or other molecules containing thiol groups is mixed with the 400 µl DTNB, producing the yellow solution which has a local maxim around 412 nm. Obviously, the concentration of the thiol groups should be given by the following equation instead of the equation 4.4 considering the volume difference after mixing(Equ. 5.5)

$$[RS^-]=\frac{3A_f-2A_i}{\varepsilon_{412}^{TNB^{2-}}} \qquad (5.5)$$

Figure 5.2 shows the meaning of A_f and A_i.

Because of the presence of the O_2 in the solution, the TNB^{2-} formed in the reaction is usually partly oxidized back to DTNB, resulting in the lose of the absorbance at 412 nm. To avoid this problem, all the reagent and the protein solution used for the absorption measurement undergo the degassing process before deposited in the cell.

In reality, 0.5 mM DTT was deposited in the same volume of 0.1% by volume weight intact α-lactalbumin. The reaction was proceeded at 5 °C in various time and the number of disulfide bond cleaved each molecule was calculated by measuring the concentrations of both thiol group and the protein. The ratio of these two concentrations gives the number of the thiol group in each protein molecule. Our measurement shows that the time it

needs for the complete cleavage of the 6-120 disulfide bridge at 5 °C can be anytime between 60 and 120 minutes.

The disulfide bond of protein was cleaved by the presence of excessive DTT. The mechanism of this reaction has been reported to be the bimolecular process (Kuwajima et al., 1990). Thus the reaction speed should be determined by the following equations if excessive DTT is present:

$$d[3SS\text{-}\alpha\text{-}LA] = k[\alpha\text{-}LA][DTT]dt \quad (5.6)$$

since $[3SS\text{-}\alpha\text{-}LA] + [\alpha\text{-}LA] = \text{const.}$, so:

$$[\alpha\text{-}LA] = \text{const} \exp(-k[DTT]t) \quad (5.7)$$

the lifetime of α-LA:

$$\tau = 1/k[DTT] \quad (5.8)$$

Therefore, the reaction time to have all 6-120 disulfide bonds cleaved is in inverse proportion to the concentration of DTT. It follows that the reaction time it takes for the mixture of 1% α-LA and 5 mM DTT to have all the 6-120 disulfide bonds cleaved at 5 °C will be from 6 minutes to 12 minutes.

5.2.2 How to trap the 3SS form of α-lactalbumin

Because those intermediates of α-lactalbumin with disulfide bond broken have both disulfides and free thiols, they must be trapped in a stable form to be structurally characterized.

There are two commonly used trapping methods: acid quench (which greatly reduces thiol reactivity by minimizing the reactive thiolate anion) and irreversible covalent modification of thiol groups with sodium iodoacetate or iodoacetamide. Acid trapped intermediates can only be characterized at acid pH, however, where the single calcium ion dissociates from α-LA and radically changes the protein's conformation. Therefore the intermediate was trapped by covalent modification, which has the advantage of being irreversible and which allowed characterization of the intermediates under the same conditions as used for the studies on disulfide formation and breakage. However, the blocking groups introduced may influence the conformational properties of the protein.

The carboxymethylated derivative of α-lactalbumin introduced by sodium iodoacetate have two units of negative electric charge attached to the blocked terminals. As a consequence, proteins are destabilized by the positive electrostatic energy between these two charges. Compared to this, the cam-3ss- α-LA (cam$^{6\text{-}120}$ α-lactalbumin) introduced by iodoacetamide, a three disulfide carboxyamidomethylated derivative of α-lactalbumin, do not have these charges existing on the blocked terminals. In addition, the introduced blocking groups might affect the conformation and stability of the protein due to their steric bulk and polar groups, but all these were demonstrated to have negligible effects on the stability (Ewbank &

Creighton, 1993(b)). In this study, we investigate the cam-3ss α-LA to eliminate the influence of ionization of the modified thiol groups in cm-3ss α-LA.

The basic principal of this blocking method is revealed in the following equation where the thiol group acts as a nuclearphile to attack the methyl group to make the I^- a leaving group.

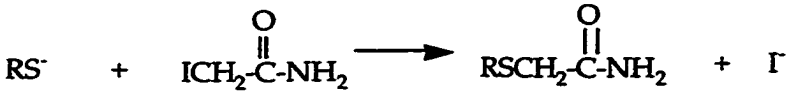

$$RS^- + ICH_2\text{-}C(=O)\text{-}NH_2 \longrightarrow RSCH_2\text{-}C(=O)\text{-}NH_2 + I^- \qquad (5.9)$$

As a results, the I^- is replaced by thiol groups which is tightly attached to the main body of protein.

5.2.3 Preparation of CAM-3SS Form

1% bovine α-LA in Tris-HCl buffer and 10mM $CaCl_2$ was mixed with same volume of 5mM DTT solution in the same buffer for 9 minutes at 5 °C and pH 7.3. The number of thiol groups of each protein molecule was 2±0.1 as determined by Ellman's method (Kuwajima et al., 1990). The reaction was quenched after 9 minutes by adding same amount of 10 mM Iodoacetamide. After the reaction proceeded for 40 minutes under dark at room temperature and pH 7.9, the pH was adjusted to 3. Then the product was dialyzed against acetic acid at same pH (Eyles et al., 1994), followed by dialysis against 0.1 M ammonium acetate (pH5) (Kuwajima et al, 1990). All

the above processes were made in the presence of excess $CaCl_2$. Then the protein solution was further dialyzed against distilled water without $CaCl_2$. The cam-3ss α-LA was lyophilized overnight and dissolved in D_2O. Then the solution was adjusted to pH* 7.0 and allowed the H-D exchange for four hours at room temperature. After this, it was lyophilized again. To further prove exactly three disulfide bridges remain in the protein molecule, excess of DTT was added to apo cam-3ss α-LA at 55 °C (the apo cam-3ss α-LA is denatured in this condition) to cleave all disulfides. Then the completely reduced protein was passed through sephadex G-25. The number of thiol groups inside protein was analyzed by Ellman's method. It was found that more than 95% of the protein sample adopt 3ss form. Prior to -SH group determination, protein was separated from DTT by a fast gel filtration on sephadex G-25. Then 200 μl degassed protein solution with concentration around 1 mg/ml was added to 400 μl degassed 2 mM DTNB to produce Ellman's reagent 2-nitro-5-thiobenzoate(TNB^{2-}). A molar extinction coefficient for TNB^{2-} of 14,045 $M^{-1}cm^{-1}$ as mentioned above at 412 nm was used (Riddles et al, 1978). After these process, the cam-3ss α-LA were produced. The broken disulfide linkage is 6-120 according to Kuwajima et al. (Kuwajima et al., 1990).

In the above process, calcium is present at the very beginning to stabilize the three disulfide derivative of α-lactalbumin. Denatured 3ss form of α-LA tends to adopt the intramolecular disulfide exchange arrangement, so the blocked thiol group may not be the cystein 6 and 120. In the native protein, as the case when the 3ss form has calcium ion bond and is put in room temperature, the protein keeps its rigidity. The broken

disulfide 6-120 can not be mobile enough to exchange with the other disulfide pairs outside the local region of SS 6-120. The other three disulfide bonds are buried inside α-LA. In the native condition, solvent is excluded from this core region. It follows that their cleaving process adopts slow phases. In the denatured protein, as the case of the 3ss form of α-LA at 55 °C, all disulfide bonds are exposed to solvent. The easy access of DTT to these SS pairs completely eliminate their sluggish reaction with DTT when protein is in its native condition.

5.2.4 Preparation of Protein Solutions

The holo bovine cam-3ss α-LA was dissolved in D_2O buffer. The apo bovine cam-3ss α-LA was made by depositing same volume of 10 mM EDTA solution in our 5 °C cold room. Before FT-IR measurement, the protein solutions were equilibrated with the reference with a sephadex G-25 column at 5 °C. Both protein and buffer samples were collected from the same elution to ensure balanced HDO present in buffer and protein solutions. For the apo cam-3ss form, the samples were in the presence of 10 μM EDTA to eliminate the possible Ca^{2+} contamination. The sample aliquots after the column were used to determine the pH* and concentration. The pH value of the protein in D_2O was adjusted by DCl and NaOD.

Similar to the reversibility of the apo form discussed in the section 4.2.3, we conclude that the transitions of the apo cam-3ss form are reversible although a small portion of them are apparently irreversible.

IR spectra were acquired on a Bruker IFS-66 Fourier-Transform Infrared Spectrometer using MCT detector. The instrument, methods and parameters used to process the data are exactly same as those described in chapter 4.

5.3 Results and Discussion

5.3.1 The holo cam-3ss form of α-lactalbumin

For our study, the reasons why the thiol groups are blocked are based on the following three facts.

1. One is the tendency for intermolecular aggregation in MG.
2. One is the tendency for oxidation of thiol groups back to disulfide bridges at high temperature. It has been shown that this reaction time constant is about two hours at room temperature with the presence of air.
3. Intramolecular disulfide exchange after the protein is denatured will give us various non-native disulfide bonds, resulting in different intermediates.

Indeed, the FTIR spectra of apo 3ss α-LA without blockage has been shown to fluctuate with time even below room temperature. This may come from either intermolecular disulfide aggregation or intramolecular disulfide exchanges.

The absorption spectra and double difference spectra at elevated temperatures are shown in figure 5.3a and 5.3b respectively. The double difference spectra in figure 5.3b are used to generate the transition curves

described below. The transition curve of the holo cam-3ss α-LA in the presence of 10 mM KCl as displayed in the figure 5.4 exhibits a major transition similar to the holo α-LA except that the transition temperature is shifted down from upper sixties to around 56 ^{o}C. In agreement, the T_m of the holo cam-3ss α-LA in 10 mM Tris buffer and H_2O as measured by calorimetric method is found to be 55 ^{o}C. This shift is easy to understand by noting that the broken disulfide connecting Cys 6 and Cys 120 destabilizes the protein. Structure studies by circular dichroism (Eyles et al., 1994) also indicate that both native state and the molten globule state of the cam-3ss protein are significantly less stable than their unmodified counterparts. Figure 5.5 shows the transition curves monitored from 1638 cm^{-1} and 1669 cm^{-1} in double difference spectra. These curves further indicate the corresponding transition is cooperative.

In addition, some structural change appear to happen around 25^{o}C and can be found from the transition curve in figure 5.4. More interestingly, the holo cam-3ss α-LA involves substantial decrease of the band 1653 cm^{-1} and increase of band 1645 cm^{-1} between 20 ^{o}C and 30 ^{o}C while the alternation of other bands are similar in the holo and holo cam-3ss α-LA. This feature can be seen from the second derivative spectra (Figure 5.6). This is different from the holo α-LA which has cooperative decrease of band 1653 cm^{-1} and increase of 1645 cm^{-1}. Not surprisingly, if we note cystein 6 and cystein 120 are close to N and C termini which are also close to protein surface, this suggests a process involving solvent penetration. It follows that some parts of the helical structures are exposed to solvent or unfold, resulting in a downshift of 1653 cm^{-1} band, while the other parts of

protein intact and rigid. ANS binding fluorescence of the holo cam-3ss α-LA at 25 °C was found to be comparable to that of the apo α-LA (Ikeguchi et al., 1992), and this was thought by Creighton to be the consequence of a local relaxation in the region of the cleaved disulfide bond (Ewbank & Creighton, 1993a; Ewbank & Creighton, 1993b) which is consistent with our results. More interestingly, the pulsed amide hydrogen exchange labeling study of lysozyme at 20 °C, which is homologous to α-lactalbumin, indicates that the protection from exchange is approximately 100-fold lower in the N and C terminal regions of cm-3ss-lysozyme, near the site of modification, than that found in intact protein (Eyles et al., 1994). This suggests that N and C terminal regions be largely accessible to solvent after the disulfide bridge is broken. Indeed, at room temperature, holo cam 3ss α-LA adopts a near-fully folded conformation (Ewbank & Creighton, 1993b) as proved by CD, electrophoresis and fluorescence spectra. The relatively slowly reducing remaining disulfide bonds (Ewbank & Creighton, 1993a) are also strong evidence that the remaining part of protein keeps its rigid structure after the disulfide bond 6-120 is broken.

The cooperative denaturation of helical domain and β-sheet domain and the downshift of T_m after disulfide 6-120 is removed further shows that the stability of β-sheet domain depends on helical domain which is stabilized partly by disulfide bridge 6-120. The broken disulfide bond 6-120 destabilizes the helical domain. It follows that β-sheet domain is destabilized simultaneously, resulting in a lower T_m than that found in intact α-LA.

5.3.2 The apo cam 3ss form of α-lactalbumin

The temperature dependence of the partial heat capacity of the apo cam-3ss form in H_2O measured by calorimetric technique shows a wide band centered at 18 °C (Hendrix et al., 1996). It was also reported that the apo cam-3ss α-LA exhibited CD spectrum somewhat similar to the native protein at 2 °C (Hendrix et al., 1996). At 25 °C, its CD spectrum was similar to the acid form. From this, Creighton proposed this form to be a molten globule (Ewbank & Creighton, 1991). These indicate some denaturation happens before room temperature.

It is interesting to further investigate the apo 3ss form of α-LA using FTIR. Due to the same reason as the apo form, the Ca^{2+} free form of the cam-3ss α-LA was investigated in AgCl windows. The transition curve (Figure 5.8) monitored by double difference spectra (Figure 5.7b) indicates a transition which is quite similar to the second transition of the apo α-LA. The approximate T_m is around 40 °C. However, there is no strong evidence that an additional transition happens at low temperature based only on double difference spectra.

Further structural analysis by second derivative spectra (Figure 5.9) indicates that the apo cam-3ss form at 5 °C is not completely folded. Its second derivative spectrum is obviously different from that of the holo form, suggesting a partially denatured protein. A relatively strong band at 1629 cm^{-1} and substantially diminished bands at 1638 and 1653 cm^{-1} as compared to the native α-LA indicates the helical domain has almost been

denatured while the β-structure domain remains folded. As temperature increases to 27 °C, the bands at 1638 and 1653 cm^{-1} disappear completely and are replaced with a wide band at 1646 cm^{-1}, a typical IR band for denatured protein. On the contrary, the intensity of the band at 1629 cm^{-1} increases a bit. This reveals that the helical domain is denatured completely at higher temperature, while the β-structure domain still keeps folded. Further elevating the temperature results in β-structure denaturation, and this is associated with the major transition around 40 °C. The small structural alteration at low temperature infers some transition may happen. However, the absence of this transition in double difference spectra suggests that the T_m of this transition may beyond the low extreme of the experimental range. As a result, the structural changes found at low temperature in our FTIR measurement would only catch the end of the transition.

Figure 5.10 shows the deconvolved double difference spectra of the apo cam-3ss form. The 80 °C spectrum is subtracted from 5 °C and 27 °C spectra respectively. The predominant band at 1629 cm^{-1} shown in the spectra at 5 and 27 °C indicates that β-structure is dominant in the protein. Compared to that at 5 °C, the bands at 1638 and 1653 cm^{-1} at 27 °C have little changes, suggesting the helical domain has been denatured almost completely at this temperature. Moreover, the diminish extend of these two bands from 5 °C to 27 °C is significantly smaller than the amplitude of the band at 1629 cm^{-1}. A α-lactalbumin contains much more helical components than β-structures. This implies that only small amount of helical structures was detected to be denatured in our experimental

temperature range. Therefore, most of the helical structures is denatured below 5 ^{o}C and, unfortunately, is not detected in our experiment.

The transition curves (Figure 5.11) based on the deconvolved double difference spectra provide us with further evidence of this separate denaturing behavior. The decreasing curve of the band at 1638 cm^{-1} ranging from 5 ^{o}C to 15 ^{o}C suggests the helical structure has already begun to be denatured. The low temperature baseline may be beyond the low extreme of the experimental range. This transition temperature can not be determined because of the absence of the low temperature baseline. It may be below 5 ^{o}C. The transition curve monitored at 1629 cm^{-1} (figure 5.11) also indicates that some transition happens at low temperature. This curve increases around 5^{o}C, suggesting the formation of β-structure at low temperature. This, together with the transition found at low temperature for helical structure, demonstrates that some β-structure is formed while most of the helical structure is unstructured through the first transition. The second transition is only associated with the denaturation of β–structure.

Noticing that the only difference between the apo form and the apo cam-3ss form is the disulfide bond 6-120, we are not surprised to see the transition temperature of the helical domain of cam-3ss shift down significantly, since the disulfide bond 6-120 is located in the helical domain and brings two ends of the polypeptide together.

As predicted, the broken disulfide bond is helpful to destabilize the helical domain, resulting in a downshift of the first transition. The smaller

overlap of the transitions makes the structure of the intermediate easier to be determined. The weaker band signals from the helical domain provide the evidence that the helical domain is largely denatured. The similarity of the transitions of the two domains to those of the apo form reveals the same non-cooperative denaturing mechanism of these two calcium free forms It is interesting to note that the T_m of the second transition coincides with the T_m found in the apo form. This suggests that the apo and apo cam-3ss forms have a similar intermediate which is denatured around 40 ^oC. This is additional evidence that the helical domain and β-structure domain are denatured independently after calcium ion is removed.

5.4 Conclusions

Our FT-IR study of the holo cam-3ss and the apo cam-3ss forms of bovine α-lactalbumin arrives at the following three direct conclusions:

1. The function of disulfide bond 6-120 in α-LA is to stabilize the folded protein as expected.
2. The cooperativity of the denaturing behavior of helical and β-structural domains is determined by the presence of the calcium ion. Upon removal of this ligand, the helical domain denatures first, followed by denaturation of the β-sheet domain.
3. The intermediate formed after the helical domain melts exhibits somewhat more β-structure than that shown in the native protein.

Figure Legends

Figure 5.1 The absorption difference ΔA as a function of the concentration of cystein. ΔA is calculated as shown in figure 5.2. Only the linear region is used to calculate the slope.

Figure 5.2 Schematic presentation of the absorption of the mixture of DTNB with the molecules containing thiol groups. The absorption was monitored by 412 nm which corresponds to the absorption maxima of TNB^{2-}. $\Delta A = 3A_f - 2A_i$ was used to calculate the absorption difference shown in figure 5.1.

Figure 5.3 The holo cam-3ss α-Lactalbumin IR absorbance spectra a) and its double difference spectra b). The spectra shown in a) is used to generate the spectra in b) where the spectrum at 5 °C in a) is subtracted from the spectra at other temperatures.

Figure 5.4 The transition curve of the holo cam-3ss form α-LA generated by subtracting the spectra minima from the maxima in double difference spectra shown in figure 5.3b). The protein was dissolved in D_2O with 10 mM KCl and pH* 6.8. The protein concentration is 3.1 mg/ml.

Figure 5.5 The transition curves of the holo cam-3ss α-LA obtained from the amplitude at 1638 cm^{-1} and 1669 cm^{-1} in the double difference spectra (see 5.3b).

Figure 5.6 The second derivative spectra of the holo cam-3ss α-LA at 5 °C, 35 °C and 95 °C. The spectrum at 5 °C is a typical spectrum of native α-LA while the spectrum at 95 °C is similar to the high temperature unfolded protein (see chapter 3). A local structural change happens at room temperature, and the spectrum at 35 °C demonstrates an asymmetric decrease of the bands at 1638 and 1653 cm^{-1} which are marker bands of the helical domain.

Figure 5.7 The IR absorbance spectra of the apo cam-3ss form in the amide I' region a) and the corresponding double difference spectra b). To generate b), the spectrum at 80 °C in a) was subtracted from the absorbance spectra at the other temperatures.

Figure 5.8 The transition curve of the apo cam-3ss form of α-LA obtained by subtracting the spectra maxima from the spectra minima in the double difference spectra in figure 5.7b. The protein concentration is 7.5 mg/ml with pH* 7.2 before measurement. The protein was present in 10 mM KCl. Obviously only one unequivocal transition can be found based on this curve.

Figure 5.9 The second derivative spectra of the apo cam-3ss form of α-LA. The temperature s of the above spectra are 5, 27 and 80 °C respectively. The spectrum at 27 °C suggests that the intermediate populated at room temperature exhibits dominant β-structure.

Figure 5.10 The deconvolved double difference spectra of the apo cam-3ss α-LA at 5 °C and 27 °C. These spectra were generated by subtracting the deconvolved spectrum at 80 °C from the deconvolved spectra at the 5 °C and 27 °C. Similar to the apo form, the dominant band at 1629 cm^{-1} shown in both spectra reflects the helical domain has been largely denatured at the corresponding temperatures.

Figure 5.11 The transition curves obtained from the deconvolved double difference spectra at 1629 cm^{-1} and 1637 cm^{-1}. The major transition shown in the curve monitored at 1629 cm^{-1} is indicative that the β-structure is denatured at higher temperature compared to the early melting behavior of the helical domain suggested by the curve monitored at 1637 cm^{-1}.

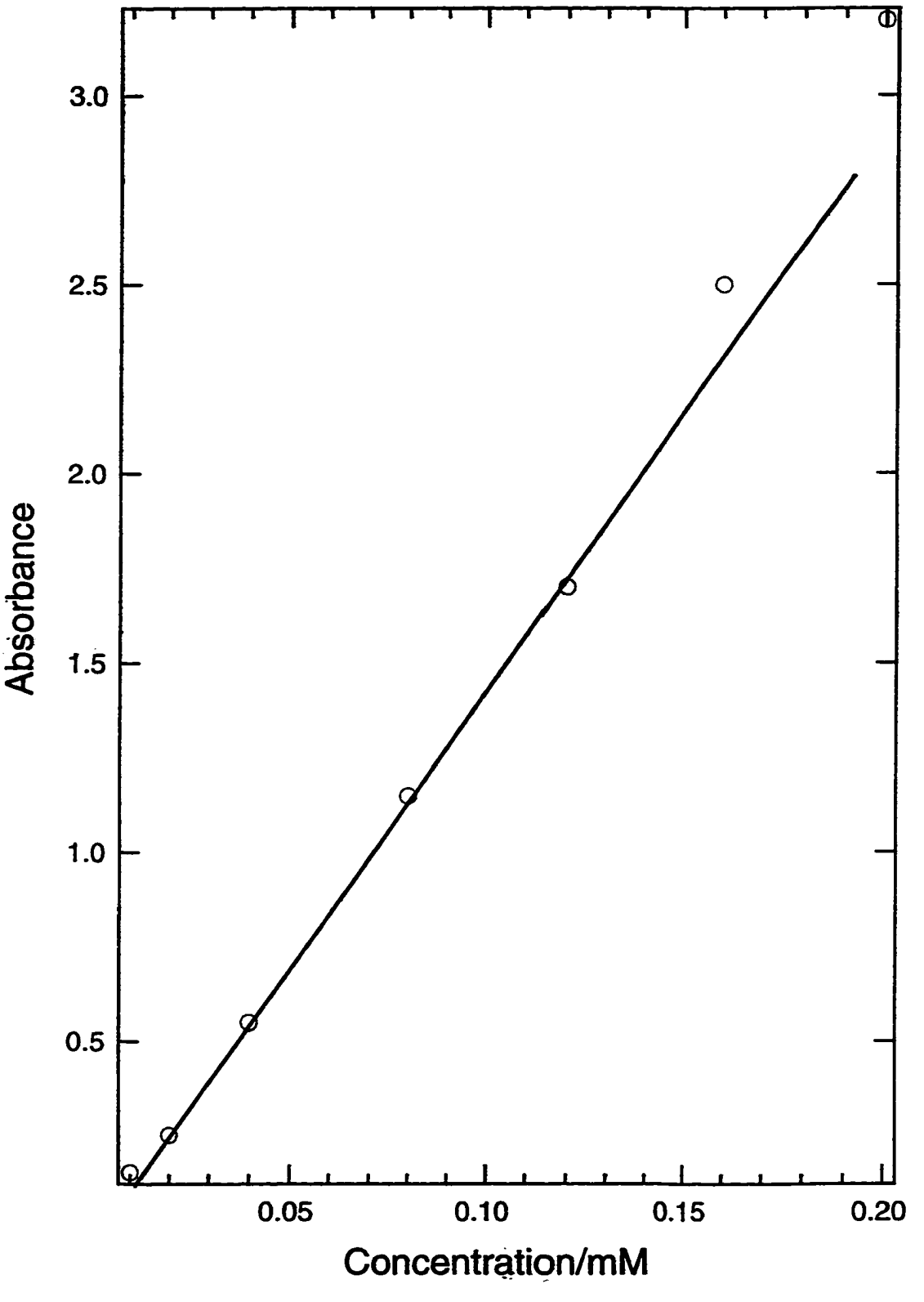

Figure 5.1

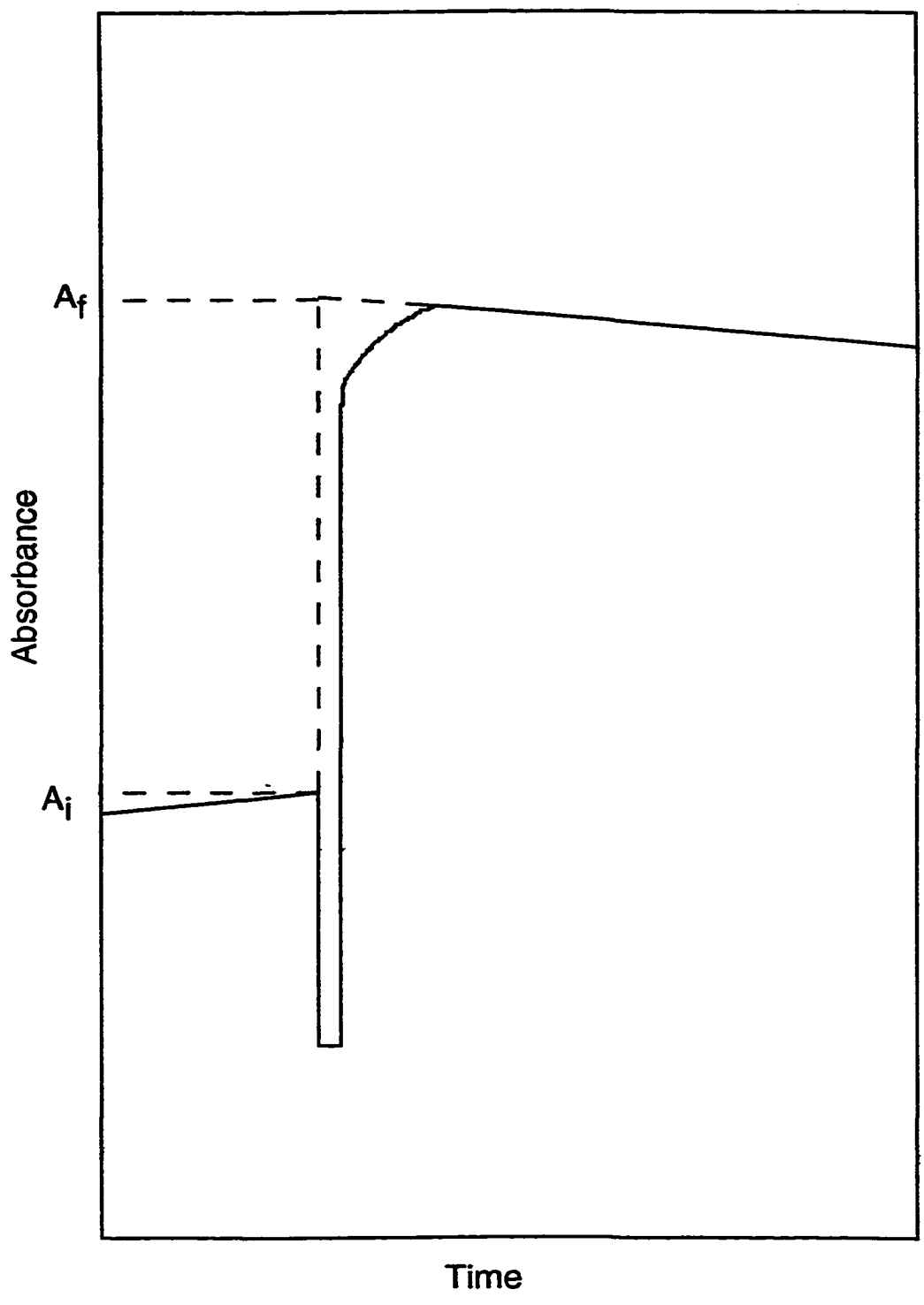

Figure 5.2

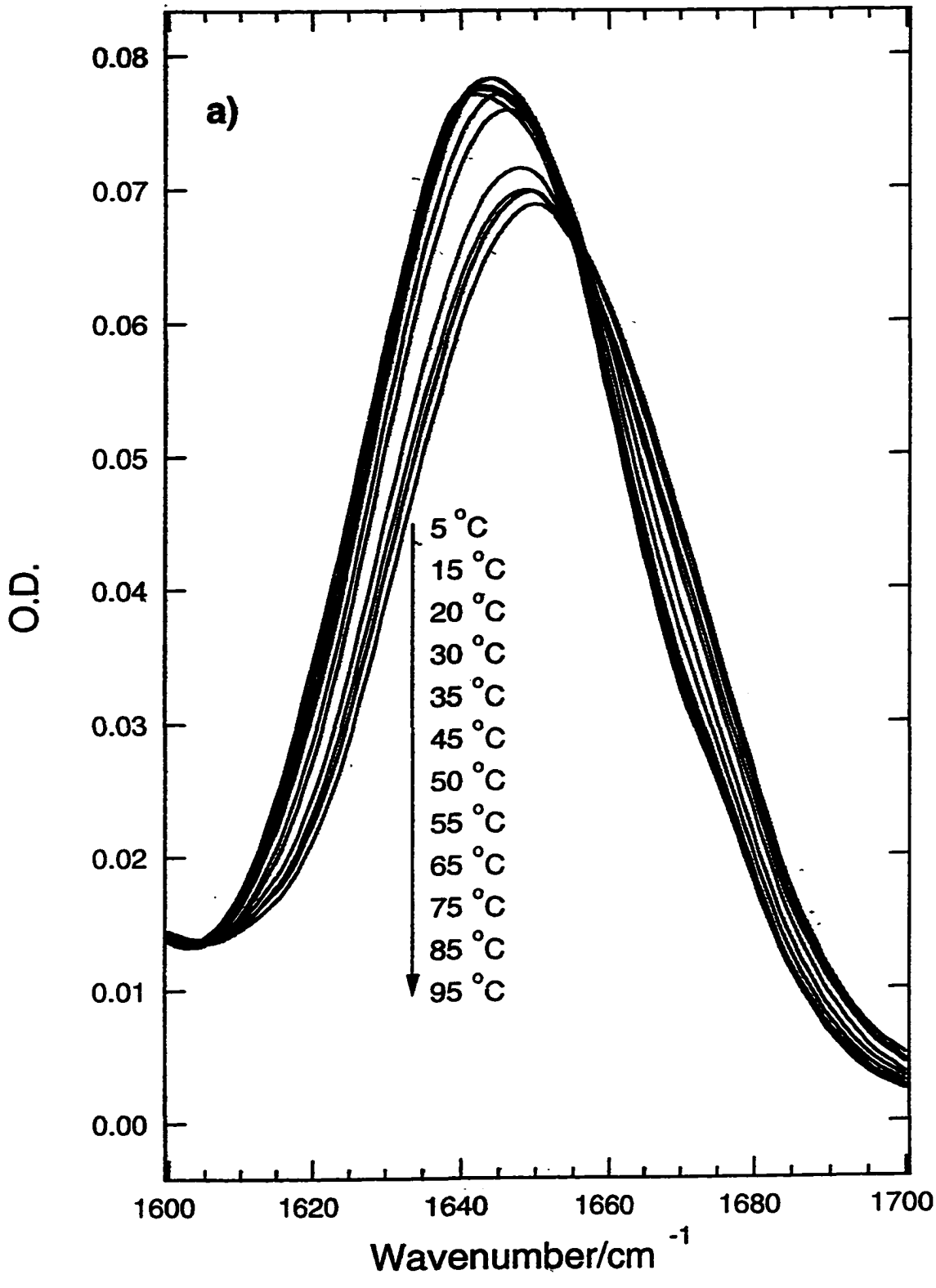

Figure 5.3a

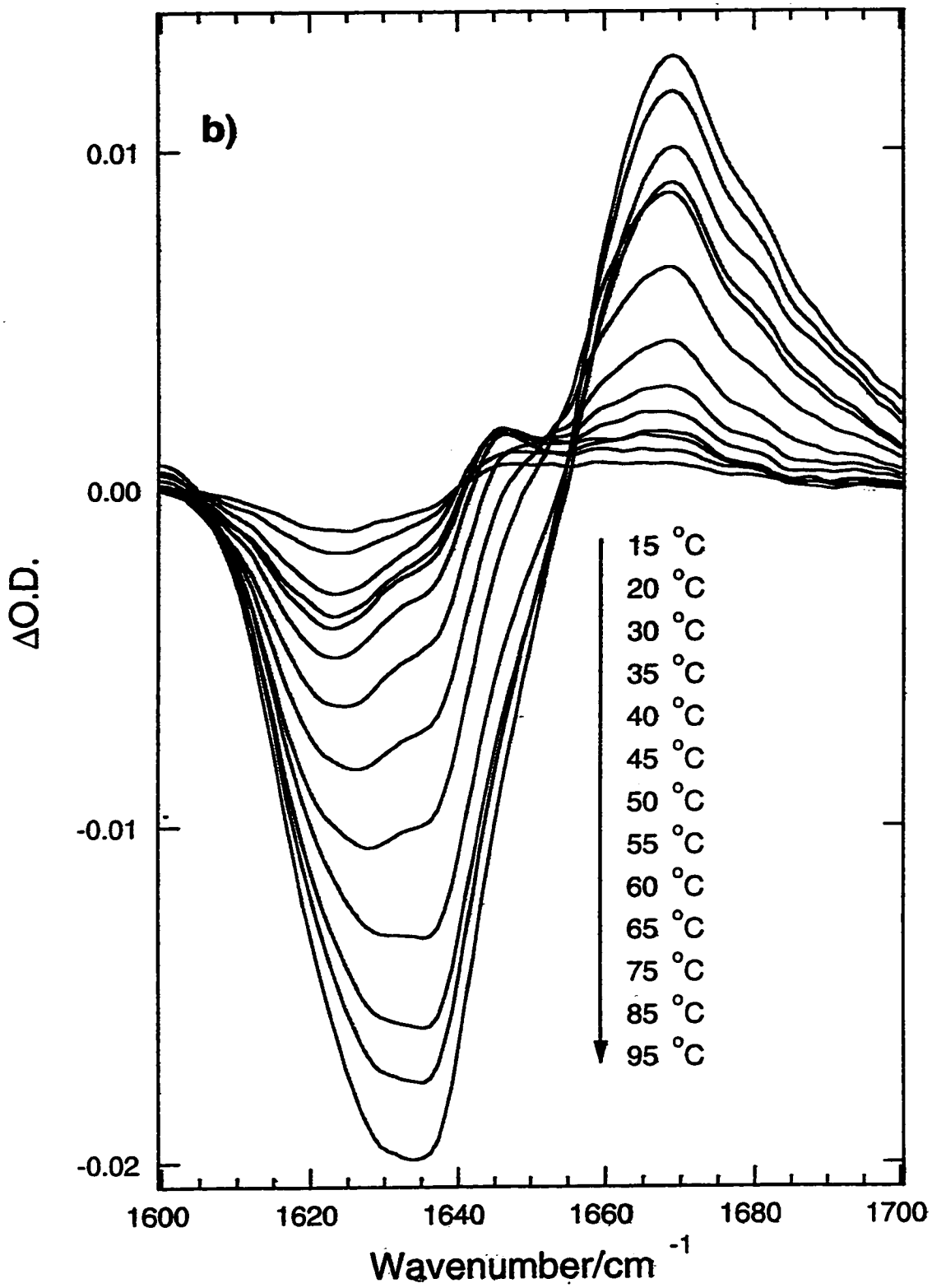

Figure 5.3b

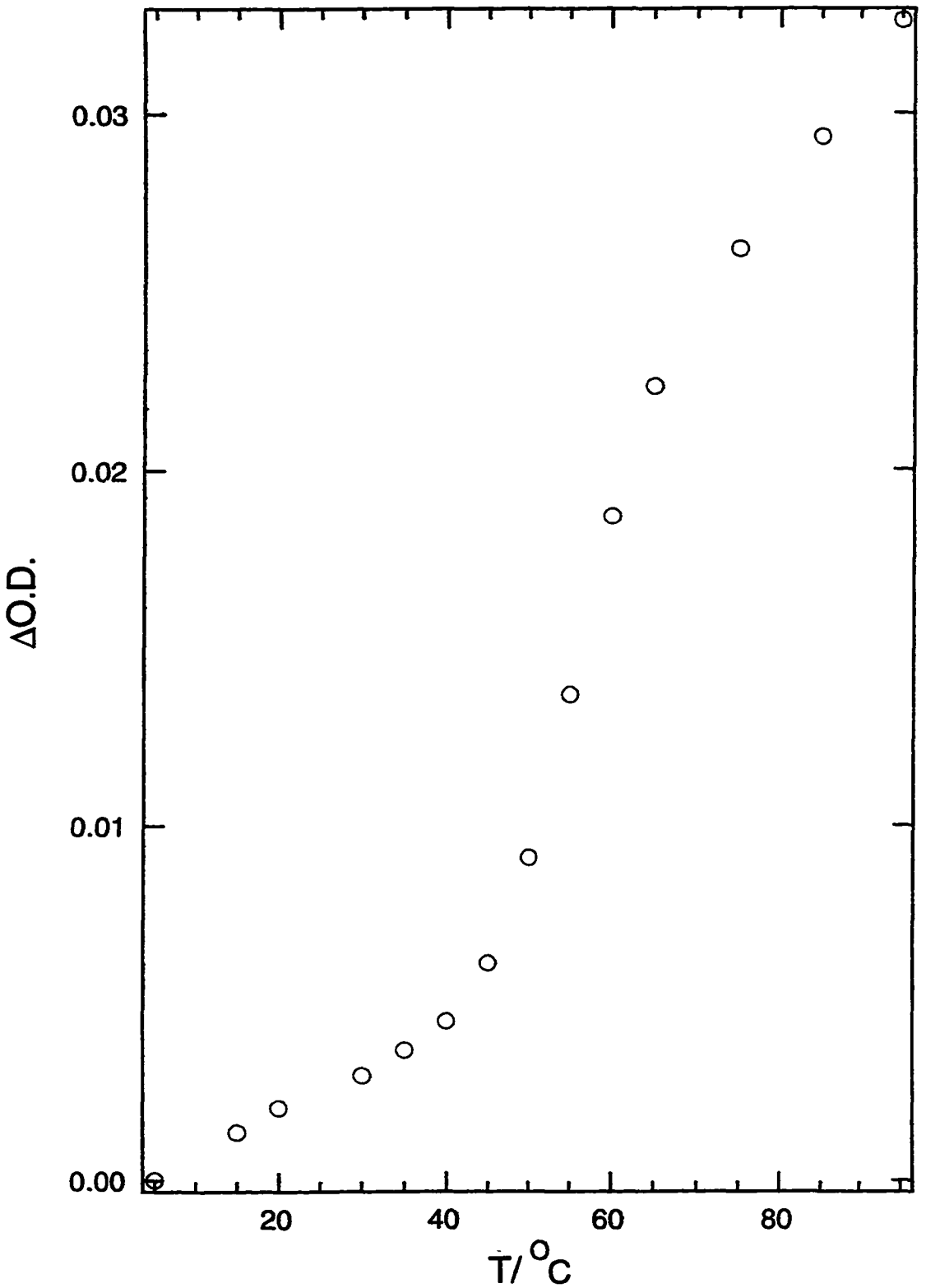

Figure 5.4

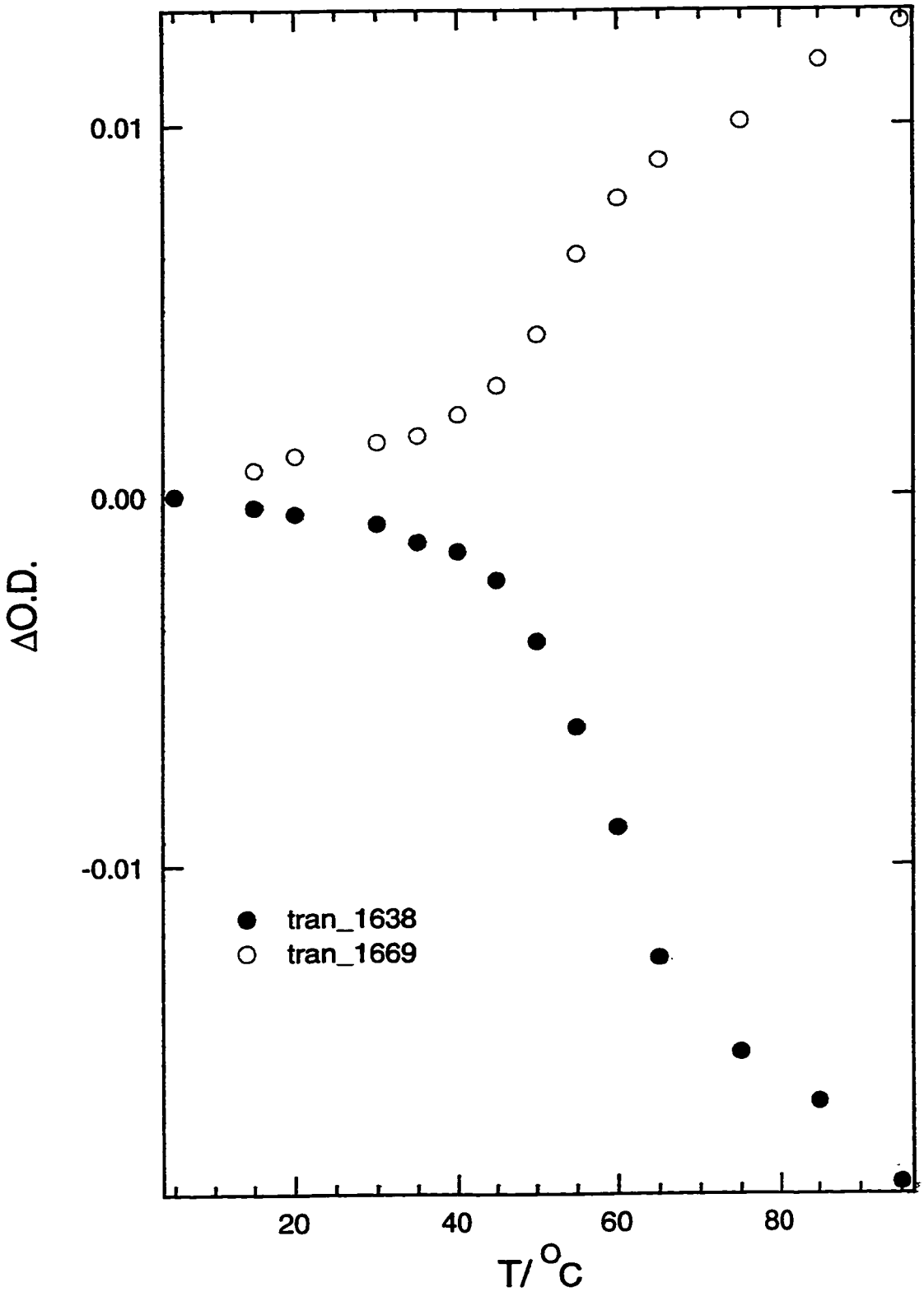

Figure 5.5

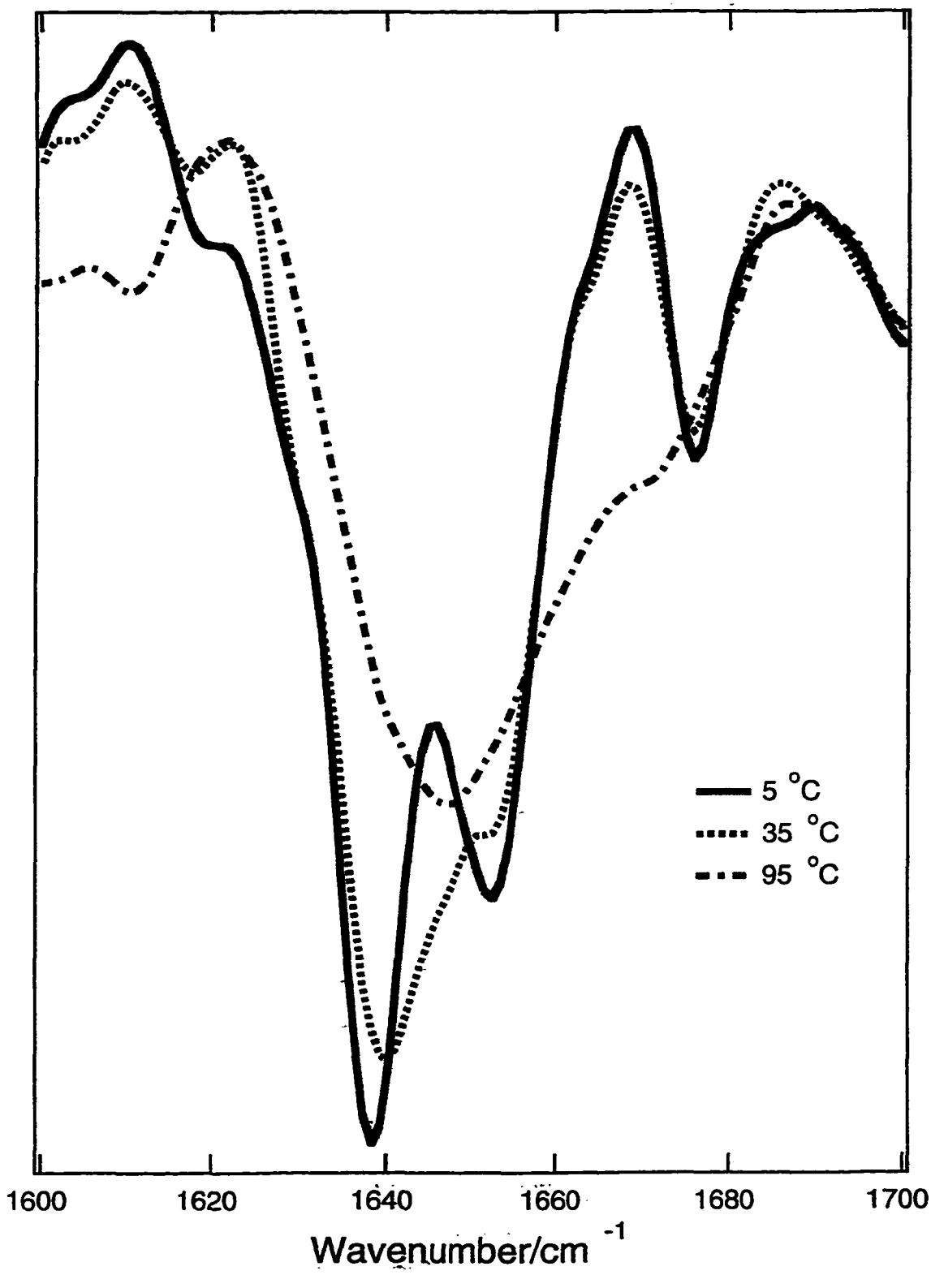

Figure 5.6

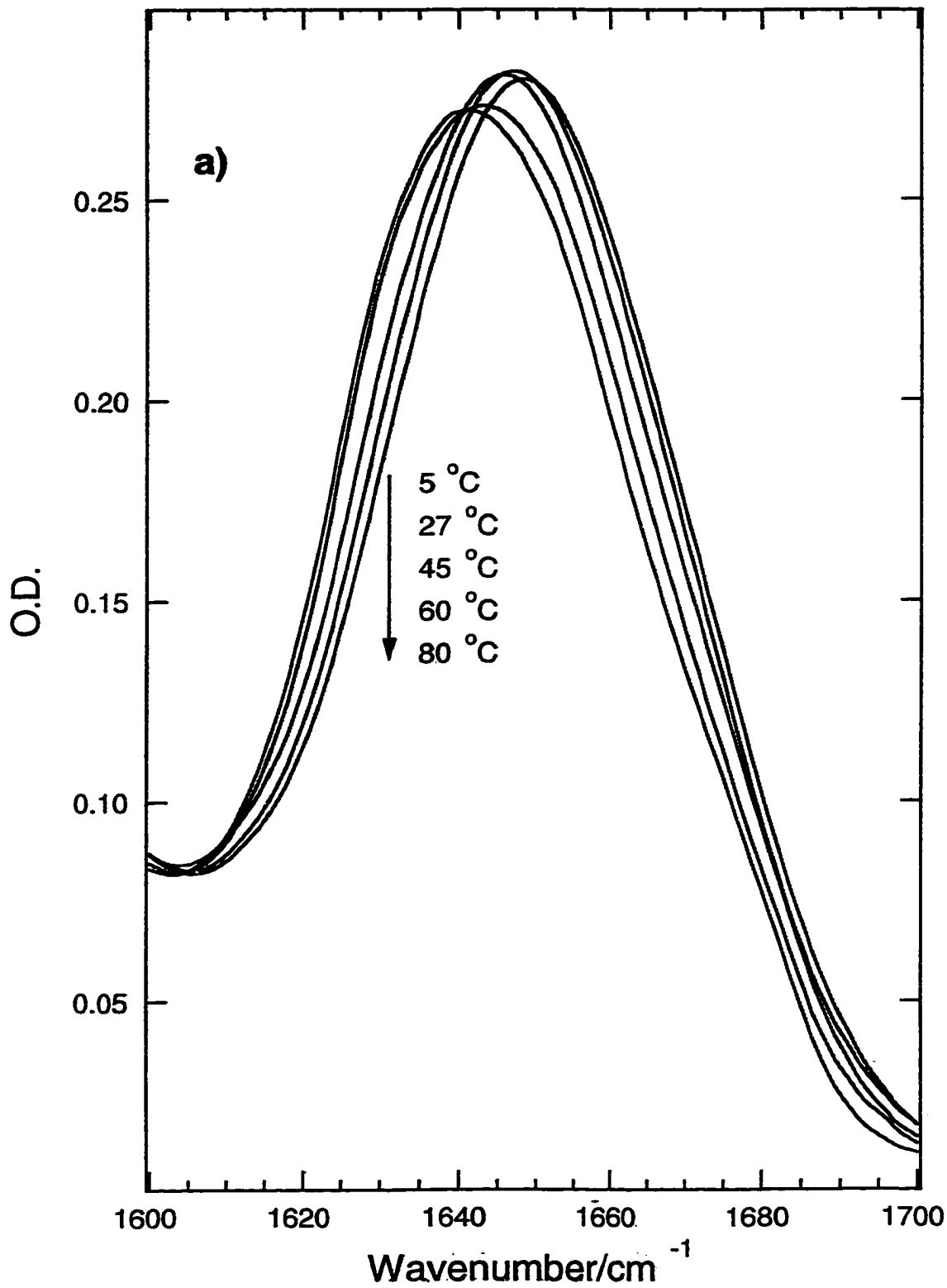

Figure 5.7a

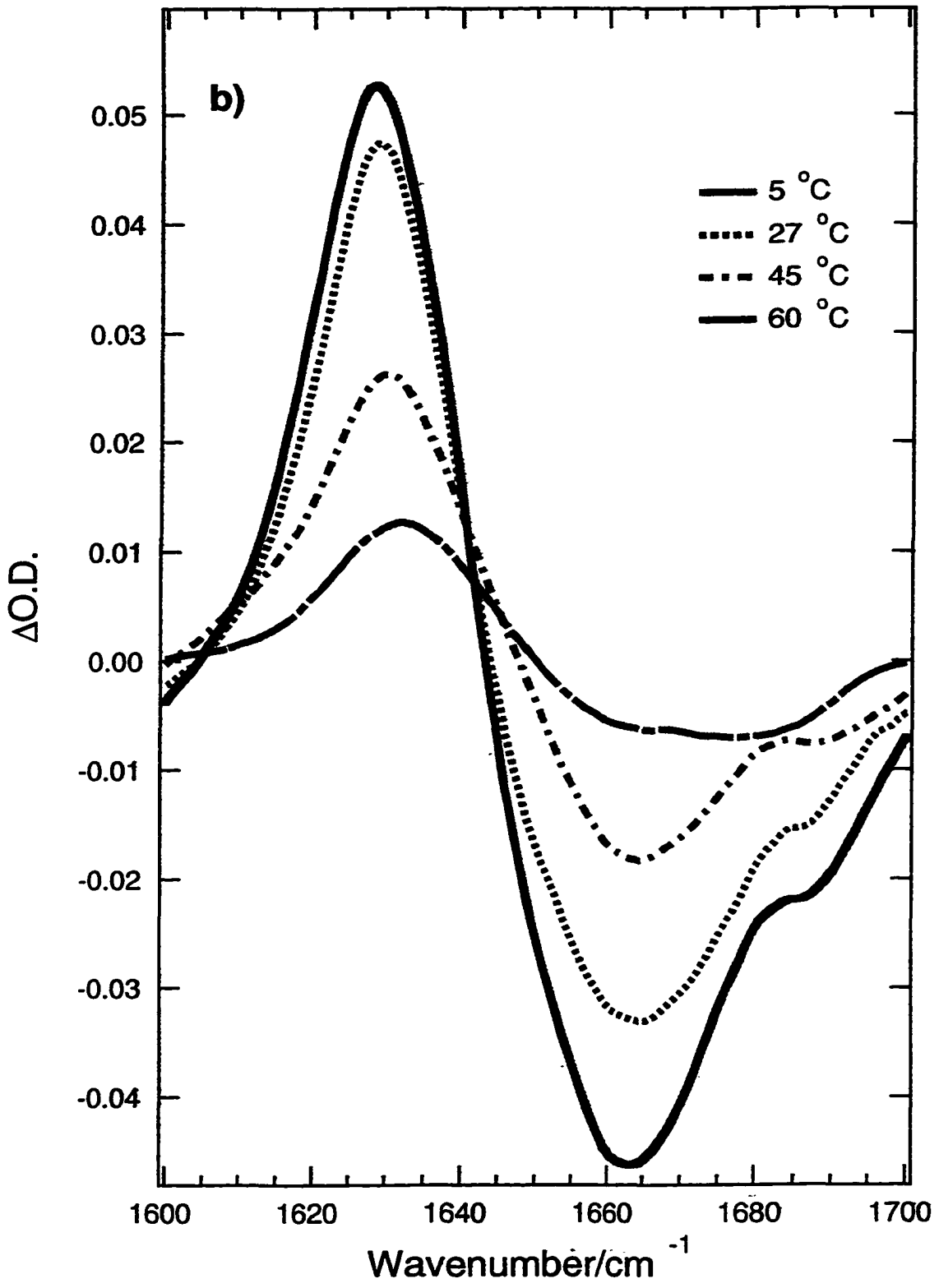

Figure 5.7b

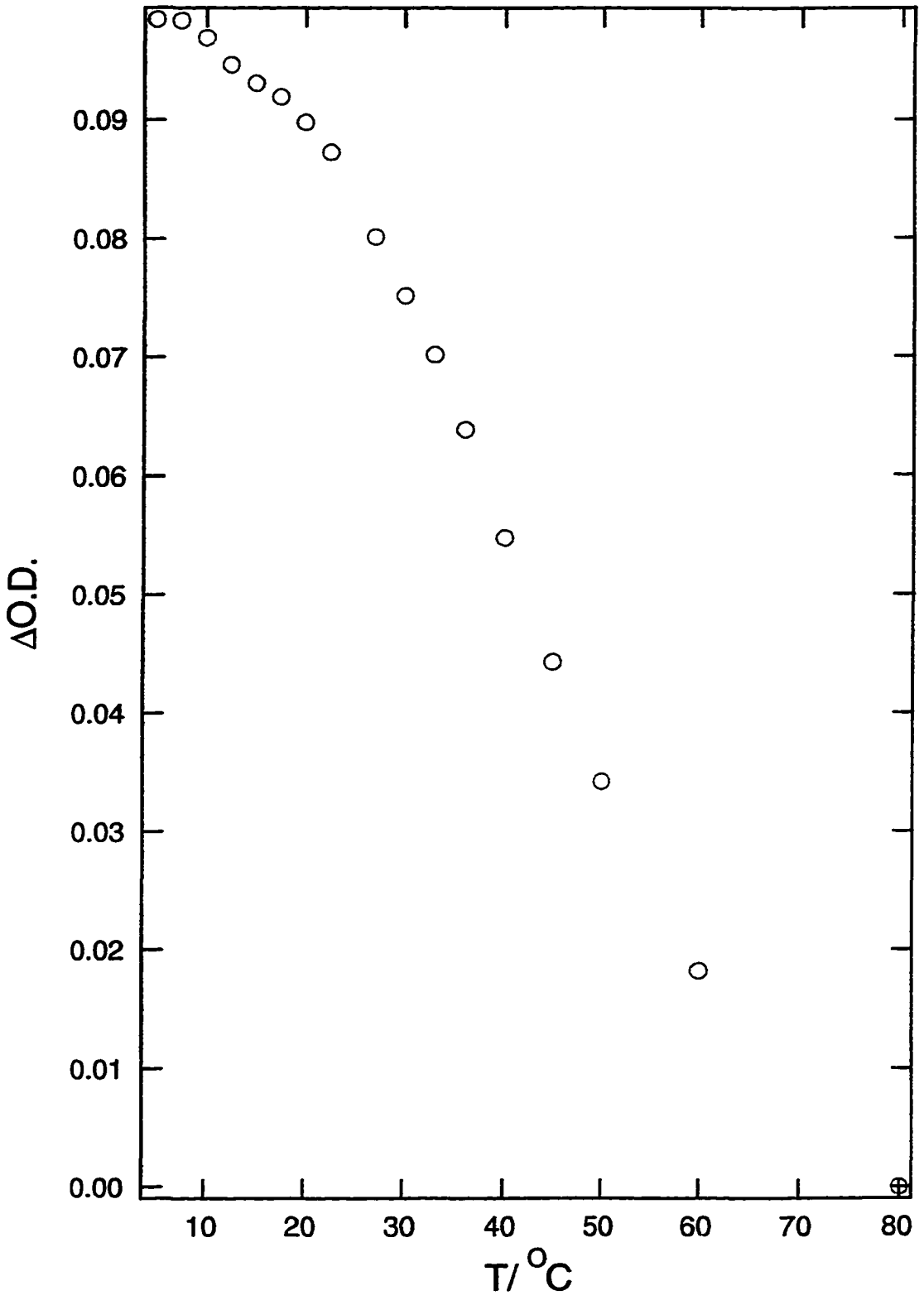

Figure 5.8

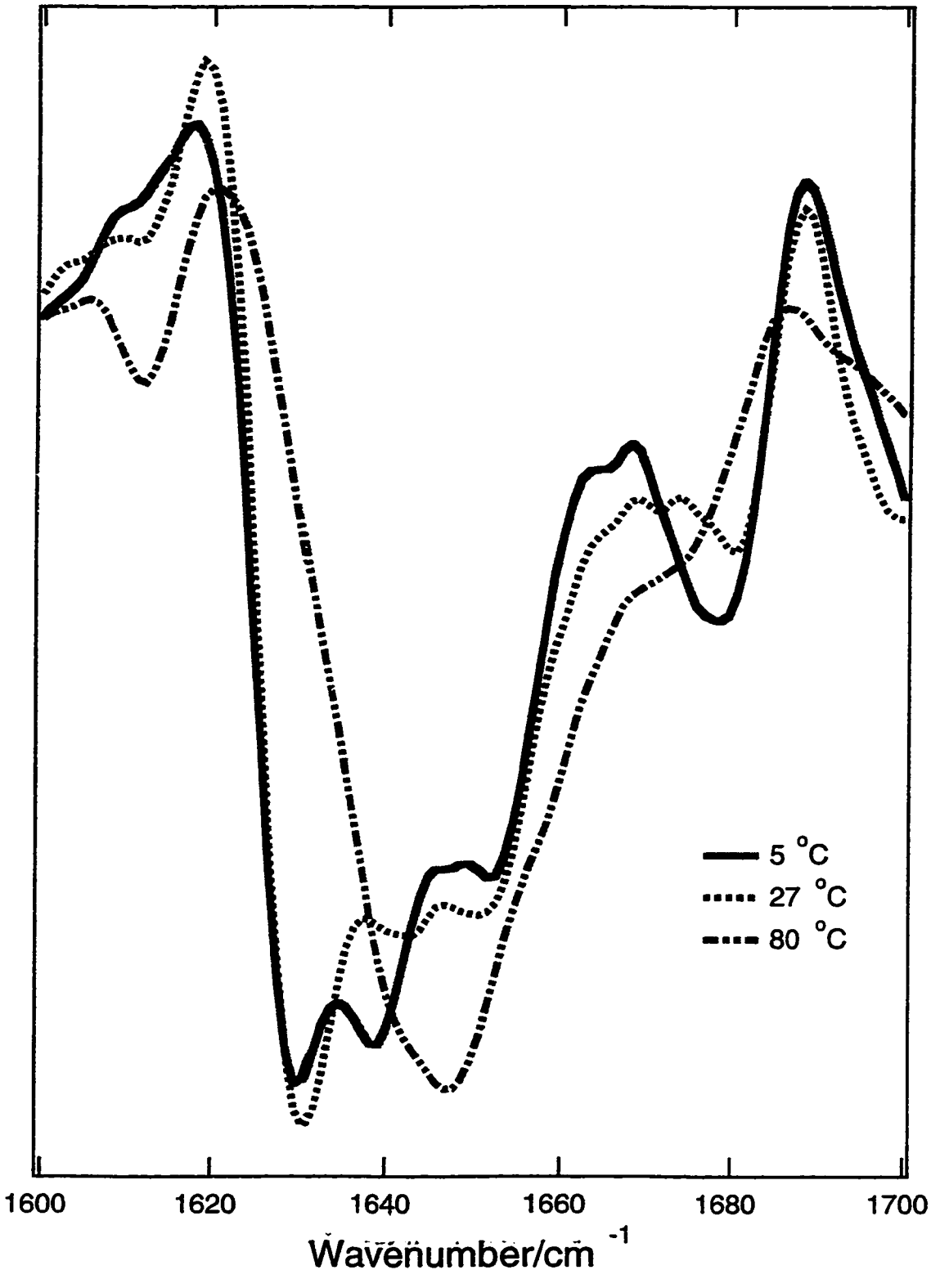

Figure 5.9

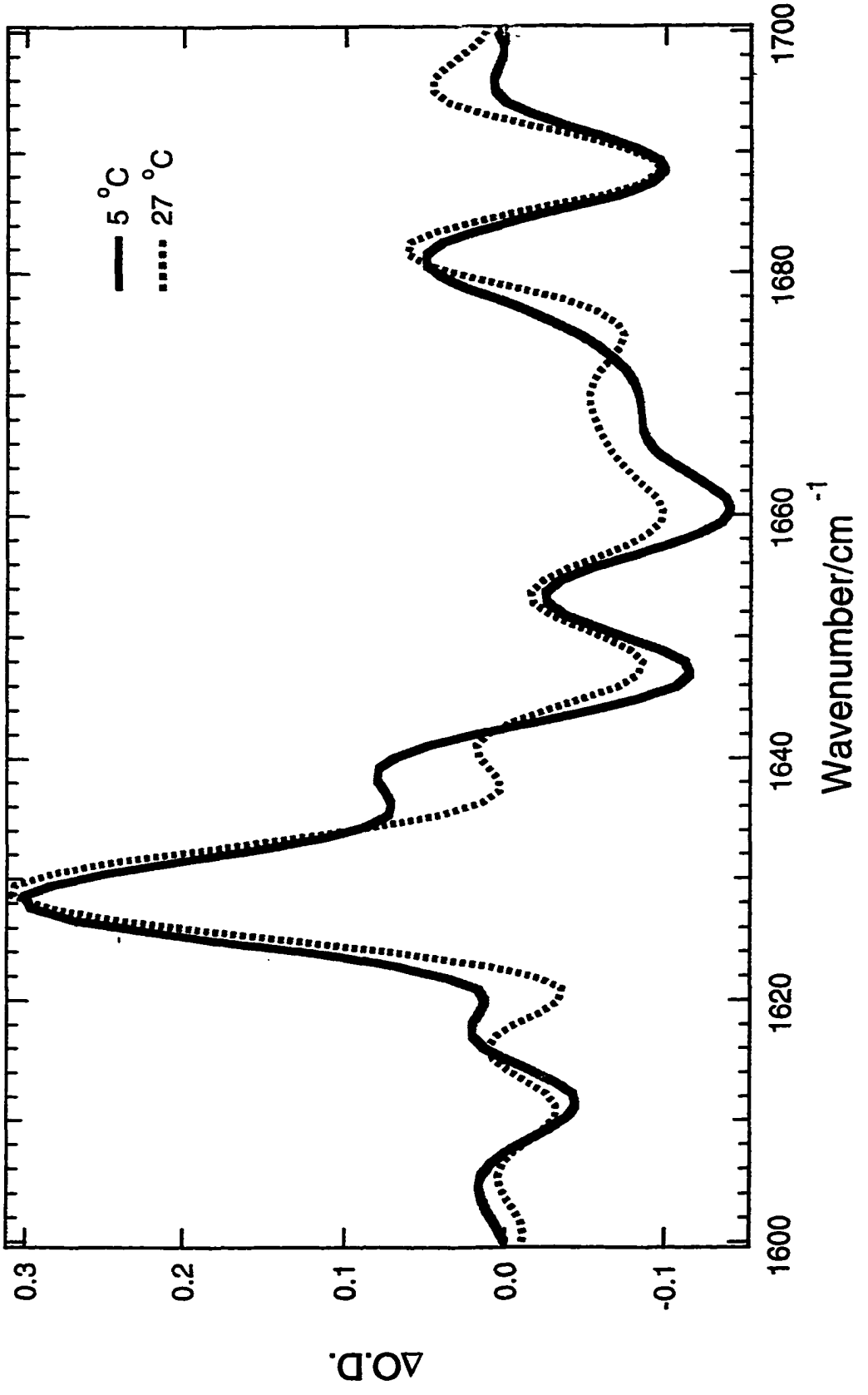

Figure 5.10

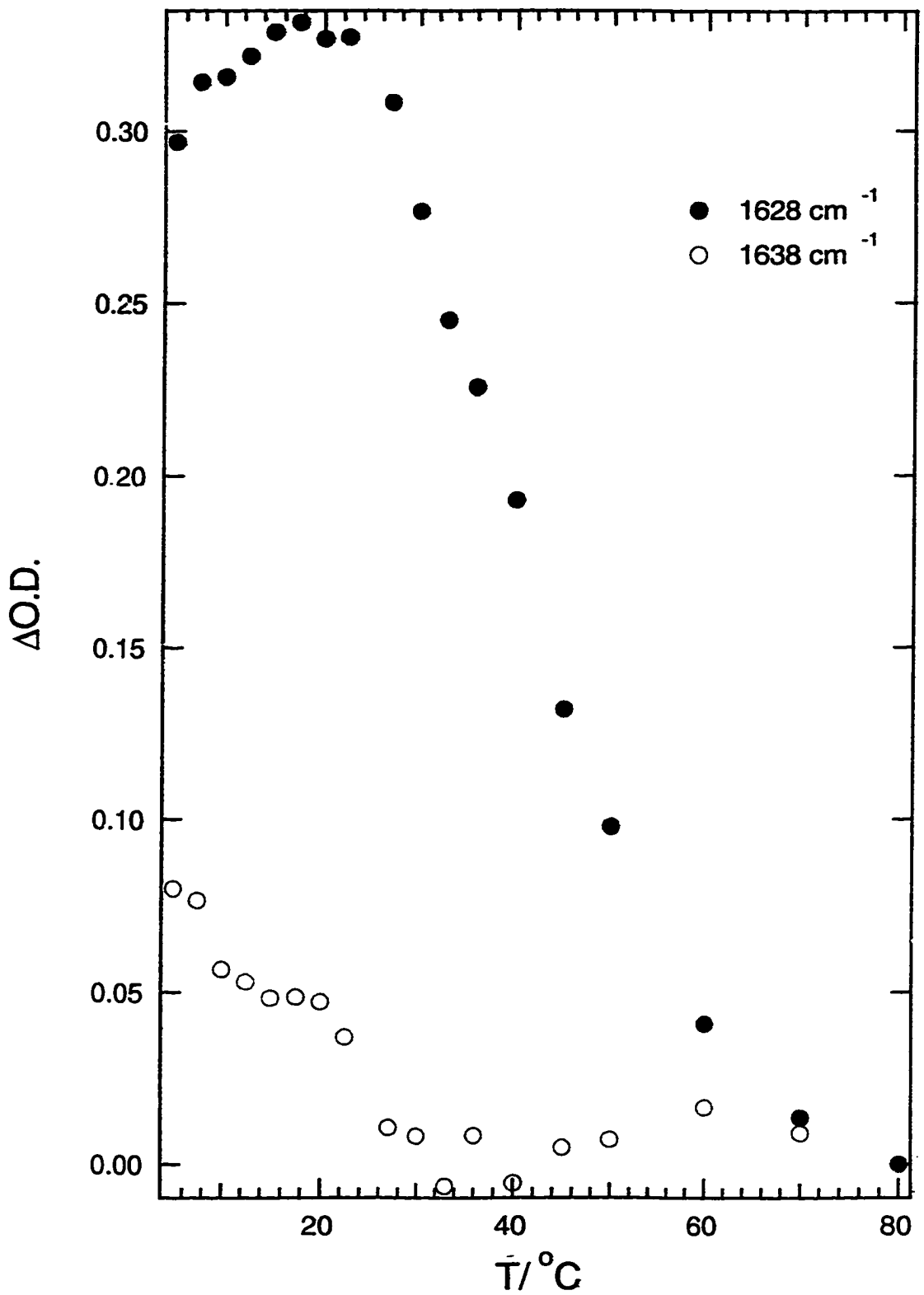

Figure 5.11

Chapter 6 The Protein Folding Pathway of α-Lactalbumin

6.1 General thought of protein folding

It has been long thought that proteins are folded by random searching from their various conformations until the lowest free energy is reached. The free energy governing these processes is shown below:

$$\Delta G = \Delta H - T\Delta S \qquad (6.1)$$

Where the G is free energy, H is enthopy and S is entropy. However, the general estimation of the time scale needed for the proteins to reach their final native structures based on this model gives an unacceptable time scale that is even larger than the age of the Universe (10^{10} years).

Consider a small protein with 100 amino acids similar to the size of α-lactalbumin (123 residues). To simplify the estimation, we assume each residue can only rotate in a two dimensional plan. Thus each amino acid has two choices to determine two different conformations of the protein. One hundred amino acids therefore will give $2^{100} \sim 10^{30}$ possible conformation of the protein. Suppose each possible conformation needs 1 ps to be reached, the average time scale necessary for this protein to arrive at its unique native conformation based on this random search model will be:

$$10^{-12} * 10^{30}\ s = 10^{18}\ s = 10^{10}\ \text{years} \sim \text{age of the Universe} \qquad (6.2)$$

which certainly is ridiculous. Actually a typical protein needs only no more than one second to fold from its complete unfolded structure to native structure, and the intact holo α-LA just takes 40 ms to be folded (Balbach et al., 1996). This suggests that proteins must follow some specific pathways, rather than a random search, to fold to their final native states.

Given the disordered feature of the polypeptide when proteins are in their unfolded state, only local interactions exist. The amino acids of protein tend to form secondary structures more easily by interacting with their neighboring amino acids. It is reasonable to think that the secondary structures are the first regular structures to be formed in protein folding pathway. It follows that these early secondary structures act as a nucleation center, with the help of other components in the native protein such as ligands and disulfide bridges, to trigger the subsequent formation of the tertiary structure which has the relative position of secondary structures fixed and well packed sidechains.

We should specially mention that this early event postulated in protein folding pathway has been proved experimentally. In Los Alamos, the temperature jump kinetic experiments have been done on some model peptides and proteins and result in many fruitful results. Our group led by our group leader, Robert Callender, is an important participant in all of these experiments.

The basic idea of these experiments are the following. An YAG infrared laser gives a short pulse to initiate the temperature jump about 10 °C within

a time scale of ps. This T-jump unfolds the target peptide or protein by heat denaturation transition behavior, previous well studied in equilibrium experiments similar to the methods we used to investigate α-lactalbumin described in details in the previous chapters. This unfolding behaviors were monitored by the changes of the marker bands of the target proteins or peptides collected by infrared spectroscopy installed with fast detector of time resolution down to 10 ~ 20 ns. The temperature will not relax within millisecond, so the early event of protein folding can be derived by its unfolding behaviors.

These experiments indicated that the secondary structures can be folded within 100 ns which is much faster than the time scale needed for the tertiary structures to be formed, 100 μs to 1 s based on other kinetic studies. These T-jump kinetic experiments gave the evidence for the first time that secondary structure formation dominates in the very early process of protein folding.

6.2 How does α-lactalbumin fold to its native state

Protein folding problem can be studied either in kinetic state or equilibrium state. The kinetic states probed by time resolved techniques reflect the reality happening in protein folding pathway. The equilibrium intermediates may not exist in protein folding pathway. However, as we have mentioned in previous chapters, the evidence of the equilibrium intermediates populated in the protein folding pathway of α-lactalbumin has been provided by a 1-D NMR study (Balbach et al., 1995; Roder, 1995). Therefore, we can establish a model of the folding of α-lactalbumin based

on our thermal denaturation study discussed in details in the previous chapters. We assume that the intermediates populated at various temperatures for different forms reflect the intermediates populated in protein folding pathway of α-lactalbumin at different stages.

6.2.1 *Helical structures are formed first*

The studies on MG of various proteins have concluded that the acid state of α-lactalbumin is closer to the unstructured α-lactalbumin (Morozova et al., 1995; Ptitsyn, 1992; Baum et al., 1989; Chyan, et al., 1993). Our FTIR study also indicates that there is no β-structure in the acid form of α-lactalbumin. The gradual melting behavior of the acid form also suggest that no tertiary structures exist in these molecules. Moreover, a large amount of helical structures are detected by CD (Dolgikh et al., 1981; Dolgikh et al., 1985) which is sensitive to helical structures. The dominant band at 1648 cm^{-1}, which can arise from random structures, solvated helical structures or the mixture of the both, suggests that these helical structures largely expose to the solvent. This supports the idea that solvated helical structures are the only regular structures existing in this very early stages of the folding of α-Lactalbumin.

6.2.2 *β-structures are formed subsequently*

As we have seen in the previous chapters, the second transition of the apo form of α-LA happens around 40 °C and involves the denaturation of β-structures. Furthermore, the first transition of the apo form with T_m around 20 °C makes the helical domain denatured to the state similar to the acid

state which has solvated helical structures but no tertiary structures. This suggests that the intermediate after the first transition and before the second transition have both denatured helical structure and β-structures. We suggest that a structure similar to this intermediate is formed at the second stage in protein folding pathway of α-LA. β-structures are formed at the stage 2.

The β-structures with denatured helical domain and without the presence of calcium ion, as shown by Kim and his colleagues (Wu et al., 1996) using CD, exhibits gradual melting behavior and no near UV-CD signal, suggesting no tertiary structures exist. This also explain why larger amount of β-structures, indicated by stronger band at 1629 cm^{-1}, are present in comparison with the native protein. Without the help of the tertiary structure, short β-structures just do not have enough stability to be folded. Only longer β-structures can be formed.

6.2.3 *Tertiary structures in β-structure region are formed at stage 3*

The holo cam-2ss form of α-lactalbumin studied by (Ewbank & Creighton, 1993(a); Ewbank & Creighton, 1993(b); Hendrix et al., 1996) has suggested a rigid β-sheet domain and denatured helical domain, indicating native β-structures. The 2ss form of α-LA studied by Kim (Wu et al., 1996) also shows some regular structures by near UV-CD when calcium is present. A sigmoidal transition of melting of this regular structures was also found. Kim et.al thought this regular structures are β-sheet. Moreover, the 2-D NMR study on the kinetic behavior of the apo form of α-LA provides the new clue that β-sheet region adopts native

environment earlier than that of helical domain region (Balbach et al., 1996).

So at stage 3 the calcium ion begins to bind to the partly formed binding site. The β-structure domain is thus stabilized. As a consequence, tertiary interactions within this domain are established.

Binding of calcium may not be the decisive step folding this protein. The ability of correct refolding of the apo form is strong evidence that it is possible that the function of the calcium is to help stabilize the β-structure domain, subsequently facilitating the whole folding process. In fact, the time constant for correct folding of the apo form is significantly slower than that of the holo form. Calcium appears to be responsible for rapid folding but not for correct folding.

6.2.4 Folding of helical domain at stage 4

At this stage the well formed β-structure domain acts as the nucleation center to trigger the folding of the helical domain. It follows that the completely folded protein is thus finally formed.

All the holo forms of α-LA exhibit cooperative melting behavior for both the helical and β-structures. On the contrary, all the apo forms we studied have non-cooperative melting of these two structural domains. Since calcium ion stabilizes the β-structural domain. This suggests that as long as β-structure domain is formed, the helical domain is folded quickly

and completely. In another words, the native β-structural domain stabilizes the native helical domain and vise versa.

6.3 Summery

Based on above discussion, we propose the following folding pathway of α-lactalbumin:

1. The classic MG is formed in the very beginning of the folding pathway of α-lactabumin. The structure of this MG is similar to the acid form which has formed solvated helical structures which may resemble the tertiary fold of α-LA but lack detailed sidechain packing.

2. In the second stage, the β-structural domain is formed but, similar to the helical domain, contains no tertiary fixed structure. This β-structure domain may contain more β-sheet than that found in the native protein.

3. The well formed secondary structures formed at stages 1 and 2 yield protein that begins to bind metal ions (Ca^{2+}). The binding of Ca^{2+} induces the rearrangement of the secondary structural components and further triggers the tertiary structure formation of β-structure domain.

4. The rigid β-sheet domain formed in the stage 3 subsequently constitutes the nucleation center and trigger the complete folding of the helical domain. Beginning this point, native protein is formed completely.

Reference:

Acharya, K. R., Stuart, D. I., Walker, N. P. C., Lewis, M., and Phillips, D. C. (1989). *Journal of Molecular Biology* **208**, 99-127.

Acharya, K. R., Ren, J., Stuart, D. I., Phillips, D. C., and Fenna, R. E. (1991) *Journal of Molecular Biology* **221**, 571-581.

Arrondo, J. L. R., Muga, A., Castresana, J., and Goni, F. M. (1993). *Prog. Biophys. molec. Biol.* **59**, 23-56.

Balbach, J. et al., (1995) *Nature Struct, Biol.* 2, 865.

Balbach, J., Forge, V., Lau, W. S., Nuland, N. A. J. V., Brew, K. , & Dobson, C. M. (1996) *Science* **274,** 1161-1163.

Baum, J., Dobson, C. M., Evans, P. A. , & Hanley, C. (1989) *Biochemistry* **28,** 7-13.

Byler, D. M. , & Susi, H. (1986) *Biopolymers* 469-487.

Casal, H., Kohler, U. , & Mantsch, H. H. (1988) *Biochim. Biophys. Acta.* **957,** 11-20.

Chirgadze, Y. N., Shestopalov, B. V., and Venyaminov, S. Y. (1973). *Biopolymers* **12,** 1337-1351.

Chirgadze, Y., Fedorov, O. V. , & Trushina, N. P. (1975) *Biopolymer* **14,** 679-694.

Chyan, C., Wormald, C., Dobson, C. M., Evans, P. A. , & Baum, J. (1993) *Biochemistry* **32,** 5681-5691.

Colon, W. , & Roder, H. (1996) *Nature Structural Biology* **3,** 1019-1025.

Creighton, T. E. , & Ewbank, J. J. (1994) *Biochemistry* **33,** 1534-1538.

Dill, K. A. (1990) *Biochemistry* **29,** 7133-7151.

Dobinson, C. M. (1994) *Curr. Biol.* **4,** 636-640.

Dolgikh, D. A., Gilmanshin, R. I., Brazhnikov, E. V., Bychkova, V. E.,Semisotnov, G. V., Venyaminov, S. Y., and Ptitsyn, O. B. (1981). *FEBS Letters* **136**, 311-315.

Dolgikh, D. A., Abaturov, L. V., Bolotina, I. A., Brazhnikov, E. V., Bychkova, E., Bushuev, V. N., Gilmanshin, R. I., Lebedev, Y. O., Semisotnov, G. V., Tiktopulo, E. I. , & Ptitsyn, O. B. (1985) *Eur. Biophys. J.* **13,** 109-121.

Ewbank, J. J. , & Creighton, T. E. (1991) *Nature* **350,** 518-520.

Ewbank, J. J. , & Creighton, T. E. (1993a) *Biochemistry* **32,** 3677-3693.

Ewbank, J. J. , & Creighton, T. E. (1993b) *Biochemistry* **32,** 3694-3707.

Eyles, S. J., Radford, S. E., Robinson, C. V. , & Dobson, C. M. (1994) *Biochemistry* **33,** 13038-13048.

Fabian, H., and Mantsch, H. H. (1995). *Biochemistry* **34**, 13651-13655.

Gilmanshin, R., Van Beek, J., and Callender, R. (1996) *Journal of Physical Chemistry* **100**, 16754-16760.

Gilmanshin, R., William, S., Callender, R. H., Woodruff, W. H. , & Dyer, R. B. (1997) *Proc. Natl. Acad. Sci. USA.* **94,** 3709-3713.

Griffiths, P. R., and Pariente, G. L. (1986)*Trends in Analytical Chemistry* **5**, 209-215.

Griko, Y. V., Freire, E. , & Privalov, P. L. (1994) *Biochemistry* **33,** 1889-1899.

Haris, P. I. , & Chapman, D. (1995) *Biopolymers* **37,** 251-263.

Haynie, D. T. , & Freire, E. (1993) *Proteins: Struct. Funct. Genet.* **16,** 115-140.

Hendrix, T. M., Griko, Y. , & Privalov, P. (1996) *Protein Science* **5,** 923-931.

Holloway, P. W. , & Mantsch, H. H. (1989) *Biochemistry* **28,** 931-935.

Holzbaur, I. E., English, A. M. , & Ismail, A. A. (1996) *Biochemistry* **35,** 5488-5494.

Ikeguchi, M., Sugai, S., Fujino, M., Sugawara, T., & Kuwajima, K. (1992) *Biochemistry* 31, 12695-12700.

Jackson, M., Haris, P. I. , & Chapman, D. (1991) *Biochemistry* **30,** 9681-9686.

Jackson, M., & Mantsch, H. H. (1995) *Critical Reviews in Biochemistry and Molecular Biology* **30,** 95-120.

Kauppinen, J. K., Moffatt, D. J., Mantsch, H. H. , & Cameron, D. G. (1981) *Applied Spectroscopy* **35,** 271-276.

Kim, P. S., and Baldwin, R. L. (1990) *Annual Review of Biochemistry* **59,** 631-660.

Kronman, M. J. , & Bratcher, S. C. (1983) *J. Biol. Chem.* **258,** 5707-5709.

Kuwajima, K., Harushima, Y., and Sugai, S. (1986). *International Journal of Peptide and Protein Research* **27**, 18-27.

Kuwajima, K. (1989) *Proteins: Struct. Funct. Genet.* **6,** 87-103.

Kuwajima, K., Ikeguchi, M., Sugawara, T., Hiraoka, Y. , & Sugai, S. (1990) *Biochemistry* **29,** 8240-8249.

Makhatadze, G. I., Clore, G. M., and Gronenborn, A. M. (1995) *Nature Structural Biology* **2**, 852-855.

Martinez, G., & Millhauser, G. (1995) *Journal of Structural Biology* **114,** 23-27.

Miyazawa, T. , & Blout, E. R. (1961) *J. Am. Chem. Soc.* **83,** 712-719.

Moffatt, D. J. , & Mantsch, H. H. (1992) *Methods Enzymol.* **210,** 192-200.

Morozova, L. A., Haynie, D. T., Arico-Muendel, C., Dael, H. V., & Dobson, C. M. (1995) *Nature Structural Biology* **2,** 871-875.

Pain, R. H. (1994) *Oxford, New York, 1994.*

Parker, M. J., and Clarke, A. R. (1997) *Biochemistry* **36**, 5786-5794.

Peng, Z., & Kim, P. S. (1994) *Biochemistry* **33,** 2136-2141.

Permyakov, E. A., Morozova, L. A., and Burstein, E. A. (1985). *Biophysical Chemistry* **21**, 21-31.

Pfeil, W. (1981) *Biophysical Chemistry* **13**, 181-186.

Prestrelski, S. J., Byler, D. M. , & Thompson, M. P. (1991a) *Biochemistry* **30,** 8797-8804.

Prestrelski, S. J., Byler, D. M. , & Thompson, M. P. (1991b) *Int. J. Peptide Protein Res.* **37,** 508-512.

Privalov, P. L. (1996) *Journal of Molecular Biology* **258**, 707-25.

Ptitsyn, O. B. (1987) *Protein Chem.* **6,** 273-293.

Ptitsyn, O. B. (1992) *Freeman, New York, 1992.* 243-300.

Riddles, P. W., Blakeley, R. L., & Zerner, B. (1979) *Analytical Biochemistry* **94,** 75-81.

Robinson, C. V., Grob, M., Eyles, S. J., Ewbank, J. J., Mayhew, M., Hartl, F. U., Dobson, C. M. , & Radford, S. E. (1994) *Nature* **372,** 646-651.

Roder, H. (1995) *Nature Structrual Biology.* **2,** 817-820.

Seshadri, S., Oberg, K. A. , & Fink, A. L. (1994) *Biochemistry* **33,** 1351-1355.

Stokkum, I. H. M., Linsdell, H., Hadden, J. M., Haris, P. I., Chapman, D. , & Bloemendal, M. (1995) *Biochemistry* **34,** 10508-10518.

Stuart, D. I., Acharya, K. R., Walker, N. P. C., Smith, S. G., Lewis, M. , & Phillips, D. C. (1986) *Nature* **324,** 84-87.

Surewicz, W. K., Mantsch, H. H. , & Chapman, D. (1993) *Biochemistry* **32,** 389-393.

Susi, H., & Byler, D. M. (1983) *Biochem. Biophys. Res. Commun.* **115,** 391-397.

Susi, H., & Byler, G. L. (1986) *Methods in Enzymology* **130,** 290-311.

Taubes, G. (1996) *Science.* **271,** 1493-1495.

Trewhella, J., Liddle, W. K., Heidorn, D. B. , & Strynadka, N. (1989) *Biochemistry* **28,** 1294-1301.

Vanderheeren, G., and Hanssens, I. (1994). *Journal of Biological Chemistry* **269,** 7090-7094.

Vanderheeren, G., Hanssens, I., Meijberg, W., and Van Aerschot, A. (1996). *Biochemistry* **35,** 16753-16759.

Venyaminov, S. Y., & Kalnin, N. N. (1990) *Biopolymer* **30,** 1243-1257.

Venyaminov, S. Y., Braddock, W. D., and Prendergast, F. G. (1996). *Biophysical Journal* **70,** A65.

Veprintsev, D., Permyakov, S., Permyakov, E., Rogov, V., Cawthern, K. , & Berliner, L. (1997) *FEBS Letters.* **412,** 625-628.

Williams, S., Causgrove, T. P., Gilmanshin, R., Fang, K. S., Woodruff, W. H., Callender, R. H., and Dyer, R. B. (1996). *Biochemistry* **35,** 691-697.

Wu, L. C., Peng, Z., & Kim, P. S. (1995) *Structural Biology* **2,** 281-286.

Wu, L. C., Schulman, B. A., Peng, Z. , & Kim, P. S. (1996) *Biochemistry* **35,** 859-863.

IMAGE EVALUATION TEST TARGET (QA-3)

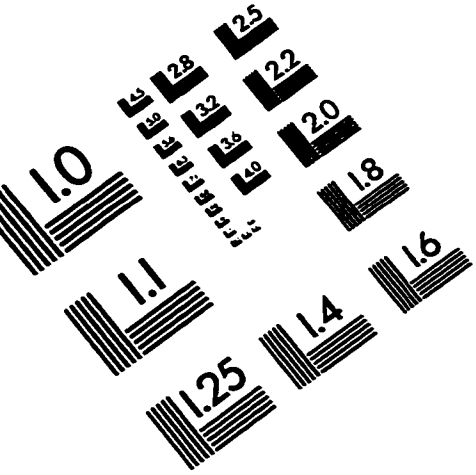

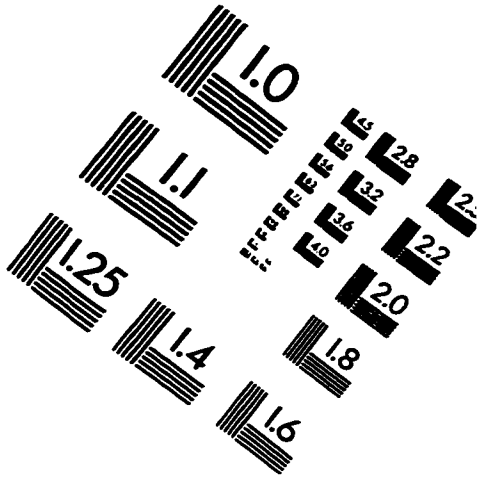

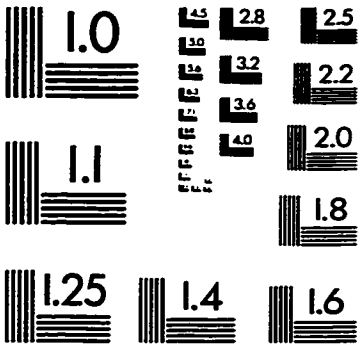

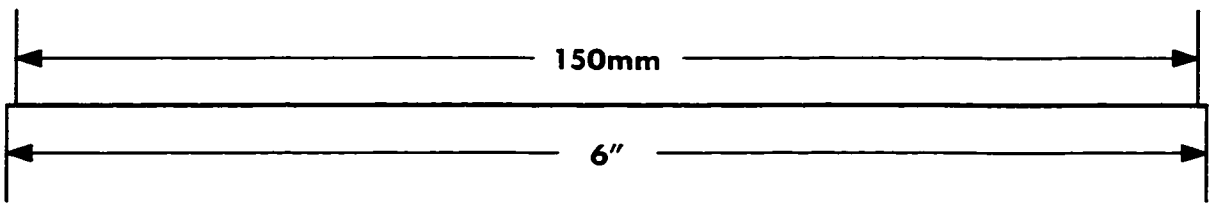

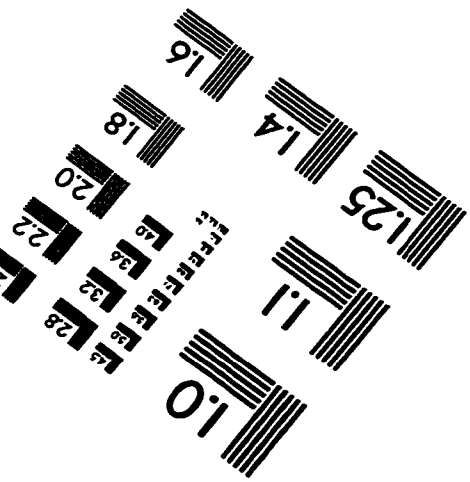

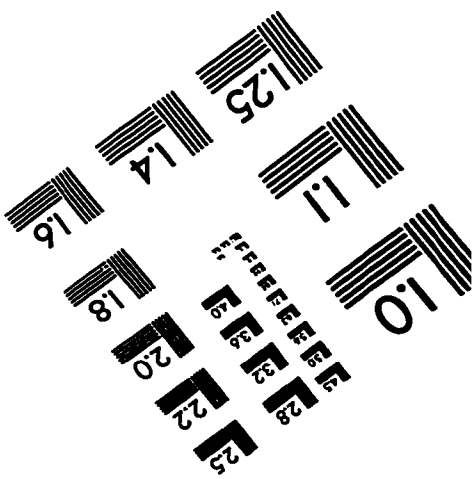

APPLIED IMAGE, Inc
1653 East Main Street
Rochester, NY 14609 USA
Phone: 716/482-0300
Fax: 716/288-5989